DEVELOPMENT OF KERATIN BASED HYDROGEL SYSTEMS

A Thesis Submitted to
the Graduate School of Engineering and Sciences of
İzmir Institute of Technology
in Partial Fulfillment of the Requirements for the Degree of

MASTER OF SCIENCE

in Chemical Engineering

by
Damla YALÇIN

July 2022
İZMİR

ACKNOWLEDGEMENTS

I would like to express my sincere thanks to my advisor Assoc. Prof. Dr. Ayben TOP for her endless support and guidance throughout my M.Sc. thesis. She has always encouraged and helped me with her deepest knowledge, patience, and support. Her research motivation, enthusiasm, and knowledge in both academia and engineering have inspired me not only in my thesis but also in my future career as a chemical engineer. I take this opportunity to thank her for helping me make this thesis possible.

I would also like to thank to my committee members, Assoc. Prof. Dr. Canan URAZ and Prof. Dr. Muhsin ÇİFTÇİOĞLU for their patience and kindness, as well as their navigation to enrich the context of the study.

I would like to thank Prof. Dr. Muhsin ÇİFTÇİOĞLU, Lecturer Dr. Özlem ÇAĞLAR DUVARCI and Pelin KELEŞ for letting me to access the rheometer, making me possible to conduct the rheological studies.

Specifically, I would like to express my sincere thanks to the members of our research group for their support, assistance, and friendship. I would also like to thank my dear all friends for their support and kind friendship throughout the period that I have been here.

I would like to express my sincere thanks to the YALÇIN family; my dear father, grandmother, brother and uncle for their unconditional warm love, their endless belief in me, and their financial and moral support. They are the honorary authors of this thesis.

Last but most definitely not the least, I would like to thank to my love, Emre Yusuf GÖL for his endless love and both physically, mentally, and spiritually support. So glad I have you.

ABSTRACT

DEVELOPMENT OF KERATIN BASED HYDROGEL SYSTEMS

In this study, keratin proteins from Merino sheep wool were obtained via oxidative extraction (Chapter 2), sulfitolysis extraction (Chapter 3) and sulfitolysis with reductive extraction methods (Chapter 4). Keratin proteins were characterized XRD and FTIR spectroscopy and thermal analysis. In the SDS-PAGE gel results of the keratins diffusive protein bands between ~23 kDa and >170 kDa and a discrete band at about 12 kDa were observed confirming highly polydisperse nature of the protein samples. Then, keratin-based hydrogel systems were obtained via different methodologies. In Chapter 2, oxidized keratins (keratoses) were crosslinked with THPC to form keratose hydrogels. Effect of the amount of the crosslinking agent on the viscoelastic, swelling, and morphological properties of hydrogels was investigated. In Chapter 3, the keratin hydrogels were obtained via reformation of disulfide bridge and self-assembly of the keratin chains. In Chapter 4, keratins reduced with DTT were crosslinked with 2000 Da PEG-$(C_2H_4\text{-mal})_2$ and 6000 Da PEG-$(C_2H_4\text{-mal})_2$ to prepare PEG-hydrogels. Storage moduli of the hydrogels were obtained in the range of 63 ± 22 and 2613 ± 254 Pa and were shown to be tuned by the amount and chain length of the crosslinker. The highest swelling ratios were obtained for the THPC crosslinked hydrogels whereas the highest pore size was observed in PEG-keratin hydrogels. Cytocompatibility of the keratin based hydrogel systems was confirmed using L929 mouse fibroblast cells by applying CCK-8 tests. Of these hydrogels, PEG-keratin hydrogels were found to support cell proliferation with a higher rate than empty TCPS wells up to 4 days. These results demonstrate that low-cost keratin-based hydrogels can be used in a variety of biomedical applications, such as drug delivery systems for cancer therapy, and scaffolds in wound healing and soft tissue engineering.

Keyword and Phrases: *Keratin, Keratose, Hydrogels, Self-assembly, Crosslinking, Rheology*

ÖZET

KERATİN BAZLI HİDROJELLERİN GELİŞTİRİLMESİ

Bu çalışmada, Merinos koyun yününden oksidatif ekstraksiyon (Bölüm 2), sülfitoliz ekstraksiyon (Bölüm 3) ve sülfitoliz ve indirgeyici ekstraksiyon yöntemleriyle (Bölüm 4) keratin proteinleri elde edilmiştir. Keratin proteinleri, XRD ve FTIR spektroskopisi ve termal analiz ile karakterize edilmiştir. SDS-PAGE jel sonuçlarında, ~23 kDa ile >170 kDa arasındaki keratin yayılımlı protein bantları ve yaklaşık 12 kDa'da ayrı bir bant gözlenmiş ve protein numunelerinin yüksek oranda polidispers doğası doğrulanmıştır. Daha sonra farklı metodolojiler ile keratin bazlı hidrojel sistemleri elde edilmiştir. Bölüm 2'de, oksitlenmiş keratinler (keratoz), keratoz hidrojelleri oluşturmak için THPC ile çapraz bağlanmıştır. Çapraz bağlayıcı ajan miktarının hidrojellerin viskoelastik, şişme ve morfolojik özellikleri üzerindeki etkisi araştırılmıştır. Bölüm 3'te, keratin hidrojelleri, disülfid köprüsünün reformasyonu ve keratin zincirlerinin kendiliğinden düzenlenmesi ile elde edilmiştir. 4. Bölümde, PEG-hidrojelleri hazırlamak için DTT ile indirgenen keratinler, 2000 Da PEG-$(C_2H_4$-mal$)_2$ ve 6000 Da PEG-$(C_2H_4$-mal$)_2$ ile çapraz bağlanmıştır. Hidrojellerin depolama modülleri 63 ± 22 ve 2613 ± 254 Pa aralığında elde edilmiş ve çapraz bağlayıcının miktarına ve zincir uzunluğuna göre ayarlanabildiği gösterilmiştir. En yüksek şişme oranları THPC çapraz bağlı hidrojellerde elde edilirken, en yüksek gözenek boyutu PEG-keratin hidrojellerinde gözlenmiştir. Keratin bazlı hidrojel sistemlerinin sito-uyumluluğu, CCK-8 testleri uygulanarak L929 fare fibroblast hücreleri kullanılarak doğrulanmıştır. PEG-keratin hidrojellerinin, 4 güne kadar boş TCPS kuyularından daha yüksek oranda hücre çoğalmasını desteklediği bulunmuştur. Bu sonuçlar, düşük maliyetli keratin bazlı hidrojellerin, kanser tedavisi için ilaç taşıyıcı sistemleri ve yara iyileşmesi ve yumuşak doku mühendisliğinde yapı iskelesi gibi çeşitli biyomedikal uygulamalarda kullanılabileceğini göstermektedir.

Anahtar Kelimeler ve Deyimler: *Keratin, Keratoz, Hidrojel, Kendiliğinden düzenlenme, Çapraz bağlanma, Reoloji*

TABLE OF CONTENTS

LIST OF FIGURES

LIST OF TABLES

CHAPTER 1

INTRODUCTION

1.1. Hydrogels

Hydrogels are viscoelastic materials with three-dimensional network structures constituted by polymeric or oligomeric chains. The hydrogels can be obtained mainly by physical and chemical crosslinking processes (Peppas et al., 2000). Chemically crosslinked hydrogels are solid-like and generally exhibit Newtonian behavior with extremely high viscosity may be higher than 105 Pa.s and more than 2000 Pa with high elasticity (Y. Chen, 2020). Hydrogels are characterized by high water swelling characteristics, which can be tuned by the structure and the composition of the precursor(s). The main application area of the hydrogels include drug delivery, tissue engineering, wound healing, cell encapsulation, biosensors, and contact lenses (Y. Cao et al., 2019; Kim et al., 2017; Lloyd et al., 2001; T.-Y. Lu et al., 2020; Varaprasad et al., 2015; J. Yang et al., 2021).

Hydrogels have many classifications. Firstly, according to their sources, hydrogels can be divided into two groups, natural and synthetic hydrogels. Natural hydrogels are obtained from biocompatible and biodegradable natural polymers such as collagen, gelatin, hyaluronic acid, fibrin, sodium alginate, agarose, and chitosan (Dang & Leong, 2006; George et al., 2019; Ishihara et al., 2019; Sionkowska, 2011; Swetha et al., 2010; Xie et al., 2010).

On the other hand, synthetic polymers like polyacrylic acid, polyvinyl alcohol, and polyethylene glycol are frequently used to prepare synthetic hydrogels. Chemically crosslinked hydrogels can be obtained by the widely exploited addition or ring-opening polymerization reactions. Compared to the natural-based hydrogels, the synthetic ones can be equipped with desired functional groups without post-modification steps and can be tailored easily to tune their physicochemical properties. However, the biocompatibility and bioactivity of physical hydrogels are the primary concern of synthetic hydrogels.

Secondly, the hydrogels are classified as physically crosslinked and chemically crosslinked hydrogels based on the formation mechanism of their three-dimensional

network structures. Common preparation routes of physical and chemical hydrogels are given in Figure 1.1. Chemically crosslinked hydrogels, thermosetting hydrogels, or permanent gels can hardly dissolve in many solvents because their chemical hydrogel network structure is held by covalent bonds. For that reason, once they are formed, the chemical hydrogels can not be shaped again.

These covalent forces impart high mechanical stability and high order of swelling properties to the hydrogels' three-dimensional network structure, and these properties can be tuned by changing the crosslinking density. The major drawback of the chemically crosslinked hydrogels is the toxicity of the crosslinking agents and crosslinking reaction product. Also, unwanted aggregations, called clusters, can be formed because of the hydrophobic side of the chemical crosslinked agent. So, the homogeneity of chemically crosslinked hydrogels could not be well-ordered. Furthermore, the swelling would not be changed equally in the hydrogel network structure because of undesired voids and macropores.

On the other hand, the three-dimensional network structure of physically crosslinked hydrogels is constituted by the self-assembly of individual molecules. Since their network structures are held by secondary forces, like van der Waals, hydrophobic interactions, and hydrogen bonding, physical hydrogels are reversible or thermoplastic gels. These hydrogels can be triggered by external stimuli such as temperature, pH, ionic strength, and irradiation. However, physically crosslinked hydrogels generally exhibit weaker mechanical properties than chemically crosslinked hydrogels (Pakkaner et al., 2019).

Hydrogels can also be classified based on their degradation properties. The intermolecular and intramolecular bonds in the biodegradable polymer network structure can be broken by enzymes or microorganisms. In the case of hydrolytically degradable hydrogels, certain functional groups such as unhindered ester bonds are attacked by water molecules, disrupting the network structure.

Another hydrogel classification is related to their response to the environment. So-called responsive hydrogels are triggered by external stimuli, for instance, pH, temperature, and ionic strength. As a result of the change in the environment, the network structure can swell or shrink. After removing the stimulus, the hydrogel network structure restores spontaneously.

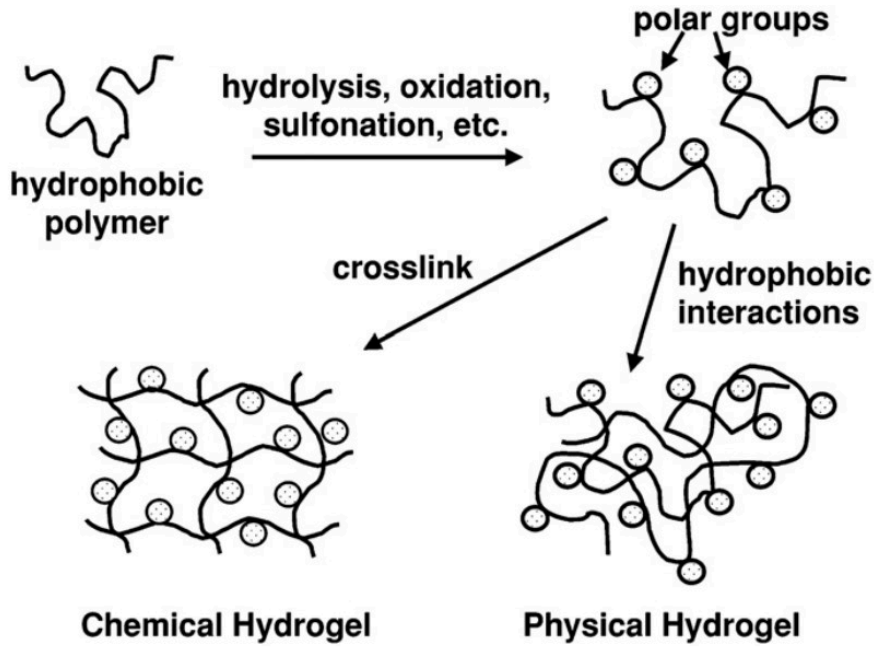

Figure 1.1. Schematic representation of chemical and physical hydrogels preparation (Source: Asif et al., 2019).

1.2. Keratin

Keratin is one of the most abundant proteins in nature, found in epithelial and epidermal appendage structures of mammals, reptiles, birds, and fishes such as hair, wool, horns, hooves, and nails (Kadirvelu & Fathima, 2016; McKittrick et al., 2012; Pakkaner et al., 2019). Keratin has high mechanical strength and stiffness and is insoluble in polar and nonpolar solvents because of intermolecular and intramolecular disulfide bonds and hydrogen bonding in its structure and high crystallinity.

Nowadays, keratin-containing biomass is produced annually million tons from the food industry, especially the wool, slaughterhouse, and meat markets. USA, Brazil, and China report that 40 million tons of keratin-containing biomass are produced annually (Sharma et al., 2019). According to the Turkish Statistical Institute data, the number of sheep and wools is about 48 million, and 76 thousand tons of wool are produced from these sheep and goats; also, the number of slaughtered poultry has been 1.2 billion last five years in Turkey (Turkish Statistical Institute, [TÜİK], 2022). Additionally, wool keratin is classified as keratin waste according to European Parliament and Council until 3rd October 2002 (Petek & Marinšek Logar, 2021).

The hierarchical structure of a wool fiber is given in Figure 1.2. The cytoskeleton of the keratins, known as intermediate filaments (IF), is constituted by α-keratins, β-keratins, and γ-keratins. β-keratins are found in the outer cuticle part and are not readily soluble. Unlike β-keratins, α-keratins are abundant in soft tissues with lower cystine content and characterized by low chemical resistance. The average molecular weight of low sulfur-containing α-keratins is between 40 kDa and 60 kDa (Duer et al., 2003). α-keratins are mainly obtained from sheep wool, hair, and skin. On the other hand, γ-keratins with high sulfur content and high tyrosine proteins, rich in glycine and tyrosine amino acids, are embedded in the microfibrils parts. The average molecular weight of high sulfur contents is between 11 kDa and 28 kDa, and that of high tyrosine proteins is between 9 kDa and 12 kDa (Gillespie, 1972; Shavandi, Silva, et al., 2017).

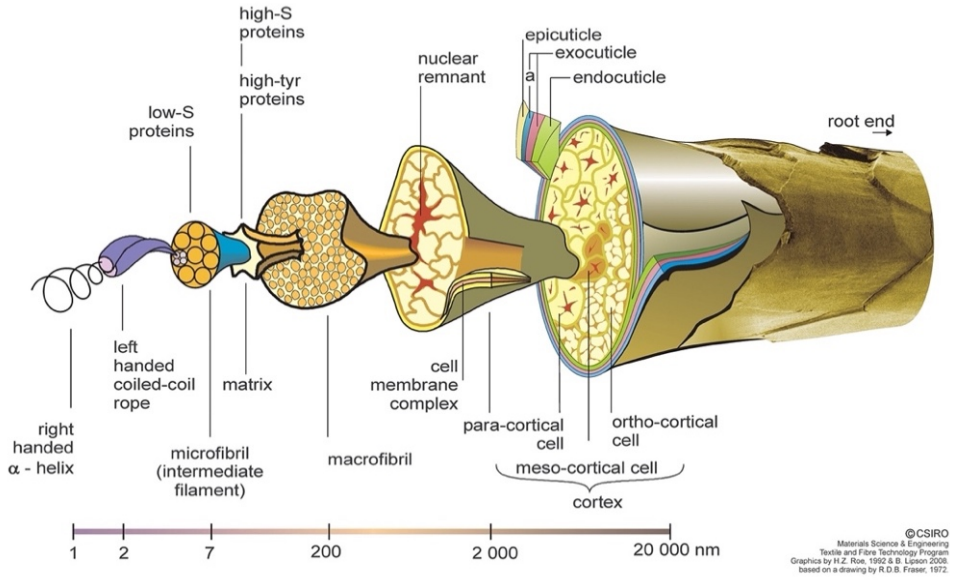

Figure 1. 2. The structure of a merino wool fiber (Source: Caven et al., 2019).

Table 1.1 shows amino acid compositions of the keratins obtained from various resources. It implies that glutamic acid, arginine, and cysteine are the primary amino acids in keratins. Wool, hair, and skin keratins are soft and flexible due to their low cystine content (between 10 and 14%). On the other hand, feathers, beaks, claws, and horns in keratins with cystine content of up to 22% are stiff, rigid, inflexible, and inextensible (Cardamone, 2010).

Table 1. 1. Amino acid composition (% of total amino acid residues) of keratin from different sources (Source: Sinkiewicz et al., 2018).

Amino acid	Buffalo horn and hoof	Cow hair	Feathers	Wool
Alanine	6.3	4.5	3.6	5.8
Arginine	6.8	11.0	5.4	7.8
Aspartic acid	6.7	6.6	4.7	4.1
Cysteine	3.7	nd	7.7	6.1
Glutamic acid	12.6	14.5	7.7	11.4
Glycine	12.3	5.5	6.2	2.9
Histidine	0.6	1.3	-	-
Isoleucine	3.0	4.2	4.3	3.9
Leucine	8.2	9.8	7.0	11.9
Lysine	2.7	5.5	0.6	2.9
Methionine	0.6	0.7	1.3	0.2
Phenylalanine	2.9	3.1	4.2	1.9
Proline	6.8	7.7	8.7	4.1
Serine	10.8	8.9	9.3	8.3
Threonine	5.6	7.5	3.5	5.6
Tyrosine	5.9	2.4	2.0	2.4
Valine	4.1	6.8	6.9	6.1

nd = not determined.

1.3. Wool

Almost half of the keratins have been extracted from wool (Reddy, 2017). Wool contains approximately 82% keratinous proteins having a high concentration of cystine, about 17% nonkeratinous proteins with a low concentration of cystine, and 1% impurities such as wool grease, dirt, and vegetable matters (Parry & Creamer, 1979; Teasdale, 1988; Zahn & Kusch, 1981). The high level of high-sulfur proteins imparts mechanical and chemical stability to the wool by forming the disulfide bonds (Figure 1.3) between cysteine amino acid residues. The amino acid sequence of wool keratin contains cell attachment motifs such as LDV (Leu-Asp-Val), EDS (Glu-Asp-Ser), and RGD (Arg-Gly-Asp) (Hill et al., 2010; Su et al., 2020). RGD constitutes the cell attachment site of fibronectin, fibrinogen, and osteopontin. On the other hand, LDV and EDS support cellular adhesion (Rajabi et al., 2020).

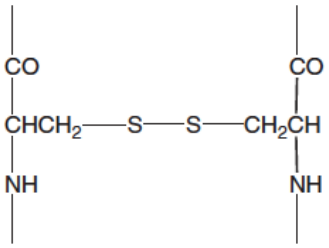

Figure 1. 3. Cystine amino acid residue structure.

Also, hydrogen bonds, hydrophobic interactions, and ionic bonds have an essential role in the stability and properties of wool (Figure 1.4). The side chains of wool contain nearly equal numbers of basic amino and carboxyl groups responsible for amphoteric structure (Rippon, 2013).

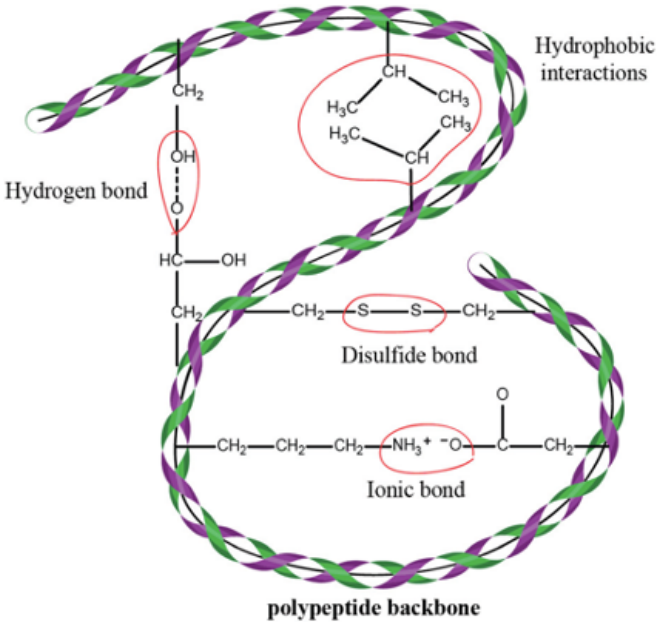

Figure 1. 4. The scheme of intermolecular and intramolecular bonding in wool keratin (Source: Shavandi, Silva, et al., 2017).

Figure 1.5 shows that wool has no net charge when the amino and the carboxyl groups are fully ionized. Thus, the ionic bonds between molecules in the wool structure depend on pH. The highest ionic bonding level is at pH 4.9 when the protein is in the fully ionized form of the amino and carboxyl groups. The carboxyl groups of keratin are protonated at low pH, and the amino groups of keratin are deprotonated at high pH. Thus,

the lowest ionic interactions are at extreme acidic or basic conditions (Rippon, 2013; Shavandi, Silva, et al., 2017).

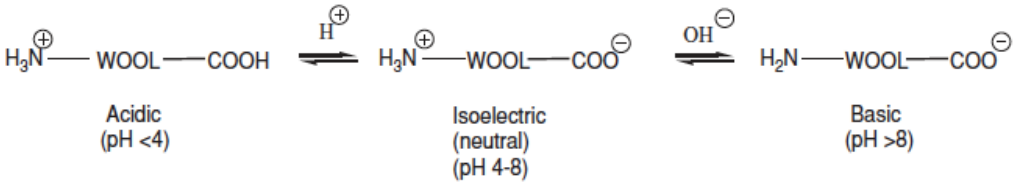

Figure 1. 5. The amphoteric structure of wool keratin (Source: Rippon, 2013).

There are many extraction methods to solubilize and isolate wool keratin, such as reduction, oxidation, microwave irradiation, alkali extraction, steam explosion, sulfitolysis, enzymatic and microbial, and ionic liquids (Costa et al., 2018; Gaidau et al., 2021; Perța-Crișan et al., 2021; Shavandi, Silva, et al., 2017; Sinkiewicz et al., 2018).

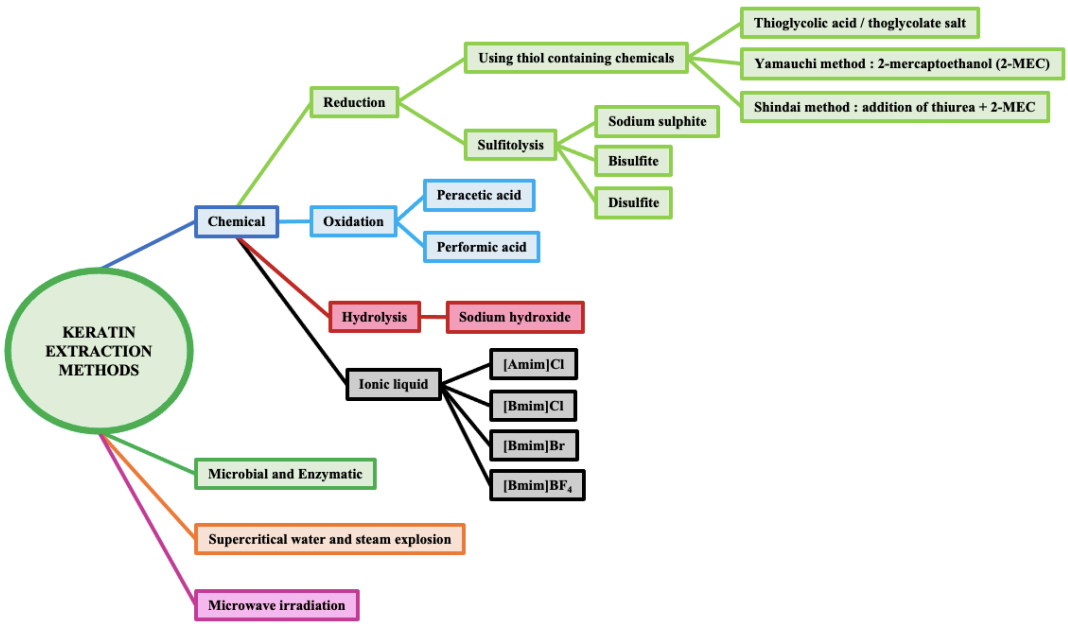

Figure 1. 6. The wool keratin extraction methods (Source: Shavandi, Silva, et al., 2017).

One of the oldest methods of extraction of wool keratin is the oxidative extraction procedure (Earland & Knight, 1955). The most popular oxidative agents are peracetic acid, hydrogen peroxide, performic acid, and potassium permanganate. They are mainly

used to extract wool or hair keratin. When the wool keratins are reacted with the oxidative agents, the disulfide bonds bridges in the protein structure are partially broken and turned into a sulfonate chemical structure (Figure 1.7). The oxidized keratins are named keratoses. Different fractions of keratoses such as α-keratose, β-keratose, and γ-keratose can be isolated according to their isoelectric points (Buchanan, 1977; Ghosh et al., 2014; Nakamura et al., 2002; Robbins, 2012; Shavandi, Silva, et al., 2017). Long extraction reaction times, a vast amount of oxidizing agents, and a low degree of extraction yield are disadvantages of the oxidative reduction of wool keratin. Examples of the oxidative extraction methods of the wool and the feather keratins are shown in Table 1.2.

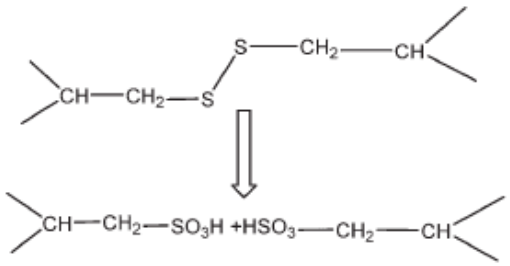

Figure 1. 7. The oxidized wool keratin structure (Source: Shavandi, Silva, et al., 2017).

On the other hand, the most stable structure of the keratin can be obtained when the disulfide bonds bridges are reduced with thiol-containing chemicals such as sodium thioglycolate, thioglycolic acid, and mercaptoethanol. After the reduction extraction process, thiol anions of the reductive agents in alkaline media form soluble keratin structures named kerateines (Figure 1.8). Urea and thiourea are the denaturants of the protein, and they are generally used to increase the water solubility of the kerateines in the reductive extraction processes. Additionally, sodium dodecyl sulfate (SDS), a surfactant, increases the rate of the keratin extraction processes and improves the stabilization of the kerateines. However, some reductive agents, such as mercaptoethanol, are toxic, harmful to the environment, and have high costs (Shavandi, Carne, et al., 2017).

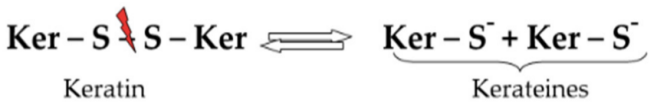

Figure 1. 8. The kerateines structure after the reductive extraction process (Source: Perța-Crișan et al., 2021).

Table 1. 2. The oxidative extraction methods of the wool keratins and the feather keratins (Table is modified by Perța-Crișan et al., (2021)).

Keratin Source	Processing Parameters		Reference
	Oxidative Agent	Conditions	
Wool	Peracetic acid 1.8% (w/v)	37 °C; overnight, 150 rpm	(Yalçın & Top, 2022)
Wool	Peracetic acid 2% (w/v)	37 °C; overnight, 150 rpm	(Pakkaner et al., 2019)
Wool	Solid sodium percarbonate 4.5% mass ratio Fiber, liquid ratio 1:35 NaOH 30%	Room temperature; 3-4 h stirring	(Brown et al., 2016)
Wool	Peracetic acid 24% Fiber, liquid ratio 1:60	2 days Room temperature Yield 57%	(Shavandi, Carne, et al., 2017)
Wool	Peracetic acid 2% Fiber, liquid ratio 1:50	25 °C; 24 h	(Rajabinejad et al., 2020)
Human hair	Performic acid (100 volume H_2O_2/98% formic acid, 1:39 v/v)	4 °C; 18 h	(Buchanan, 1977)
Human hair	Peracetic acid 2% Hair mass, liquid ratio 1:20	37 °C; 10 h, 150 rpm	(de Guzman et al., 2011)
Human hair	Peracetic acid 2.5%	Room temperature; Overnight	(Agarwal et al., 2019)
Human hair	Thioglycolic acid 0.5 M	37 °C; 15 h, pH 10.4	(Agarwal et al., 2019)

Tris (2-carboxyethyl)phosphine), TCEP, is another reductive agent less toxic than mercaptoethanol and odorless. Additionally, TCEP provides increased stability due to its high water solubility. Compared with mercaptoethanol and TCEP, sodium sulfite is an excellent reductive agent to break down sulfide bonds and obtain keratin structure at the end of the reductive extraction named sulfitolysis extraction. Sodium sulfite, bisulfite,

and disulfite are the popular chemical agents used in sulfitolysis extraction. Additionally, sodium sulfide reductive agent is primarily used as a reductive agent in industrial and laboratory scales to obtain keratin from wool (Shavandi, Silva, et al., 2017). At the end of the extraction, disulfide bond bridges are broken and transformed into cysteine thiol and S-sulfonated residues (Figure 1.9).

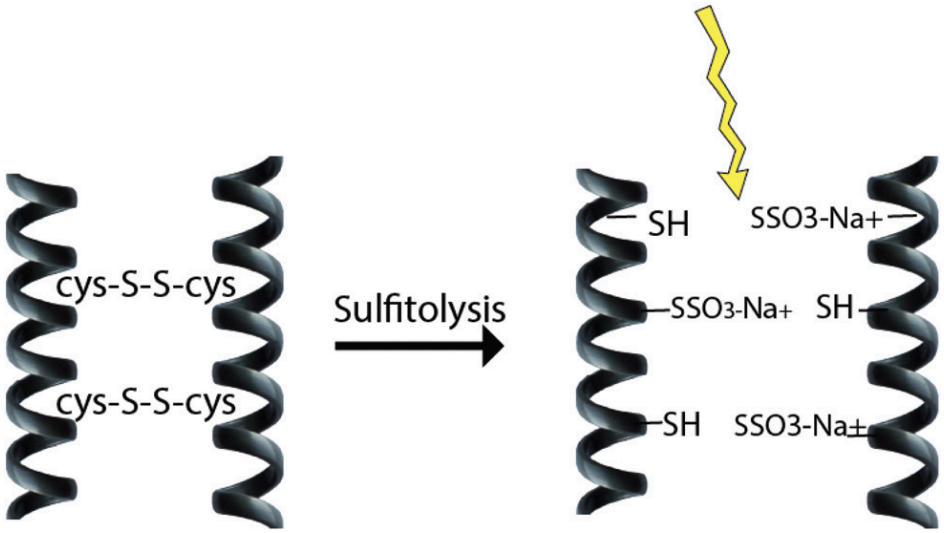

Figure 1. 9. Scheme of the sulfitolysis extraction reaction of the wool keratin (Source: Shavandi, Silva, et al., 2017)

Like mercaptoethanol extraction reaction, urea and SDS are used to improve the solubilization of the keratins in sulfitolysis extraction. Examples of the reductive and sulfitolysis extraction methods of the wool keratins, the feather keratins, and the human hair keratins are shown in Table 1.3.

Table 1. 3. The reductive and sulfitolysis extraction methods of the wool keratins, the feather, and the human hair keratins (Table is modified by Perța-Crișan et al., (2021)).

Keratin Source	**Processing Parameters**		**Reference**
	Reductive Agent	**Conditions**	
Wool	Extractive liquor: sodium sulfide 125 mM	40 °C; 4 h; 150 rpm	This study

Cont. on the next page

Cont. of Table 1.3

Wool	Extractive liquor: sodium sulfide 125 mM, HCl	40 °C; 4 h, 150 rpm, pH 4.0	This study
Wool	Extractive liquor: sodium sulfide 125 mM, urea 8 M, EDTA 3 mM	40 °C; 4 h, 150 rpm	This study
Wool	Extractive liquor: sodium sulfide 125 mM, 500 mg DTT	40 °C; 4 h, 150 rpm	This study
Wool	Extractive liquor: thiourea 2.6 M; urea 5M; 2-mercaptoethanol 5%	50 °C; 3 days; pH 8.5, 100 rpm	(Brown et al., 2016)
Wool	Extractive liquor: urea 8 M; SDS 0.25%; 2 g soidum metabisulfite Fiber to liquid ratio > 1:70	65 °C; 5 h, 120 rpm	(Brown et al., 2016)
Wool	Extractive liquor: urea 8 M; Tris 0.5 M; DTT, 0.14 M; EDTA 6 mM Fiber to liquid ratio 1:25	25 °C; 2.5 h; pH 8.6	(Rajabinejad et al., 2020)
Wool (red sheep hair)	Extractive liquor: urea 8 M; SDS 0.26 M; mercaptoethanol 1.66 M Fiber to liquid ratio 1:20	50 °C; 12 h, under shaking	(Ramya et al., 2020)
Wool	Extractive liquor: urea 7 M, thiourea 2 M, Tris 50 mM, TCEP 50 mM Fiber to liquid ratio 10:1	18 h, pH 4.3	(Deb-Choudhury et al., 2016)
Wool	Extractive liquor: urea 8 M, 75 g SDS, 150 g sodium disulfite.	100 °C; 30 min	(Park et al., 2015)
Wool	Extractive liquor: urea 8M, SDS 0.2 M, sodium metabisulfite 0.5 M.	95 °C	(G. Yang et al., 2018)

Cont. on the next page

Cont. of Table 1.3

Feathers	Extractive liquor: sodium sulfite 0.5 M Fiber to liquid ratio 1:20	40 °C; 6 h mixing	(Pourjavaheri et al., 2019)
Feathers	Extractive liquor: sodium sulfide 10g/L, urea 9 M, SDS 10 g/L	30 °C; 130 rpm	(Poole et al., 2011)
Feathers	Extractive liquor: sodium hydroxide 1.78%; sodium bisulfite 0.5% Fiber to liquid ratio 1:5	87 °C; 111 min Yield 68.2	(Fagbemi et al., 2020)
Human hair	Extractive liquor: urea 5 M, Tris-HCl 25 mM, β-mercaptoethanol 5%, thiourea 2.6 M	50 °C; 72 h	(Lin et al., 2019)
Human hair	Extractive liquor: soidum sulfide 0.125 M	40 °C; 2 h	(Yue et al., 2018)
Human hair	Extractive liquor: Tris-HCl 25 mM pH 8.5, thiourea 2.6 M, urea 5 M, 2-mercaptoethanol 5%	50 °C; 1-3 day	(Nakamura et al., 2002)
Human hair	Extractive liquor: Tris-HCl 25 mM pH 9.5, urea 8 M, 2-mercaptoethanol 5%	50 °C; 1-3 day	(Nakamura et al., 2002)

The third keratin extraction method is alkaline extraction, in which hot concentrated alkaline solutions break peptide bonds and cystine disulfide bonds (Bertini et al., 2013; Blackburn & Lee, 1956). After the bonds rupture, soluble fractions are formed. However, the strong odor of alkaline sulfide is a problem. Additionally, high amounts of alkali reagents are required in this extraction method. Neutralization and precipitation of the solubilized keratin fraction require high amounts of acids (X. Wang

et al., 2021). Examples of the alkaline extraction methods of the wool keratins are shown in Table 1.4.

Table 1. 4. The alkaline extraction methods of the wool keratins (Table is modified by Perța-Crișan et al., (2021)).

Keratin Source	**Processing Parameters**		**Reference**
	Extracting Solution	**Conditions**	
Wool	KOH; CaO 5% 10% 15%	140 °C/170°C/1 h	(Bhavsar et al., 2017)
Wool (red sheep hair)	Extractive liquor: NaOH 0.5 N Fiber to liquid ratio 1:20	60°C; 3 h	(Ramya et al., 2020)

The fourth wool keratin extraction method is based on the use of ionic liquids (ILs). Low melting point (below 100°C) salt groups composed of an organic cation and some organic or inorganic anions are used in ILs extraction (Fernández et al., 2008; Gough et al., 2020; Leitner, 2004). ILs show some unique properties. For example, they have chemical and thermal stability, low volatility, high solvation, and non-flammability. They are miscible with other solvents and environmentally friendly. For these reasons ILs are used in a wide range of areas, such as extraction of biomass or organic synthesis and electrochemistry and as ion conductive media and catalysts (D. Han & Row, 2010; Isik et al., 2014; Sowmiah et al., 2009). 1-allyl-3-methylimidazolium chloride [AMIM]Cl, 1-Ethyl-3-methylimidazolium chloride [EMIM]Cl, 1-butyl-3-methylimidazolium chloride [BMIM]Cl, 1-allyl-3-methylimidazoliumdicyanamide [AMIM][dca], 1-Ethyl-1,5-diazabicyclo-non-5-enium diethyl phosphate [DBNE]DEP, and 1-methyl-1,5-diazabicyclo[4.3.0]non-5-enium dimethyl phosphate ([DBNM]DMP) are mostly used as ILs in these kinds of applications (Chaitanya Reddy et al., 2021; Gough et al., 2020; Ventura et al., 2017). The temperature is the most important parameter in the ILs extraction. The dissolution process is improved when the temperature increases by providing higher mobility for ions due to lower viscosity. However, the high temperature may damage the structure of the keratin. Thus, there should be a compromise between the extraction yield and temperature to avoid damaging

the protein structure (Ghosh et al., 2014). Examples of the ILs extraction methods of the wool keratins and the feather keratins are shown in Table 1.5.

Table 1. 5. The ionic liquids (ILS) extraction methods of the wool keratins, the feather, and the human hair keratins (Table is modified by Perța-Crișan et al., (2021)).

Keratin Source	**Processing Parameters**		**Reference**
	Extracting Solution	**Conditions**	
Wool	[DBNE]DEP Solid, liquid ratio: 8 wt%	120°C, 3h Yield: 0.447 g/g	(X. Liu et al., 2017)
Wool	[DBNM]DMP Solid, liquid ratio: 8 wt%	120°C, 3.5 h Yield: 0.4 g/g	(X. Liu et al., 2017)
Wool	[Amim]Cl	130°C, 10 h Solubility: 8 wt %	(H. Xie et al., 2005)
Wool	[Amim]Cl	130°C, 640 min Solubility: 21 wt%	(Li & Wang, 2013)
Wool	[Amim]Cl	130°C Solubility: 10 wt%	(Idris et al., 2014)
Wool	[Amim][dca]	130°C Solubility: 23 wt%	(Idris et al., 2014)
Wool	[Bmim]Br	130°C, 10 h Solubility: 2 wt%	(H. Xie et al., 2005)
Wool	[Bmim]Cl	100°C, 10 h Solubility: 4 wt%	(H. Xie et al., 2005)
Wool	[Bmim]Cl	130°C, 10 h Solubility: 11 wt%	(H. Xie et al., 2005)
Wool	[Bmim]Cl	130°C, 535 min Solubility: 15 wt%	(Li & Wang, 2013)
Wool	[Bmim]Cl Solid, liquid ratio: 1:6	120°C, 30 min Yield: 57%	(Ghosh et al., 2014)

Cont. on the next page

Cont. of Table 1.5

Wool	[Bmim]Cl Solid, liquid ratio: 1:6	150ºC, 30 min Yield: 35%	(Ghosh et al., 2014)
Wool	[Bmim]Cl Solid, liquid ratio: 1:6	180ºC, 30 min Yield: 18%	(Ghosh et al., 2014)
Wool	[Bmim]Cl	130ºC Solubility: 12 wt%	(Idris et al., 2014)
Wool	[Bmim]BF_4	130ºC, 24 h Insoluble	(H. Xie et al., 2005)
Wool	[Choline][thioglycolate]	130ºC Solubility: 11 wt%	(Idris et al., 2014)
Feathers	[Amim]Cl Solid, liquid ratio: 1:2	130ºC; 10 h Solubility: 50 wt% Yield: 60%	(Idris et al., 2014)
Feathers	[Amim]Cl + 10% wt Na_2SO_3 Solid, liquid ratio: 1:20	90ºC; 1 h Solubility: 4.8 wt%	(Ji et al., 2014)
Feathers	[Bmim]Cl Solid, liquid ratio: 1:2	130ºC; 10 h Solubility: 50 wt% Yield: 60%	(Idris et al., 2014)
Feathers	[Bmim]Cl 500 mg in 20 g	130ºC; 2 h	(Azmi et al., 2018)
Feathers	[Bmim]Cl	100ºC; 48 h Solubility: 23 wt%	(P. Sun et al., 2009)
Feathers	[Bmim]Cl + 10% wt Na_2SO_3 Solid, liquid ratio: 1:20	90ºC; 1 h Solubility: 4.8 wt%	(Ji et al., 2014)
Feathers	[Bmim]Cl: dimethylsulfoxide mixture 35:65 500 mg in 20 g Ultrasonic treatment: 200 W	52 min	(Azmi et al., 2018)
Feathers	[Bmim]Cl 500 mg in 20 g Ultrasonic treatment: 200 W	20 min	(Azmi et al., 2018)

Cont. on the next page

Cont. of Table 1.5

Feathers	[Bmim]Br + 10% wt Na_2SO_3 Solid, liquid ratio: 1:20	90°C; 1 h Solubility: 4.2 wt%	(Ji et al., 2014)
Feathers	[Bmim]NO_3 + 10% wt Na_2SO_3 Solid, liquid ratio: 1:20	90°C; 1 h Solubility: 4.2 wt%	(Ji et al., 2014)
Feathers	[Bmim]HSO_4 + 10% wt Na_2SO_3 Solid, liquid ratio: 1:20	90°C; 1 h Solubility: 4.1 wt%	(Ji et al., 2014)
Feathers	[HOEMIm][NTf2] + 1.0 g $NaHSO_3$ Solid, liquid ratio: 1:45	80°C; 4 h Yield: 21.75%	(Y.-X. Wang & Cao, 2012)

The fifth group of the extraction method is enzymatic and microbial procedures. Unfortunately, the wool keratins are not completely bio-degraded by using enzymatic and microbial treatments because of disulfide bonds and hydrophobic interactions in the wool keratin protein structure (Feroz et al., 2020). Bacteria, actinomycetes, and fungi are used in microbial extraction to produce keratinase residues. Enzymes can also hydrolyze the wool keratin structure and produce soluble wool keratin proteins (Holkar et al., 2018; Korniłłowicz-Kowalska & Bohacz, 2011). Compared with chemical extraction methods, enzymatic extraction can consume lower energy and have mild treatment conditions (Brandelli, 2008). Keratinases belong to neutral or alkaline enzyme groups, and their optimum activities are at pH 6.0 and 9.0 values (de Oliveira Martinez et al., 2020; Gupta & Ramnani, 2006). The optimum process temperature interval is between 45°C and 60°C (Purchase, 2016). Thus, enzymatic and microbial extractions are green, environmentally friendly methods and do not damage the wool keratin protein structure under extraction conditions (Brandelli, 2008; Gupta & Ramnani, 2006; Onifade et al., 1998). Furthermore, keratinases are used in many areas such as cleaning and treatment of obstruction in sewage systems, cleaning of wool, and finishing of textiles (Brandelli et al., 2015; Chaturvedi et al., 2014; Saleem et al., 2012). Examples of the enzymatic and microbial extraction methods of the wool keratins, feather keratins, and human hair keratins are shown in Table 1.6.

Table 1. 6. The enzymatic and microbial extraction methods of the wool keratins, the feather, and the human hair keratins (Table is modified by Perța-Crișan et al., (2021)).

Microorganism	Substrate	Degradation Condition		Reference
		pH	Temp. (°C)	
Bacillaceae				
Bacillus subtilis	Feathers, human hair	9	50	(Villa et al., 2013)
Bacillus cereus Wu2	Feathers	7	30	(Lo et al., 2012)
Bacillus sp. MTS	Chicken feathers	8-12 (8-10)	35 (40-70)	(Rahayu et al., 2012)
Bacillus amyloliquefaciens 6B	Feathers	8	50	(Bose et al., 2014)
Bacillus pumilus	Bovine hair	8	35	(Kumar et al., 2007)
Bacillus safensis LAU 13	Feathers	7.5	40	(Lateef et al., 2015)
Brevibacillus brevis US575	Feathers, hair	8	55	(Jaouadi et al., 2013)
Kocuria rosea	Feathers	-	40	(Vidal et al., 2000)
Gram negative bacteria				
Meiothermus sp. 140	Feathers, wool, hair	8	70	(Kuo et al., 2012)
Stenotrophomonas maltophilia BBE11-1	Feathers, wool	9 (7-11)	40-60	(Fang et al., 2013)
Chryseobacterium sp. P1-3	Feather meal			(Hong et al., 2015)
Chryseobacterium sp. Strain kr6	Feathers	8	30	(Riffel et al., 2003)
Lysobacter NCIMB 9497	Feathers	7.5	50	(Allpress et al., 2002)

Cont. on the next page

Cont. of Table 1.6

Actinobacteria				
Streptomyces gulbargensi	Feathers	8 (7-9)	45 (30-60)	(Syed et al., 2009)
Aphanoascus fulvescens *Chrysosporium articulatum*	Feathers	7.5	28.7	(Bohacz, 2017)
Fungi				
Aspergillus niger	Feathers, human hair, sheep's wool	5	-	(Mazotto et al., 2013)
Aspergillus fumigatus	Feathers	9	45	(Santos et al., 1996)
Purpureocillium lilacinum	Hair	6 (4-9)	60 (20-65)	(Cavello et al., 2013)
Trichopyton sp. HA-2	Chicken feathers	8	35	(Anbu et al., 2008)
Trichoderma asperellum, *Trichoderma atroviridae*	Feathers	7.5	26	(Calin et al., 2019)
Fusarium sp. 1A	Horse hair	7.5	27	(Călin et al., 2017)
Doratomyces microsporus	Feathers	8-9	50	(Gradišar et al., 2000)

Another wool extraction is the superheated water and steam explosion method. Steam flash explosion (SFE) extraction is a green hydrolysis process to produce bio-based materials. Temperature, resistance time, particle size, and moisture content of the wool affect the yield of the SFE extraction process (Sánchez & Cardona, 2008; X. F. Sun et al., 2005). In the SFE extraction process, high temperature saturated steam (180–240^{o}C) under pressure (1–3.5 MPa) are used for a short timeframe (Chaitanya Reddy et al., 2021). The SFE method improves digestibility and solubility of the products with fast processing time, but cysteine residues are destroyed during the process. This process also yields low product quality (Miyamoto et al., 1982; Shavandi, Silva, et al., 2017; Tonin et al., 2006; W. Zhao et al., 2012). For example, an unwanted product, lanthionine, is formed through crosslinking between cysteine and lysine residues. Additionally, the

keratin is degraded into oligopeptides by water under high temperature and pressure. Compared with alkaline hydrolysis, the superheated water extraction method is more economical and environmentally friendly. The yield of wool keratin obtained using the superheated water extraction method is similar to those of the oxidative, reductive, and sulfitolysis technique (Bhavsar et al., 2017). The main disadvantage of the superheated water extraction method is that proteins with a low molecular mass form at the end of the process, and some of the amino acids are lost (Rajabinejad et al., 2018). Nevertheless, the superheated water extraction method can be used on an industrial scale with reduced processing time and operating cost and environmentally friendly properties without using any chemicals. Examples of the superheated water and the steam explosion extraction methods of the wool keratins and the feather keratins are shown in Table 1.7.

Table 1. 7. The superheated water and the steam explosion extraction methods of the wool keratins and the feather keratins (Table is modified by Perța-Crișan et al., (2021)).

Keratin Source	**Processing Parameters**			**Reference**
	Temp. (°C)	**Pressure (MPa)**	**Time (min)**	
Wool	164.2	0.2 – 0.6	2 - 8	(Xu et al., 2006)
Wool	220	-	10	(Tonin et al., 2006)
Feathers	50	0 – 2.0	< 3	(W. Zhao et al., 2012)
Feathers	-	0.5 – 2.5	1	(Zhang et al., 2014)
Feathers	220	2.2	120	(Yin et al., 2007)
Feathers	Saturated steam	1.6	1	(Zhang et al., 2015)
Feathers	Saturated steam	1.8 – 2	1	(Guo et al., 2020)

Wool keratin can also be extracted by microwave treatment. In microwave extraction, the processing time is lowered with fast heating in the reactor (Feroz et al., 2020). In the microwave treatment extraction process, The maximum yield of the wool

keratin proteins was reported as 62%. However, extracted keratin proteins have very low molecular weights (between 3 and 8 kDa), and cysteine residues are significantly lost at higher temperatures (Zoccola et al., 2012). On the other hand, the microwave treatment extraction process provides some economic benefits with low energy consumption in industrial-scale processes compared with the SFE extraction. Examples of the microwave treatment extraction methods for the wool and the feather keratins are shown in Table 1.8.

Table 1. 8. The microwave treatment extraction methods of the wool keratins and the feather keratins (Table is modified by Shavandi et al., (2017)).

Keratin Source	Processing Parameters			Reference
	Temp. (^{o}C)	Time (min)	Yield (%)	
Wool	150 – 180	Up to 60	60	(Zoccola et al., 2012)
Wool	180	30	31	(Bertini et al., 2013; Canetti et al., 2013)
Feathers	160 – 200	20	71.83	(J. Chen et al., 2015)

1.4. Thesis Overview

The main objective of this MSc thesis is to develop keratin hydrogels from Merino sheep wool.

The contents of each chapter are described below:

i. In Chapter 2, the keratose proteins were obtained using the peracetic acid oxidization extraction method. To improve the mechanical properties of the keratose hydrogels, we used a low-cost, water-soluble, and amine-reactive crosslinking agent, tetrakis(hydroxymethyl) phosphonium chloride (THPC). The effect of the crosslinking agent on the viscoelastic and swelling properties and morphology of the keratose hydrogels was investigated. These chemically

crosslinked hydrogels were shown to support the proliferation of fibroblasts. Moreover, unlike our previous study (Pakkaner et al., 2019), Merino wool was used as the biopolymer source, and the previously used peracetic acid oxidation procedure was slightly modified. Molecular weight distribution, crystallinity, conformational, and thermal properties of the Merino wool keratoses were determined.

ii. In Chapter 3, keratin proteins were obtained by using three different sulfitolysis methods. After the appropriate method was determined, the hydrogels were prepared at 15 wt.% keratin concentration, and their viscoelastic, swelling, and morphological properties were investigated. Additionally, cytotocompatibility of the 15 wt.% keratin hydrogels was tested on L929 fibroblast cells.

iii. In Chapter 4, keratin proteins were obtained by sulfitolysis method using sodium sulfide, and the amount of free thiol groups increased by applying DTT reduction method. Then, these reactive thiol groups in the keratin protein structure reacted with 6000 Dalton PEG-$(C_2H_4\text{-mal})_2$ and 2000 Dalton PEG-$(C_2H_4\text{-mal})_2$ to form crosslinked hydrogel network structure. The effect of molecular weight of PEG-MAL on the viscoelastic and swelling properties, and morphology of the chemically crosslinked keratin hydrogels was investigated.

CHAPTER 2

NOVEL BIOPOLYMER - BASED HYDROGELS OBTAINED THROUGH CROSSLINKING OF KERATOSE PROTEINS USING TETRAKIS (HYDROXYMETHYL) PHOSPHONIUM CHLORIDE

2.1. Introduction

Keratin is a family of fibrous proteins that constitute bulk of cytoplasmic epithelia and epidermal appendageal structures of birds, reptiles, and mammalians such as hair, wool, horns, hooves, and nails (Kadirvelu & Fathima, 2016; Pakkaner et al., 2019; Rouse & van Dyke, 2010). Inter- and intra-chain disulfide bonds play important role in the mechanical integrity of the keratins but these crosslinks also lower the solubility of these proteins (Rajabi et al., 2020; Shavandi, Silva, et al., 2017). Various extraction techniques such as reduction (Fernández-d'Arlas, 2018), oxidation (Potter & van Dyke, 2018), sulfitolysis (Aluigi et al., 2008), alkali hydrolysis (Fagbemi et al., 2020), enzymatic hydrolysis (Su et al., 2020), ionic liquid treatment (Ji et al., 2014), microwave irradiation (Rodríguez-Clavel et al., 2019), and steam explosion (Zhang et al., 2015) have been used to solubilize keratins. Ionic liquid, microwave irradiation and steam explosion assisted solubilization methods require extreme processing conditions. Alkali hydrolysis and enzymatic hydrolysis cleave peptide bonds and, hence, degrade keratin structures whereas much more intact keratin proteins can be obtained via reduction, oxidation, and sulfitolysis processes (Pourjavaheri et al., 2019; Shavandi, Silva, et al., 2017).

Soluble keratin extracts or its blends with other polymers can be fabricated into fibers (Edwards et al., 2015), films (Tran & Mututuvari, 2015), sponges (Tachibana et al., 2006), and hydrogels (S. Wang et al., 2015) and these processed forms find many applications in the biomedical field. More specifically, there exist many reports

This chapter has been published as:
Yalçın D. & Top A. (2022). Novel biopolymer-based hydrogels obtained through crosslinking of keratose proteins using tetrakis (hydroxymethyl) phosphonium chloride, *Iranian Polymer Journal*, 1-11.

demonstrating the potential of keratin hydrogels in the delivery of therapeutics (Cohen et al., 2018; Saul et al., 2011; Tomblyn et al., 2016a), wound healing (Park et al., 2015; Veerasubramanian et al., 2018; J. Wang et al., 2017), nerve regeneration (Pace et al., 2013; Sierpinski et al., 2008), ossointegration of dental implants (Duncan et al., 2018), and vascular smooth muscle differentiation (Ledford et al., 2017). Most of the keratin hydrogels were prepared via oxidation of thiol groups of the reduced keratins to form disulfide linkages (Y. Cao et al., 2019; M. Chen et al., 2021; Esparza et al., 2018; Ham et al., 2016; J. Wang et al., 2017). Modification of the parent keratin proteins used in these hydrogel formulations allowed to tune the release of therapeutic molecules by controlling the erosion of the hydrogels (S. Han et al., 2015; Nakata et al., 2015). More stable hydrogels can be obtained by photocrosslinking and using chemical crosslinking agents. However, these kinds of crosslinked hydrogels were not explored as much as the keratin hydrogels prepared via the reformation of the disulfide bonds. Keratin hydrogels prepared by the photochemical reaction between thiol and norbornene groups (Yue et al., 2018), dityrosine crosslinked keratose (oxidized keratin) hydrogels formed by using ruthenium based photochemistry (Sando et al., 2010) are a few examples of photocrosslinked keratinous hydrogels. Additionally, sodium trimetaphosphate was employed as a crosslinking agent in the preparation of hydrogels composed of konjac glucomannan and keratin (Veerasubramanian et al., 2018).

We prepared self-assembled hydrogels by using keratose proteins extracted from Akkaraman sheep wool in our previous study (Pakkaner et al., 2019). In the current study, in order to improve the mechanical properties of the keratose hydrogels, we used a low cost, water soluble, and amine reactive crosslinking agent, tetrakis(hydroxymethyl) phosphonium chloride (THPC), which was introduced by Chung et al. (2012). Effect of the concentration of the crosslinking agent on the viscoelastic, swelling and morphology of the keratose hydrogels was investigated. These chemically crosslinked hydrogels were shown to support proliferation of fibroblasts. Moreover, different from our previous study, Merino wool was used as the biopolymer source and previously used peracetic acid oxidation procedure applied to solubilize keratose proteins was slightly modified. Molecular weight distribution, crystallinity, conformational, and thermal properties of the Merino wool keratoses were determined.

2.2. Experimental

2.2.1. Materials

Wool samples obtained from Karacabey Merino sheep breed were kindly provided by the Ministry of Agriculture and Forestry, Sheep Breeding Research Institute (Balıkesir, Turkey). Chloroform (Sigma-Aldrich) and methanol (Sigma-Aldrich) were used for the defatting of the wools. Peracetic acid solution (Sigma-Aldrich, 32 w % in dilute acetic acid), Tris-base (Merck), Tris-HCl (Sigma-Aldrich) and cellulose membrane dialysis tubing (Sigma-Aldrich, MWCO ~14000) were employed in the extraction and isolation of the keratoses. FT-IR grade potassium bromide was purchased from Sigma-Aldrich. Acrylamide (Sigma-Aldrich), bisacrylamide (Amresco), sodium dodecyl sulfate (Merck), ammonium persulfate (Merck), tetramethylethylenediamine (TEMED, Merck), bromophenol blue (Amresco), glycerol (Merck), 2-mercaptoethanol, PageRulerTM pre-stained protein ladder (Thermo Fisher Scientific), glycine (Amresco), coomasie brilliant blue G-250 (Merck), acetic acid (Sigma-Aldrich), methanol (Sigma-Aldrich), Tris-HCl (Sigma-Aldrich), Tris-base (ChemCruz) were employed in sodium dodecyl sulfate polyacrylamide gel electrophoresis (SDS-PAGE) analysis. 2,4,6-trinitrobenzene sulfonic acid solution (TNBSA, 5% w/v in H2O) and sodium tetraborate were obtained from Sigma-Aldrich. Sodium phosphate dibasic (Na_2HPO_4) and potassium phosphate monobasic (KH_2PO_4) purchased from Merck, NaCl (Sigma-Aldrich) and KCl (Panreac) were used in the preparation of phosphate buffer saline. Sodium hydroxide (Sigma-Aldrich) and hydrochloric acid (Merck) were used to adjust pH of the solutions. Tetrakis (hydroxy methyl) phosphonium chloride (THPC, Acros) was used as a crosslinking agent in the preparation of hydrogels. DMEM cell culture medium (high glucose), fetal bovine serum (FBS, European grade), gentamycin sulfate, 0.25% trypsin-EDTA solution and trypan blue solution (5 mg/ml) were obtained from Biological Industries. CCK-8 cell counting kit were purchased from Cayman Chemical Company.

2.2.2. Methods

2.2.2.1. Extraction of the keratose proteins

Merino sheep wools were cut, cleaned, defatted, and oxidized with peracetic acid similarly to the procedures described previously (Pakkaner et al., 2019). However, in the current study, 200 ml 1.8 w/v % peracetic acid solution was used to oxidize 5 g defatted wool. After the oxidation process, keratose proteins were extracted and isolated by following the methods used before (Pakkaner et al., 2019). Finally, the keratose samples were stored at -20^{o}C.

2.2.2.2. Characterization of the wools and the keratose

Scanning electron microscopy (SEM) was performed to monitor the morphologies of the cleaned wool and lyophilized keratose. The samples were coated with a thin layer of gold prior to the observations and an FEI Quanta 250 FEG (Oregon, USA) model instrument was used. Fourier transform infrared (FTIR) spectra of the defatted wool and the keratose were taken between 400 – 4000 cm^{-1} wavelength range by applying a scan number of 32 and a resolution of 2 cm^{-1}. The samples were prepared by using KBr pellet technique and the spectra were acquired on a Shimadzu 8400 (Tokyo, Japan) spectrophotometer. Thermogravimetric analyses (TGA) of the defatted wool and the keratose were carried out using a Shimadzu TGA-51 (Tokyo, Japan) instrument. The samples were heated from room temperature to 1000^{o}C with a heating rate of 10^{o}C/min under nitrogen flow. X-ray diffraction (XRD) experiments were conducted using a Philips PANalytical X'Pert Pro (Almelo, Netherlands) model diffractometer with an incident CuKα radiation at 1.54 Å. XRD patterns were recorded between 2θ range of 5^{o} and 80^{o} with a scan rate of 0.08 degree/s. SDS–PAGE analysis of the keratose was performed using a 4% stacking gel and 10% resolving gel on a Mini-Protein Tetra system (Bio-Rad Lab. Inc., USA). The protein sample with a concentration of 6 µg/µL was prepared in a buffer solution containing 8 M urea and 50 mM Tris at pH 8.0. The protein solution was mixed with 4x sample buffer (0.25 M Tris-HCl at pH 6.8, 40% glycerol, 0.28 M SDS, 0.008% bromophenol blue and 20% 2-mercaptoethanol) and the mixture was incubated at 90^{o}C for 10 min and 10 µL of the mixture was loaded onto the gel. The separation was performed at 100 V for 80 min and the gel was stained with coomassie

brilliant blue (R-250) solution (0.05% coomassie brilliant blue, 50% methanol and 10% acetic acid) for 1 h. Excess stain was removed by washing the gel with 12.5% acetic acid and 5% methanol solution.

2.2.2.3. Preparation of the chemically crosslinked keratose hydrogels

TNBSA (2,4,6-trinitrobenzene sulfonic acid) assay was used to determine amine content of the keratose by applying the method proposed by Snyder and Sobocinski (1975). Known amount of keratose sample was dissolved in 0.01 M sodium tetraborate solution at pH 9.3. 1 ml protein solution is mixed with 25 µL 0.03 M TNBSA solution and the mixture was incubated at room temperature for 30 min. Absorbance of the mixture at 420 nm was measured using a UV-Vis spectrophotometer (Shimadzu UV-2450, Tokyo, Japan). Amine concentration was determined using the extinction coefficient of 11.2×103 cm^{-1} M^{-1} at 420 nm (Snyder & Sobocinski, 1975). The hydrogels were prepared by crosslinking keratose containing amine functional groups (7.5 w/v %) using THCP in PBS (10 mM Na_2HPO_4, 1.8 mM KH_2PO_4, 137 mM NaCl and 2.7 mM KCl) at pH 7.4 or in deionized water at ~ pH 7.5 by simply mixing the keratose and THPC solutions at room temperature. The ratio of keratose and THPC functional groups were changed as 1:1, 1:2, and 1:4.

2.2.2.4. Characterization of the hydrogels

Oscillatory rheology tests were performed at 25°C, and by using a Thermo Fisher Scientific HAAKE MARS (Waltham, MA, USA) model rheometer equipped with a 35 mm diameter of stainless steel parallel plate. The keratose hydrogels crosslinked in PBS were placed onto the plate and, 0.5 mm gap distance was used. For the strain sweep experiments, frequency was set to 1 Hz. Frequency sweep tests were performed at 0.05% strain. Three independent measurements were taken for each set of experiment. FTIR spectra of the hydrogels recorded on the same instrument used for the wool and freeze dried keratose. 2 µL of the hydrogels crosslinked in deionized water was spread on a ZnSe window and dried in a vacuum oven at 37°C. The spectra were collected at 2 cm^{-1} resolution using 256 scans. Effect of the hydrogels on the proliferation of L929 mouse fibroblast cells was investigated using CCK-8 assay by applying the procedure reported earlier (Pakkaner et al., 2019). Absorbance values at 450 nm (A450) correlated to cell

viability were measured using Thermo Fisher Varioskan Flash microplate reader (Waltham, MA, USA). Relative proliferation rate was determined using three replicates of each hydrogel prepared in PBS. Empty tissue culture treated polystyrene (TCPS) wells were used as the control sample. Thus, relative proliferation rate was calculated by the following equation:

$$\text{Relative cell proliferation rate} = \frac{A_{450} \text{ of the hydrogel}}{A_{450} \text{ of TCPS at the end of Day 1}} \quad (2.1)$$

For swelling tests, keratose hydrogels were prepared inside the wells of a 24-well flat-bottom plate. Crosslinking reactions of the hydrogels were performed in deionized water. The hydrogel samples were lyophilized and the mass of each freeze dried sample (number of replicates = 3) was determined. Dry samples, then, were immersed in excess deionized water at room temperature and the samples swollen during specified time periods (3 h, 6 h and 24 h) were weighed after removing excess water. Swelling ratio values at time t were determined using the following equation (Y. Chen et al., 2020):

$$\text{Swelling ratio at time t} = \frac{W_t - W_d}{W_d} \quad (2.2)$$

where W_d is the initial weight of the freeze-dried sample, and W_t is the weight of the swollen hydrogel measured at time t. Pore structures of the hydrogels crosslinked in deionized water were observed using the same SEM instrument given in Section 2.2.2. The hydrogels were prepared in deionized water, frozen in liquid nitrogen, and freeze dried at -80°C. The samples were coated with gold and cross-sectionally fractured portion of the samples were investigated.

All the statistical analyses were performed using Minitab software (Minitab Inc., PA, US). $p < 0.05$ obtained in the t-test method was considered as statistically significant. Origin data analysis and graphing software (OriginLab, MA, US) was employed in the deconvolution of amide I region of FTIR spectra of the samples into optimum number of Gaussian peaks. Average pore size values of the freeze-dried hydrogels were measured using ImageJ software.

2.3. Results and Discussions

In this study, Karacabey Merino wool fibers was used as the biopolymer source. SEM pictures of the wool fibers and freeze dried extracted keratose are given in Figure A.1 a and Figure A.1 b, respectively. Figure A.1 a indicates that the fiber diameters are in the range of 17 μm to 48 μm. Average diameter of the fibers was measured to be 28 ± 7 μm, very close to that of Akkaraman sheep wool fibers (29 ± 10 μm) used in our previous study (Pakkaner et al., 2019). The fiber structure, on the other hand, collapsed after the extraction process as indicated in the SEM picture of the keratose.

Wool contains highly heterogeneous mixture of proteins with different molar masses and compositions held together by the disulfide bonds, which render wool insoluble (C Marshall & Gillespie, 1977; Shavandi, Silva, et al., 2017). Karacabey Merino wool proteins were solubilized by the peracetic acid oxidation of the disulfide bonds. Molar mass distribution of these water-soluble wool proteins was determined by SDS-PAGE analysis. Figure 2.1 shows SDS-PAGE gel image of the extracted protein sample along with the molecular weight marker. Diffusive protein bands between ~23 kDa and >170 kDa and a discrete band at about 12 kDa confirm highly polydisperse nature of the protein sample. Similar distribution was also observed in the SDS-PAGE result of another Merino wool keratose protein sample (Sando et al., 2010). Especially, a quite intense band between ~40 kDa and ~55 kDa is noticeable and this band cluster corresponds to low-sulfur content α-keratose proteins (Sando et al., 2010; Shavandi, Silva, et al., 2017). The fractions separated above 55 kDa can be attributed to the highly stable (undenatured) protein aggregates or the proteins with some uncleaved disulfide bonds (Sando et al., 2010). The diffusive band between ~20 kDa and ~40 kDa separated with relatively lower intensity and this band is likely to composed of some high sulfur content proteins (γ-keratoses) with a proposed molecular weight range between 11 and 28 kDa (Sando et al., 2010; Shavandi, Silva, et al., 2017). In our previous study, intensity of γ-keratose proteins' band cluster was observed to be higher than that of α-keratose protein band in the SDS-PAGE gel image of the oxidized Akkaraman wool proteins (Pakkaner et al., 2019). In the current study, we decreased the amount of peracetic acid in the oxidation process and obtained higher α-keratose protein fraction. Thus, it can be concluded that the amount of peracetic acid used for oxidation affects the composition of the proteins extracted. More specifically, our results indicate that increasing the amount

of peracetic acid can facilitate the extraction of high sulfur content proteins. Finally, the molecular weight of the proteins identified with the discrete band (~12 kDa) is in the range of those of the wool protein fractions rich in glycine and high tyrosine content (7.4–12.3 kDa) (Gillespie, 1972).

FTIR spectra of the defatted wool and the keratose are given in Figure 2.2 a and Figure 2.2 b, respectively. Both spectra indicate characteristic infrared bands of peptide bond including amide I (1600-1690 cm^{-1}), amide II (1480–1575 cm^{-1}), amide III (1229−1301 cm^{-1}) and amide A (~3300 cm^{-1}) bands (Kong & Yu, 2007). Amide I region in the FTIR spectrum of the keratose was deconvoluted to a single Gaussian peak with a maximum at 1658 cm^{-1} indicating that secondary structure of the Merino wool keratose is rich in α-helical conformation (Figure A.2) (Jackson & Mantsch, 1995; Ko & Yu, 2007) However, in addition to α-helical secondary structure, small amount of β-turn and β-sheet content was also revealed in the deconvoluted FTIR spectrum of the keratose used in our previous study (Pakkaner et al., 2019). In the sulfoxide region of the FTIR spectrum of the Merino wool keratose, a sharp band at 1041 cm^{-1}, a shoulder at 1075 cm^{-1} and another small shoulder at 1130 cm^{-1} were observed indicating the presence of mostly cysteic acid, small but detectable amount of cystine monoxide and cystine dioxide, respectively in the composition of the keratose (Cardamone et al., 2009; Hilterhaus-Bong & Zahn, 1987).

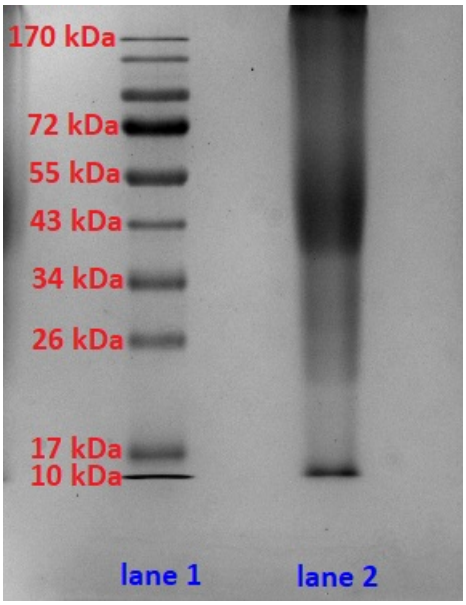

Figure 2.1. SDS-PAGE results of the extracted wool proteins. Lane 1 = protein molecular weight marker, Lane 2 = extracted wool proteins.

XRD patterns of the defatted wool and the keratose are given in Figure 2.3 a and Figure 2.3 b, respectively and were used to compare the crystallinity of these samples. Defatted wool has two broad peaks at 2Θ values of 9° and 20° in its XRD spectrum whereas these peaks disappear in that of the keratose indicating loss of crystallinity during the extraction process. The diffraction peak at 2Θ = 9° (0.98 nm) is attributed to both α-helix and β-sheet structures. Additionally, α-helix and β-sheet structures can also manifest at 2Θ = 17.8° (0.51 nm) and 2Θ = 19° (0.47 nm), respectively. Crystallinity of the regenerated wool keratins obtained from deep eutectic solvents and ionic liquids also was also reported to decrease compared to the parent wools (Idris et al., 2014; Nuutinen et al., 2019). However, intensity of the diffraction peak at 2Θ = 20° increased in the XRD spectra of the keratose used in our previous study and the regenerated wool obtained by using L-cysteine, which can be explained by the increase in the β-sheet content of these samples (Pakkaner et al., 2019; K. Wang et al., 2016). Thus, decrease in the crystallinity of the Merino wool keratose sample investigated in the current study can be attributed to the absence of β-sheet conformation as revealed by the its deconvoluted FTIR spectrum. It is also likely that the contribution of the β-sheet structures to the intensity of the XRD peaks at 2Θ values of 9° and 20° is much higher than that of the α-helices.

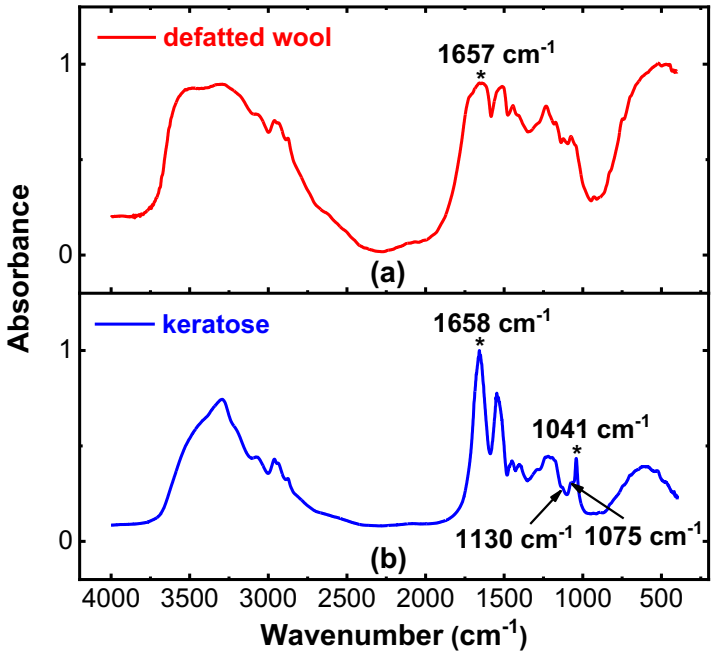

Figure 2.2. FTIR of the defatted wool and extracted keratose.

TGA and DTGA curves of the defatted wool and the keratose given in Figure A.3. The curves are similar to each other and follow the same trend as our previously investigated Akkaraman wool and keratose samples (Pakkaner et al., 2019). The first endotherm observed at ~ 82 ± 1 ºC represent the desorption of volatile components, mostly moisture. The second and the third endotherms can be due to the degradation of the side chains of the proteins and pyrolytic decomposition reactions, respectively (Kakkar et al., 2014; Rama Rao & Gupta, 1992).

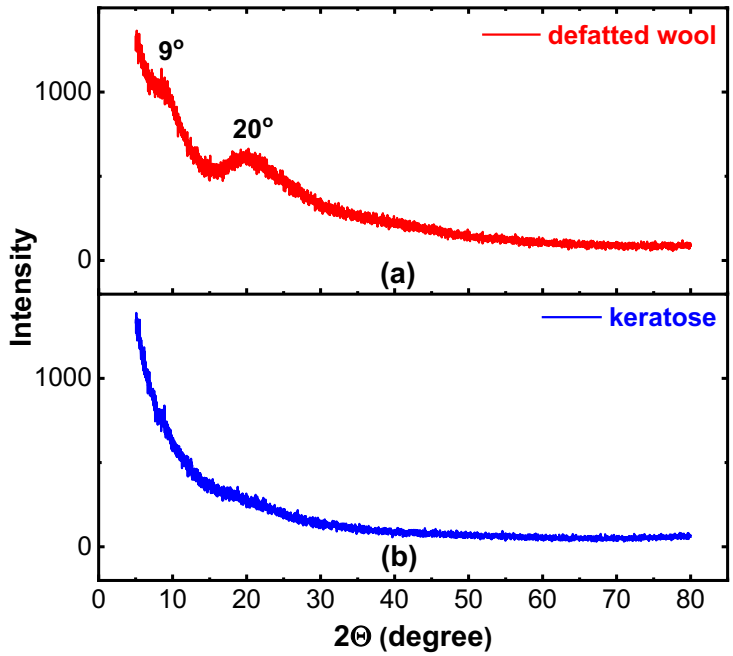

Figure 2.3. XRD of the defatted wool and extracted keratose.

Keratose samples at 7.5 w/w % concentrations were crosslinked using tetrafunctional THPC to form hydrogels. Suggested overall hydrogel formation reaction between the keratose and THPC is given in Scheme 2.1. The mechanism of the reaction between the THPC and the primary amine groups was studied by Chung et al. (2012). They proposed that first step of the reaction is the generation of formaldehyde by a hydroxymethyl arm of THPC. In the second step, amine and formaldehyde undergo a Mannich-type reaction to form immonium ion. Finally, amine coupling occurs by the reaction between phosphorous and immonium ion. Other unreacted hydroxymethyl arms follow the same reaction mechanism to crosslink different polymer chains to promote gelation (Chung et al., 2012).

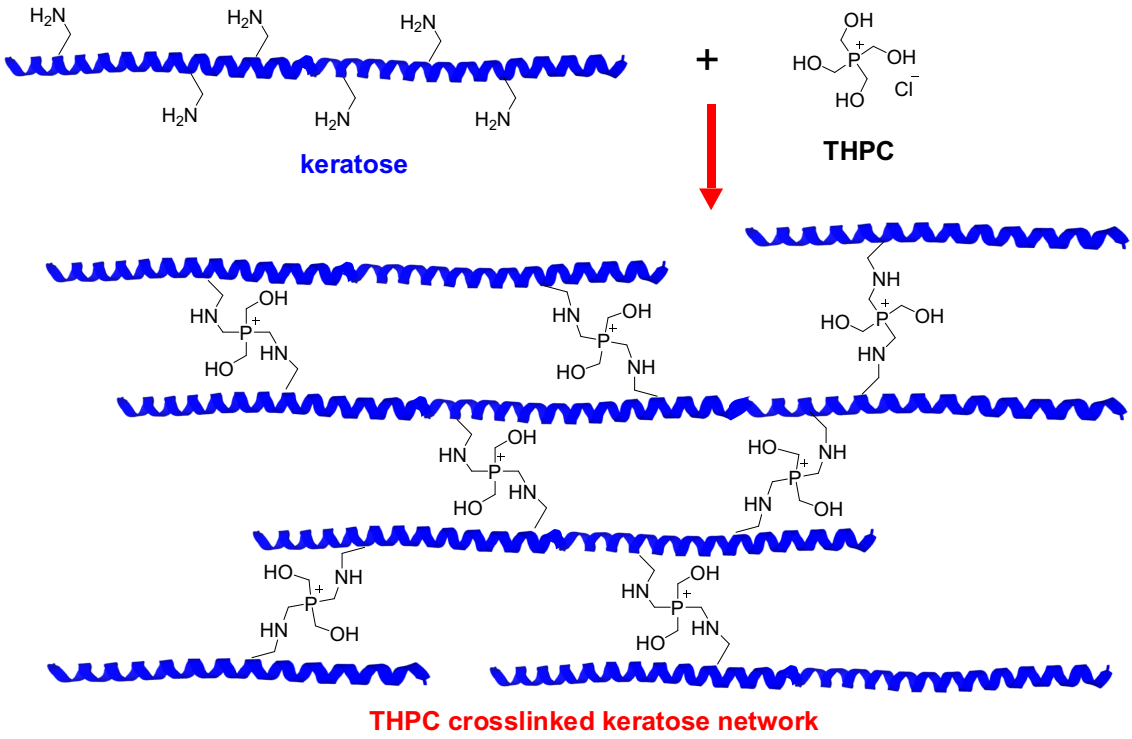

Scheme 2.1. Proposed reaction mechanism of the crosslinked hydrogel formation (Chung et al., 2012)

In the crosslinking reactions, keratose to THPC reactive group ratios were changed as 1:1, 1:2, and 1:4. Self-standing hydrogels were obtained at all three stoichiometric ratios used (Figure A.4). Mechanical properties of the hydrogels were investigated by oscillatory rheology tests. First, linear viscoelastic regions of the hydrogels were determined using strain sweep tests and the plots are given in Figure A.5. All frequency sweep experiments were performed at 0.05% strain constant value, which is within the linear viscoelastic limit (constant G' as strain is varied) (Zuidema et al., 2014).

Table 2.1. Notations and storage modules values of the crosslinked hydrogels

Notation	**keratose:THPC reactive groups ratio**	**Storage Modulus (Pa)**
1:1 gel	1:1	63 ± 22
1:2 gel	1:2	291 ± 21
1:4 gel	1:4	804 ± 53

Figure 2.4 indicates frequency sweep data of the crosslinked hydrogels. For all three samples, storage modulus (G') values are independent of frequency between 0.1 and 10 rad/s. Additionally, G' values are greater than loss modulus (G'') values verifying rigid, cross-linked viscoelastic network characteristics of the hydrogels obtained (Ham et al., 2016; Ozbas et al., 2004). Table 2.1 summarizes the G' values as a function of keratose to THPC reactive group ratio. G' values range between ~60 Pa and ~800 Pa and increase as the amount of the crosslinker increases confirming THPC joins different keratose chains together effectively rather than capping single polymer chains in this crosslinker concentration range (Chung et al., 2012).

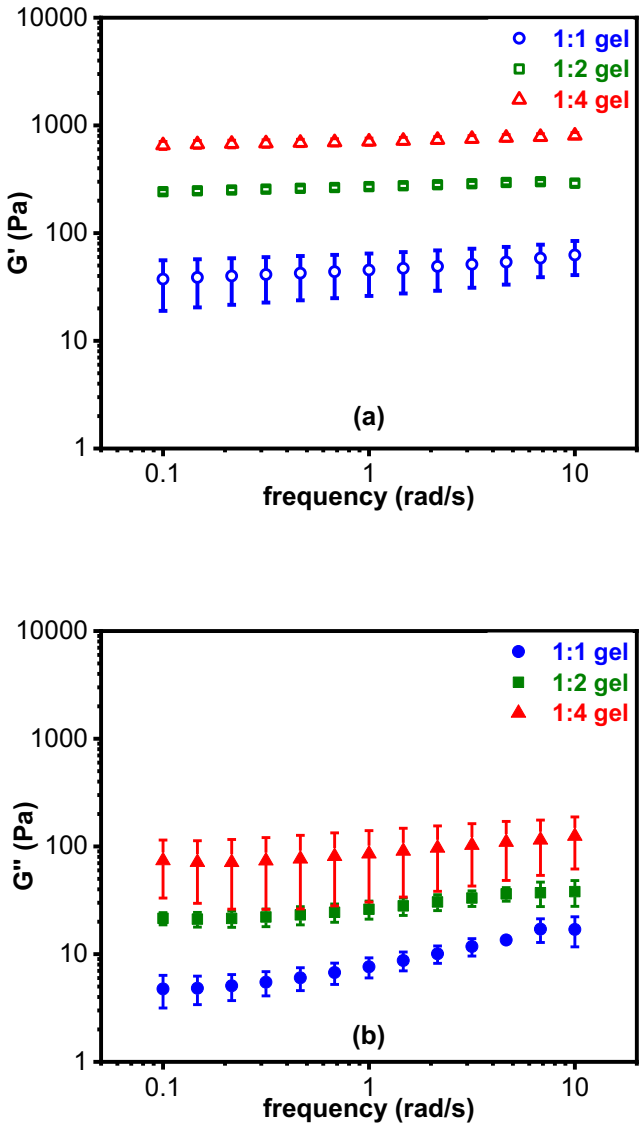

Figure 2.4. Frequency sweep data of the crosslinked hydrogels.

In our previous study, a self-assembled keratose hydrogel was prepared at physiological temperature and at 10 w% keratose concentration. Its storage modulus was measured as ~170 Pa (Pakkaner et al., 2019). Thus, in the current study, we demonstrated that it is possible to obtain keratose hydrogels with a higher mechanical strength but at a lower keratose concentration (7.5 w %) via simple chemical crosslinking procedure.

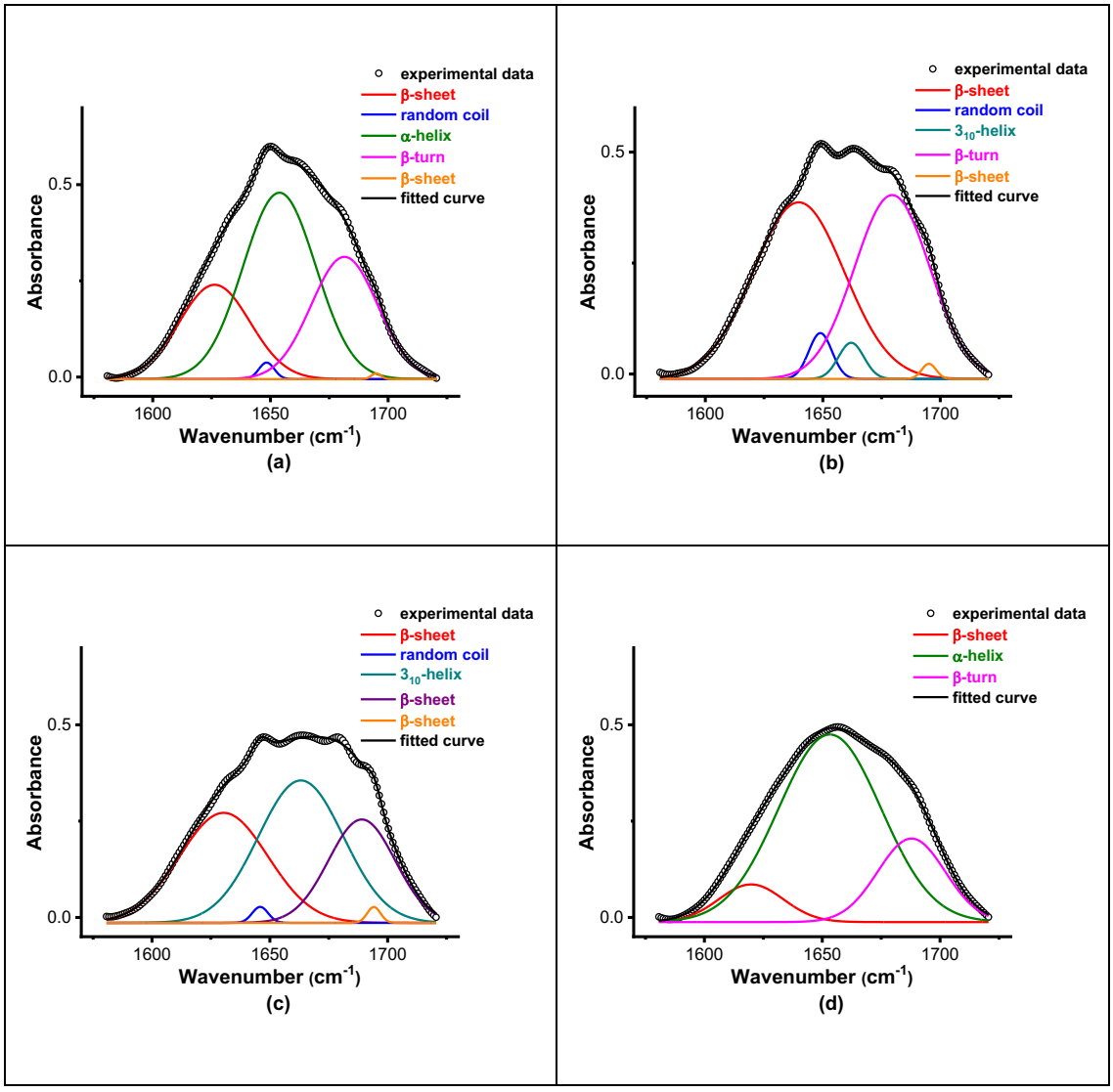

Figure 2.5. Deconvoluted FTIR spectra of (a) uncrosslinked keratose, and crosslinked keratose hydrogels prepared at (b) 1:1, (c) 1:2, and (d) 1:4 keratose:THPC reactive groups ratio.

Figure 2.5 shows the deconvoluted amide I region of FTIR spectra of the dried films of uncrosslinked keratose and the chemically crosslinked keratose hydrogels deposited on ZnSe plates. The deconvolution results and peak assignments of the samples are given in Table 2.2. Unlike the freeze-dried keratose sample, which has predominantly

α-helix structure (Figure A.2), uncrosslinked and crosslinked keratose films have some degree of β-sheet conformation as well suggesting the formation of β-sheet structures in concentrated keratose solutions (7.5 w%). Similarly, alanine-rich polypeptides also exhibited α-helix to β-sheet transformation at high concentrations (400 μM = ~ 0.3-0.6 w%) (Farmer et al., 2006; Farmer & Kiick, n.d.). However, it was also reported that secondary structure of bovine hoof derived keratin is similar both in lyophilized powder and film states and it is composed of mixture of helix and β-sheet structures (Kakkar et al., 2014). Keratose films exhibit different conformations as the crosslinking degree is changed. For example, uncrosslinked keratose film and the keratose film obtained with the highest amount of crosslinker have α-helix, β-sheet, and β-turn secondary structures. 1:2 gel film adopts appreciable amount of 3_{10} helix structure rather than α-helix structures and 1:4 gel film has the highest α-helix content. Thus, it is likely that most of the native conformation of the keratose can be preserved if crosslinking density of the keratose films is high.

Table 2.2. FTIR deconvolution results and peak assignments of the samples.

		uncrosslinked sample	1:1 gel	1:2 gel	1:4 gel
peak 1	position (nm)	1626	1640	1630	1620
	% area	23.3	50.1	33.3	8.9
	assignment	β-sheet	β-sheet	β-sheet	β-sheet
peak 2	position (nm)	1648	1649	1646	1653
	% area	0.9	3.3	0.9	70.5
	assignment	random coil	random coil	random coil	α-helix
peak 3	position (nm)	1654	1662	1663	1688
	% area	47.3	2.9	41.5	20.6
	assignment	α-helix	3_{10}-helix	3_{10}-helix	β-turn/β-sheet
peak 4	position (nm)	1681	1680	1689	
	% area	28.4	43.1	23.6	NA
	assignment	β-turn	β-turn	β-sheet	
peak 5	position (nm)	1695	1695	1694	
	% area	0.2	0.7	0.7	NA
	assignment	β-sheet	β-sheet	β-sheet	

Figure 2.6 presents cell proliferation results of the crosslinked hydrogels and empty tissue culture polystyrene (TCPS) wells. All the hydrogel samples and TCPS wells promote cell proliferation as indicated by the statistically significant differences between

relative cell proliferation rates obtained at the end of the first and the third day. Thus, these results reveal that the crosslinker (THPC) is not cytotoxic at the concentration range applied.

Chemical crosslinking is used to prepare stable and mechanically strong hydrogels, but the toxicity of the crosslinking agent and by-products of the crosslinking reaction is the primary concern. In the current study, formaldehyde evolved in the first step of the crosslinking reaction is cytotoxic at high concentrations. However, our results indicate that using THPC at low concentrations (< ~ 6 mM) renders the formaldehyde concentration below its toxicity level. Chung et al. (2012) showed that the use of millimolar concentration of THPC (~ 2.3 – 9.2 mM) did not cause significant cell death, consistent with our study (Chung et al., 2012).

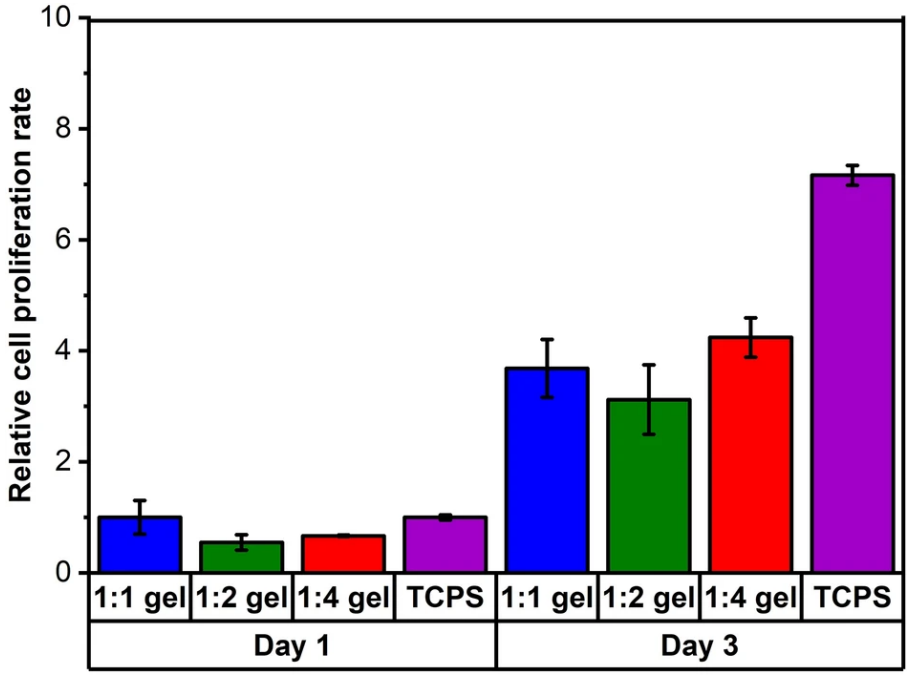

Figure 2.6. Cell proliferation results of the crosslinked hydrogels and empty TCPS wells.

Swelling ratio values of the freeze dried 1:2 and 1:4 gels swollen in deionized water are given in Figure 2.7 1:1 gel samples lost their integrity within less than 6 h. At the end of 24 h, the swelling ratios of 1:2 and 1:4 gels were determined as 69 ± 4 and 23 ± 3, respectively. Decrease in the swelling ratio with increasing crosslinking density of the network was observed in many network systems. Low solvent imbibition capacity of the highly crosslinked networks can be explained by the narrow gaps located between

crosslinking points and restricted mobility of the polymer chains (Y. Chen et al., 2020; McBath & Shipp, 2010; Suvarnapathaki et al., 2019; J. Zhao et al., 2017).

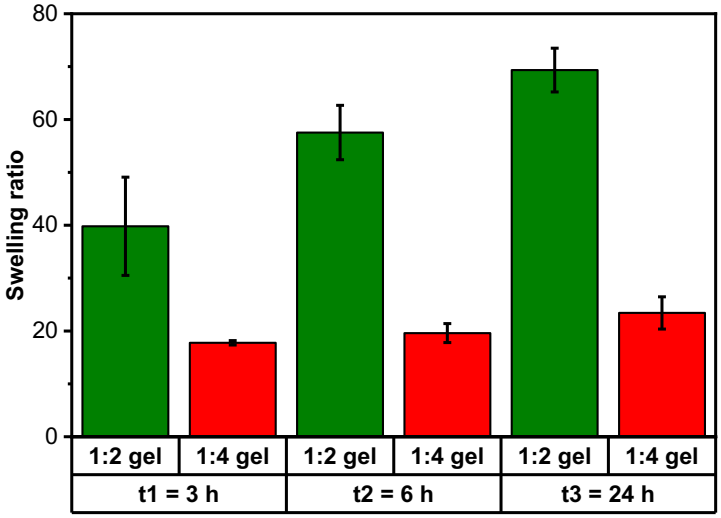

Figure 2.7. Swelling results of the freeze-dried crosslinked hydrogels.

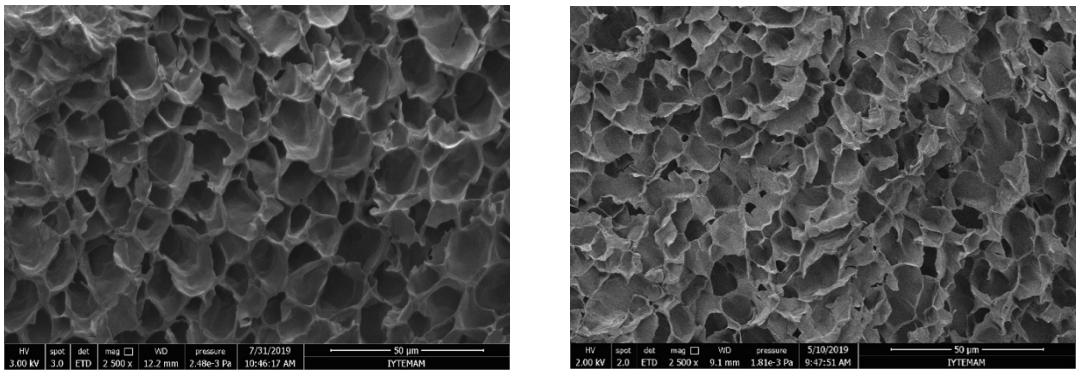

(a) (b)

Figure 2.8. SEM pictures of the freeze-dried (a) 1:2, and (b) 1:4 gels. Scale bars = 50 μm

Figure 2.8 indicates SEM images of the freeze-dried crosslinked keratose hydrogels. Porous structures are revealed in both 1:2 and 1:4 gels. However, denser network with more irregular and occasional closed pore structure resulted from its higher crosslinking density is apparent in the morphology of the 1:4 gel. Average pore size values were measured as 12 ± 3 μm and 10 ± 3 μm for the 1:2 and 1:4 gels, respectively. These values are close to those of the self-assembled keratose hydrogels investigated in

our previous study (Pakkaner et al., 2019). However, the hydrogels obtained from the mixtures of hair derived kerateine (reduced keratin) and keratose exhibited higher pore size (~20 μm) at higher biopolymer concentration (15 w%) indicating the source of biopolymer and the nature of crosslinking can alter the network characteristics of these kind of hydrogels (Ham et al., 2016).

2.4. Conclusions

Chemically crosslinked keratose hydrogels were prepared using THPC as a crosslinker. Viscoelastic properties, swelling properties and morphology of these hydrogels were shown to be tuned by changing the crosslinker amount. THPC crosslinking afforded stronger hydrogels at lower keratose concentration compared to its self-assembled counterpart prepared in our previous study. All the THPC crosslinked hydrogels supported the growth of L929 mouse fibroblasts cells with cell proliferation rates higher than those of the empty TCPS wells confirming cytocompatibility of these hydrogels. Consequently, our results suggest that THPC crosslinked keratose hydrogels can serve as low cost and efficient scaffolds in the biomedical applications as an alternative to other polymer/biopolymer-based materials.

CHAPTER 3

KERATIN BASED HYDROGELS PREPARED BY SELF ASSEMBLY & REFORMATION OF DISULFIDE LINKAGES

3.1. Introduction

Keratin is one of the most abundant proteins found in epithelial and epidermal appendage structures of mammals, reptiles, birds, and fishes such as hair, wool, horns, hooves, and nails (Kadirvelu & Fathima, 2016; McKittrick et al., 2012; Pakkaner et al., 2019). Keratin-containing biomass has been produced in the food industry, wool industry, slaughterhouse, and meat market. USA, Brazil, and China report that 40 million tons of keratin-containing biomass have been produced annually (Sharma et al., 2019). According to the Turkish Statistical Institute released data, the number of sheep and goats are about 48 million, and 76 thousand tons of wool are produced from these sheep and goats. The number of slaughtered poultry was 1.2 billion in the last five years in Turkey (Turkish Statistical Institute, [TUIK], 2022).

Almost half of the keratins can be extracted from wool (Reddy, 2017). Not surprisingly, wool keratin has been classified as keratin waste according to European Parliament and Council since 3rd October 2002 (Petek & Marinšek Logar, 2021). The high content of high-sulfur proteins imparts high strength and chemical resistance to the wool by forming the disulfide chemical crosslinked bond between cysteine residues. Thus, wool has high strength, stiffness, and it is insoluble in both polar and nonpolar solvents. There are many extraction methods to solubilize and isolate wool keratin such as reduction, oxidation, microwave irradiation, alkali extraction, steam explosion, sulfitolysis, enzymatic and microbial, and ionic liquids (Costa et al., 2018; Gaidau et al., 2021; Perța-Crișan et al., 2021; Shavandi, Silva, et al., 2017; Sinkiewicz et al., 2018). The solubilized keratins have ability to form hydrogels by self-assembly or through various crosslinking reactions.

In our previous study, keratose proteins were obtained by the oxidative extraction method, and self-assembled keratose hydrogels were prepared (Pakkaner et al., 2019). In another study, oxidized keratin (keratose) proteins and reduced keratin proteins extracted from hair were blended to form hydrogels via self assembly and reformation of disulfide bonds (Ham et al., 2016).

In the current study, keratin proteins were obtained Merino wool by using three different sulfitolysis methods. Keratins solubilized by sodium sulfide were prepared at 15 wt.% concentration and were shown to form hydrogels upon incubating at 37^{o}C. Their viscoelastic, swelling, and morphological properties were investigated. Additionally, cytocompatibility of the hydrogels were tested on L929 fibroblast cells.

3.2. Experimental

3.2.1. Materials

Wool samples obtained from Karacabey Merino sheep breed were kindly provided by the Ministry of Agriculture and Forestry, Sheep Breeding Research Institute (Balıkesir, Turkey). Chloroform (Sigma-Aldrich) and methanol (Sigma-Aldrich) were used for defatting of the Merinos wools. Sodium sulfite (Sigma-Aldrich), hydrochloric acid (HCl) (Sigma-Aldrich), urea (Sigma-Aldrich), ethylenediaminetetraacetic acid (EDTA) (Sigma-Aldrich) and cellulose membrane dialysis tubing (Sigma-Aldrich, MWCO ~14000) were employed in the extraction and isolation of the keratoses. FT-IR grade potassium bromide was purchased from Sigma-Aldrich. Sodium hydroxide (NaOH) (Sigma-Aldrich) and hydrochloric acid (HCl) (Merck) were used for adjusting pH value of the solutions. Also $NaH_2PO_4.H_2O$ (Merck) was used in the preparation of phosphate buffer saline. Acrylamide (Sigma-Aldrich), bisacrylamide (Amresco), sodium dodecyl sulfate (Merck), ammonium persulfate (Merck), tetramethylethylenediamine (TEMED, Merck), bromophenol blue (Amresco), glycerol (Merck), 2-mercaptoethanol, PageRulerTM pre-stained protein ladder (Thermo Fisher Scientific), glycine (Amresco), coomasie brilliant blue G-250 (Merck), acetic acid (Sigma-Aldrich), methanol (Sigma-Aldrich), Tris-HCl (Sigma-Aldrich), Tris-base (ChemCruz) were employed in sodium dodecyl sulfate polyacrylamide gel electrophoresis (SDS-PAGE) analysis. DMEM cell

culture medium (high glucose), fetal bovine serum (FBS, European grade), gentamycin sulfate, 0.25% trypsin-EDTA solution and trypan blue solution (5 mg/ml) were obtained from Biological Industries. CCK-8 cell counting kit were purchased from Cayman Chemical Company.

3.2.2. Methods

3.2.2.1. Cleaning and defatting of the Merino wool

In this study, keratin proteins were obtained from Merino sheep wool provided by Forestry Sheep Breeding Research Institute (Balıkesir, Turkey). The Merino sheep wool was cleaned and defatted according to the previously reported methods (Pakkaner et al., 2019; Yalçın & Top, 2022).

3.2.2.2. Extraction of the keratin proteins with sodium sulfide

1 gram defatted wools was treated with 125 mM sodium sulfide in 50 ml solution at 40^{o}C by shaking at 150 rpm for 4 h by avoiding exposure to the light. Extracted keratins were separated from the undissolved solid by using a ceramic filter. The solution was dialyzed against deionized water using a pretreated dialysis membrane tubing. Dialysis medium was changed thrice a day, and the dialysis process was carried out for 3 days. Lastly, the dialyzed keratin proteins were lyophilized and stored at -20 ^{o}C.

3.2.2.3. Extraction of the keratin proteins with sodium sulfide and HCl

1 M HCl solution was added to the keratins extracted with sodium sulfide as described above was treated until pH of solution was adjusted ~4.0. Precipitated keratins were isolated by centrifugation, then, they were dissolved in deionized water at pH 8.0. Lastly, the keratin protein solution was dialyzed against deionized water, lyophilized and stored at -20 ^{o}C.

3.2.2.4. Extraction of keratin proteins with sodium sulfide, urea and EDTA

1 gram cleaned, and defatted wool was treated with 8 M urea, 3 mM EDTA and 125 mM sodium sulfide in 50 ml solution at 40°C by shaking at 150 rpm for 4 h by avoiding exposure to the light. Solubilized keratin proteins were filtered, and pH of the keratin solution was adjusted to 8.0 with 1 M NaOH. Then, the keratin solution was dialyzed against deionized water using a pretreated dialysis membrane tubing. Dialysis medium was changed thrice a day, and the dialysis process was performed for 3 days. Lastly, the dialyzed keratin proteins were lyophilized and stored at -20 °C.

3.2.2.5. Characterization of the keratin proteins

The yield of keratin proteins from the different extraction methods was calculated using the following equation:

$$\text{Yield } \% = \left(\frac{\text{Amount of obtained keratin proteins}}{\text{Amount of initial Merino sheep wool}}\right) * 100\% \qquad (3.1)$$

DTNB (Ellman's Reagent) (5,5-dithio-bis-(2-nitrobenzoic acid)) assay was used to determine the free thiol groups of the keratin protein structures by applying the method proposed by Aitken and Learmonth (1996). Keratin proteins were dissolved in the phosphate buffer solution (0.1 M NaH_2PO_4 and 1 mM EDTA at pH 8.0) at a concentration of 1 mg/ml. Then, the keratin solution was diluted five times with 10 mM DTNB in the phosphate buffer and incubated at room temperature for 15 minutes. Absorbance of the solution was measured at 412 nm using a UV-Vis spectrophotometer (Shimadzu UV-2450, Tokyo, Japan). Free thiol content concentration was determined using the extinction coefficient of 14150 $M^{-1}cm^{-1}$ at 412 nm (Riddles et al., 1983).

Fourier transform infrared (FTIR) spectra of the secondary structure of the extracted keratin proteins with different methods were taken between 400 – 4000 cm^{-1} wavelength range by applying a scan number 32 and a resolution of 2 cm^{-1}. The samples were prepared by using KBr pellet technique and the spectra were performed by Shimadzu 8400 (Tokyo, Japan) model spectrophotometer.

Thermogravimetric analyses (TGA) of the extracted keratin proteins were carried out using a Shimadzu TGA-51 (Tokyo, Japan) type instrument. The samples were heated from room temperature to 1000 °C with a heating rate of 10 °C/min under nitrogen flow.

X-ray diffraction (XRD) experiments were conducted using a Philips PANalytical X'Pert Pro (Almelo, Netherlands) model diffractometer with an incident CuKα radiation at 1.54 Å. XRD patterns were recorded between 2θ range of 5° and 80° with a scan rate of 0.08 degree/s.

SDS-PAGE gel analysis of the keratin proteins was performed using a 4% stacking gel and 10% resolving gel on a Mini-Protein Tetra system (Bio-Rad Lab. Inc., USA). The keratin samples with a concentration of 15 µg/µL was prepared in a buffer solution containing 8 M urea and 50 mM Tris at pH 8.0. The protein solution was mixed with 4× sample buffer (0.25 M Tris-HCl at pH 6.8, 40% glycerol, 0.28 M SDS, 0.008% bromophenol blue and 20% 2-mercaptoethanol). The mixture was incubated at 90°C for 10 min and 10 µL of the mixture was loaded into the gel. The separation was performed at 100 V for 80 min and the gel was stained with coomassie brilliant blue (R-250) solution (0.05% coomassie brilliant blue, 50% methanol and 10% acetic acid) for 1 h. Excess stain was removed by washing the gel with 12.5% acetic acid and 5% methanol solution.

3.2.2.6. Preparation of the keratin hydrogels

To prepare hydrogels, aqueous solutions (PBS at pH 7.4 or deionized water) of the keratin proteins extracted with only sodium sulfide (Method NP) were prepared at 15 wt. % concentration. Then, the keratin solution was incubated at 37°C for overnight to obtain the hydrogel.

3.2.2.7. Characterization of the keratin hydrogels

Oscillatory rheology tests were performed at room temperature, and by using a Thermo Fisher Scientific HAAKE MARS (Waltham, MA, USA) model rheometer equipped with a 35 mm diameter of stainless-steel parallel plate. The protocol of rheological experiment was followed as like Chen et al. study (2017). The keratin hydrogels in PBS were placed onto the plate and, 0.5 mm gap distance was used. The time sweep experiments were performed at 0.2% strain and 1 Hz for 2 minutes to condition or recondition the hydrogels. For the frequency sweep tests, strain was set to

0.2%. After the frequency tests, the time sweep experiments were done again. Then the strain sweep experiments were performed constant frequency value at 1 Hz. After that, low strain (LVE region) and high strain (not LVE region) cyclic strain time sweep tests were conducted for 2 min and 1 min, respectively. The cyclic strain time sweep tests were repeated as 5 times. Lastly, the continuous flow test was performed using a different hydrogel sample to analyze shear-thinning behavior.

Scanning electron microscopy (SEM) was performed to monitor the pore structures of the keratin hydrogels. The hydrogels were prepared in pH 7.4 deionized water and freeze dried at -80°C. The samples were coated with a thin layer of gold prior to the observations and an FEI Quanta 250 FEG (Oregon, USA) model instrument was used. Average pore size values of the freeze-dried hydrogels were measured using ImageJ software.

Effect of the 15 wt.% keratin hydrogels on the proliferation of L929 mouse fibroblast cells was investigated using CCK-8 assay by applying the procedure reported earlier (Pakkaner et al., 2019; Yalçın & Top, 2022). Absorbance values at 450 nm (A450) correlated to cell viability were measured using Thermo Fisher Varioskan Flash microplate reader (Waltham, MA, USA). Relative proliferation rate was determined using three replicates of 15 wt.% keratin hydrogel prepared in PBS. Empty tissue culture treated polystyrene (TCPS) wells were used as the control sample. Thus, relative proliferation rate was calculated by the following equation:

$$\text{Relative cell proliferation rate} = \frac{A_{450} \text{ of the hydrogel}}{A_{450} \text{ of TCPS at the end of Day 1}} \tag{3.2}$$

For swelling test, the keratin hydrogels were prepared inside the wells of a 24-well flat-bottom plate. 15 wt.% keratin hydrogel was performed in deionized water. The hydrogel sample was lyophilized, and the mass of each freeze-dried sample (number of replicates = 3) was determined. Then dry samples were immersed in excess filtered PBS and weight of the swollen hydrogel was measured at different time intervals. Swelling ratio values at time t were determined using the following equation (Y. Chen et al., 2020):

$$\text{Swelling ratio at time t} = \frac{W_t - W_d}{W_d} \tag{3.3}$$

where W_d is the initial weight of the freeze-dried sample, and W_t is the weight of the swollen hydrogel measured at time t.

3.3. Results and Discussions

Wool contains approximately 82% keratinous proteins with high concentration of cysteine amino acids these proteins are crosslinked by disulfide bonds between cysteine residues. During the sulfitolysis process, first sodium sulfide was reacted with water to form hydrosulfide (inorganic thiol) and hydroxide ions are formed as shown in Figure 3.1. Formation of hydrosulfide and hydroxide ions increases pH of extraction solution. (D. K. Liu & Chang, 1987). Then, the disulfide bonds are broken by hydrosulfide ion, as given in Figure 3.2. After the cleavage of disulfide bonds, cysteine and perthiocysteine are formed as highly reactive protonated and deprotonated amino acid residues, respectively.

Figure 3.1. Dissolution of sodium sulfide in water and formation of hydrosulfide and hydroxide ion.

Keratin proteins were obtained from Merino sheep wool with three different sulfitolysis methods, sodium sulfide extraction method (Method NP), sodium sulfide extraction followed by HCl precipitation (Method P) and sodium sulfide, urea & EDTA extraction (Method UE).

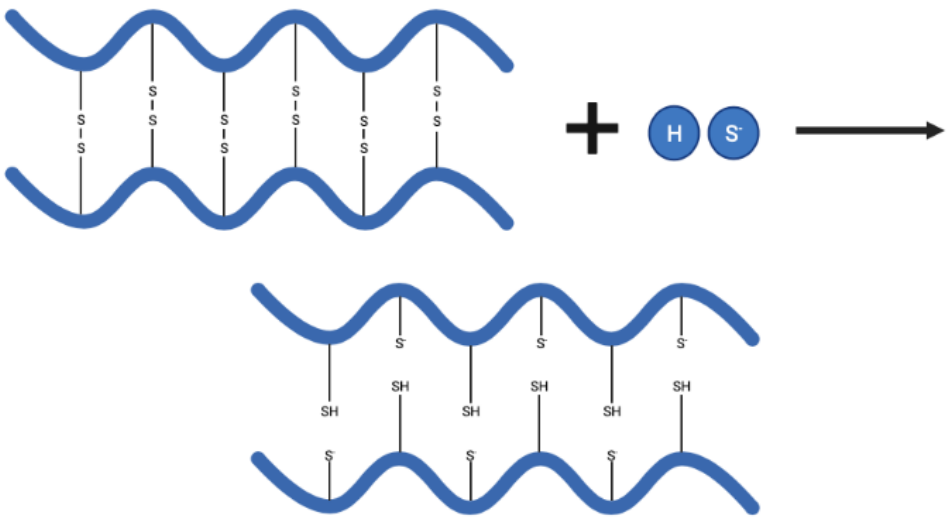

Figure 3.2. The reduction of disulfide bonds in cystine by hydrosulfide ion.

Table 3.1. The yields and the free thiol amounts obtained in different keratin extraction methods

Method	Final pH	Reduction Extraction Method	Yield (%)	Free Thiol Amounts [mmol/g keratin]
NP	11.0	Sodium sulfide	44 ± 2	0.07 ± 0.02
P	11.0	Sodium sulfide + HCl	27 ± 1	0.06 ± 0.01
UE	8.0	Sodium sulfide + Urea + EDTA	42 ± 2	0.05 ± 0.01

The yield and free thiol amounts obtained in the different keratin extraction methods are shown in Table 3.1. The yields of Method NP and Method UE are similar and higher than that of Method P. Urea was used as a denaturant to access the disulfide bonds in the intra-molecular structure of the keratin proteins during the extraction process. Thus, it was expected that using urea in the extraction would increase the yield and the amount of the free thiol amounts of Method UE. The initial pH value of Method UE was 8.0, and it was less than Method NP pH value (11.0). Thus, it is likely that high pH value of Method NP facilitates the extraction without using a denaturant. In method P, Method NP is followed by a precipitation. The isoelectronic point of α-keratin proteins is at pH 4.0. Thus, at this pH value only keratins with isoelectric point of 4 precipitated and the yield of Method P is the lowest. Similar to our study, keratin proteins from red

sheep hair were treated with extraction solution 0.125 M sodium sulfide at 40°C for 4 hours and extraction yield was calculated as 54.98 ± 0.7 % (Ramya et al., 2020). Additionally, it was also shown that as the amount of sodium sulfide increases keratin extraction yield increases (Poole et al., 2011).

The average value of the free thiol amounts was calculated as 0.06 ± 0.01 mmol SH/g keratin for all extraction methods. The free thiol amount of keratin obtained from human hair by extracted nearly similar method was determined as < 0.01 mmol/g keratin. The reason for the low free thiol content could be reformation of disulfide bonds due to the oxidization of free thiols during dialysis step (Yue et al., 2018).

Fourier transform infrared (FTIR) spectra of the extracted keratin proteins from NP, P and UE methods are given in Figure 3.3. All spectra indicated characteristic infrared bands of the peptide bond, including amide I (1600-1690 cm^{-1}), amide II (1480-1575 cm^{-1}), amide III (1229-1301 cm^{-1}), and amide A (~3300 cm^{-1}) bands (Jackson & Mantsch, 1995; Kong & Yu, 2007).

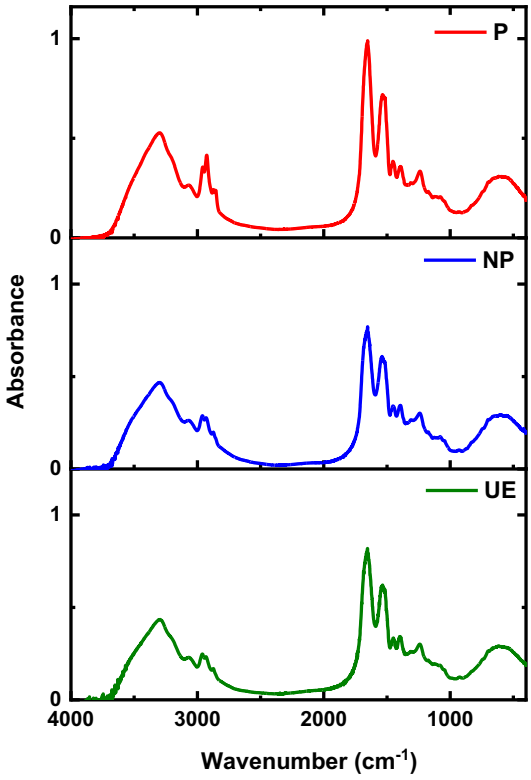

Figure 3.3. FTIR spectra of the keratin proteins obtained by different extraction methods.

X-ray diffraction (XRD) patterns of the extracted keratin proteins from NP, P and UE methods are given in Figure 3.4, and were used to compare the crystallinity of these samples. The keratins obtained by different extraction methods exhibit similar diffraction peak at $2\Theta = 20°$ which corresponds to α-helix and β-sheet structures. However, the intensity of this peak is somewhat lower for the keratin obtained in Method P. In our previous study, defatted wool had two broad peaks at 2Θ values of 9° and 20° in its XRD spectrum whereas these peaks disappear in that of the keratose indicating loss of crystallinity during the extraction process (Yalçın & Top, 2022). Similarly, the crystallinity of the regenerated wool keratin proteins obtained from deep eutectic solvents and ionic liquids also was reported to decrease compared to that of the parent wools (Idris et al., 2014; Nuutinen et al., 2019).

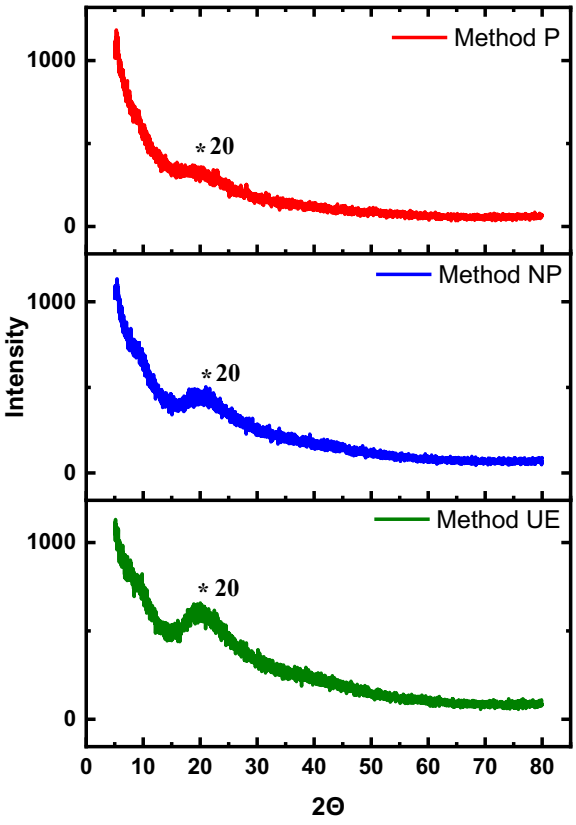

Figure 3.4. XRD patterns of the keratin extracted by different sulfitolysis methods.

Thermal behavior of the NP, P and UE methods was investigated using thermogravimetric analysis (TGA) and derivative thermogravimetric analysis (DTGA)

methods. Figure 3.5 indicates that the keratins obtained from different methods follow different degradation profiles attributed to the differences in the compositions of the keratins. However, the TG and DTG curves of Method UE are similar to the previously investigated Akkaraman wool, Merino wool and the keratose samples (Pakkaner et al., 2019; Yalçın & Top, 2022). All keratins extracted by using sulfitolysis processes exhibited three major thermal transitions by giving less than 3% residue at the end of 1000 °C. First endotherms were observed at ~95 °C, ~71 °C and ~79°C for the keratins obtained in Method NP, Method P and Method UE, respectively. The first endotherm corresponded to removal of moisture and volatile materials which constitutes ~3.61 % of the total weight of all extracted keratin proteins. The second endotherm was obtained between 310°C and 350 °C mainly indicating the degradation of the side chains of the keratin proteins (Kakkar et al., 2014; Rama Rao & Gupta, 1992). In this region, the corresponding weight losses were 33%, 25%, and 43% for the keratins extracted by Method NP, Method P, and Method UE, respectively. Similarly, ~45% weight loss associated with the second endotherm was reported for keratin proteins from a bovine hoof (Kakkar et al., 2014). However, there was a shoulder in the Method UE curve at ~300 °C which was probably due to the elimination of sulfur containing gases or other small molecules more cooperative manner. Additionally, the weight loss at this shoulder was 23.5%. The last endotherm was observed at ~944 °C for Method NP, appeared as two shoulders at ~736 °C and ~973 °C for Method P and resolved as two peaks at ~515 °C and ~575 °C for Method UE. The third endotherm can be attributed to pyrolytic decomposition reactions (Rama Rao & Gupta, 1992).

Sodium dodecyl sulfate-polyacrylamide gel electrophoresis (SDS-PAGE) analysis results of the extracted keratin proteins with the molecular weight marker are given in Figure 3.6. Molar mass of extracted keratin proteins were populated between >170 kDa and ~17 kDa as diffusive bands, and ~10 kDa as a discrete band. The SDS-PAGE results proved the highly polydisperse nature of the extracted keratin protein samples. In the SDS-PAGE analysis of the keratin extracted from another Merino wool sample similar distribution was observed (Aluigi et al., 2014). Especially, for the keratin extracted by Method P diffusive band between ~72 kDa and ~40 kDa which corresponds to low-sulfur content α-keratin proteins was quite intense compared to those of the other keratins (Sando et al., 2010; Shavandi, Silva, et al., 2017). Bands above ~55 kDa represent highly stable undenatured protein aggregates or the proteins with some uncleaved disulfide bonds (Sando et al., 2010). Second diffusive band between ~26 kDa

and ~17 kDa indicate high sulfur content proteins of γ-keratoses (Sando et al., 2010; Shavandi, Silva, et al., 2017). A discrete band at ~10 kDa is due to the wool protein fractions rich in glycine and high tyrosine content (between 7.4 kDa and 12.3 kDa) (Gillespie, 1972).

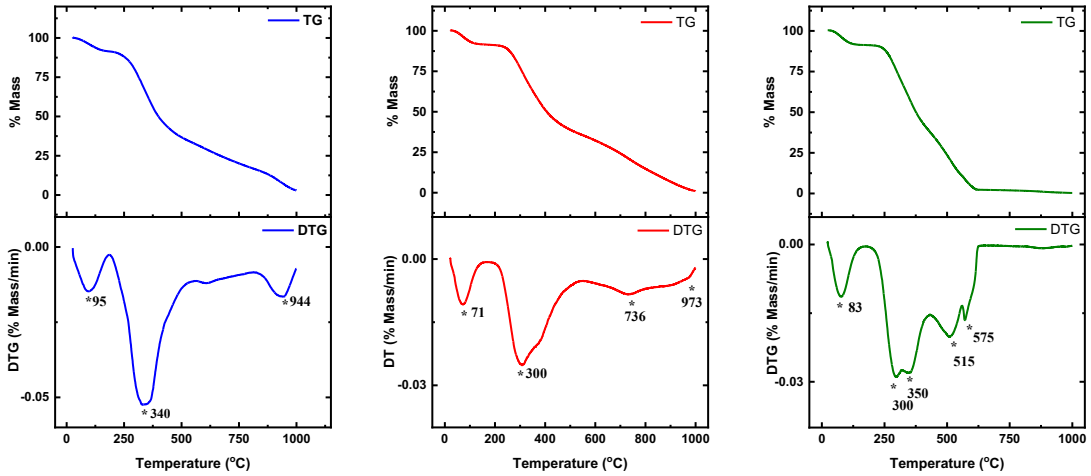

Figure 3.5. TGA and DTG of the keratins obtained by (a) Method NP, (b) Method P and (c) Method UE.

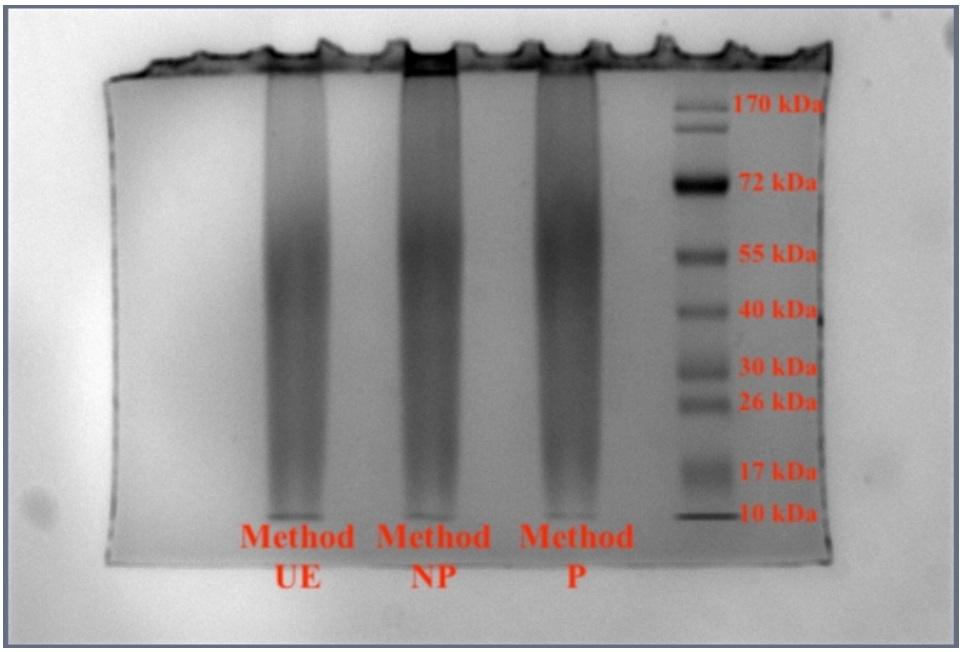

Figure 3.6. SDS-PAGE results of the extracted keratin proteins; from the left to right, lane 1 = Method UE, lane 2 = Method NP, lane 3 = Method P, and lane 4 = protein molecular weight marker.

Keratin solution prepared at 15 wt. % concentrations in PBS incubated at 37 °C for overnight formed hydrogel as given in Figure 3.7. The hydrogel formation is triggered by both self-assembly and the reformation of disulfide linkages because of the oxidation of thiols. Viscoelastic properties of the hydrogel were determined by using an oscillatory rheometer.

Figure 3.7. Picture of the 15 wt.% keratin hydrogel.

The frequency sweep tests were done between 0.1 Hz and 15 Hz at constant 0.2% strain, and the resultant curves are given in Figure 3.8. The purpose of the frequency sweep test is to determine elastic and viscous properties under constant strain. G' (storage modulus) and G" (loss modulus) give the information about the elastic and viscous response behaviors of the hydrogels. Plateau values of storage and loss moduli were obtained as 1343 ± 196 Pa, and 81 ± 8 Pa respectively. Thus, G' (storage modulus) value was obtained to be higher than G'' (loss modulus) value confirming gel-like behavior of the keratin hydrogel.

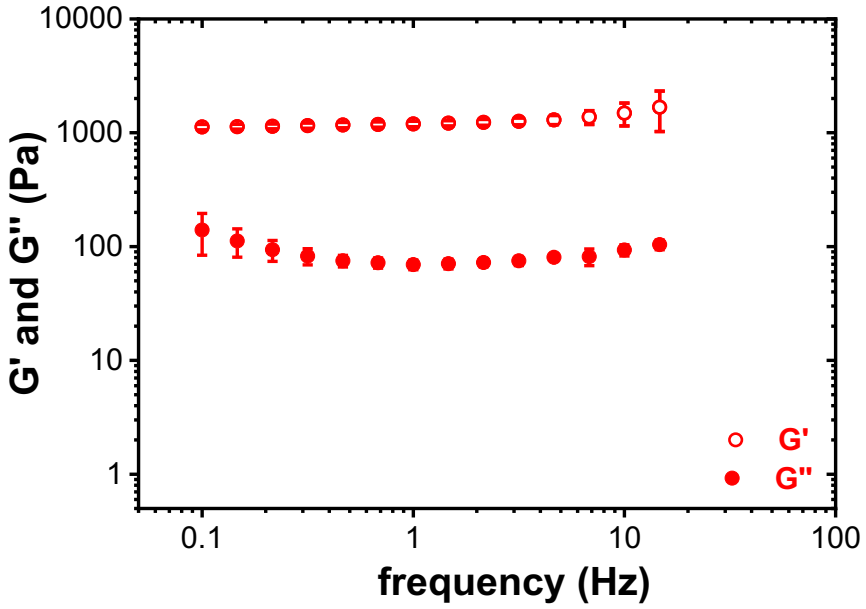

Figure 3.8. Frequency sweep data of the keratin hydrogel

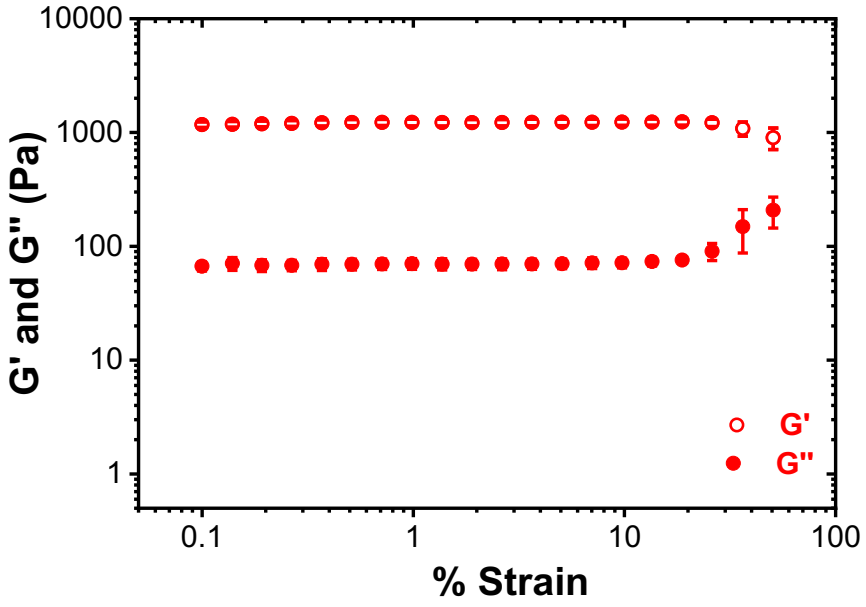

Figure 3.9. Strain sweep data of the keratin hydrogel.

Next, the strain sweep experiments were performed between 0.1% and 50% strain at a constant frequency value of 1 Hz, and the data obtained are presented in Figure 3.9. The linear viscoelastic region (LVE) was observed between 0.1% and 10%. Similar to the frequency test results, the plateau value of G' was obtained as 1218 ± 76 Pa, and 70

± 7 Pa for G'' at the LVE region. These values are much higher than the storage and loss moduli values of the self-assembled 10 wt.% keratose-based hydrogels prepared at 37 °C (Pakkaner et al., 2019). Additionally, G' and G'' values of the crosslinked keratose-based hydrogel with THPC were less than those of the 15 wt.% keratin-based hydrogels' values (Yalçın & Top, 2022). Because concentration of the keratin-based hydrogel is higher than those of the self-assembled and crosslinked keratose hydrogels. Secondly, there are small amount of thiol groups in the reduced keratins forming disulfide bonds, resulted in stiffer and stronger gel structure.

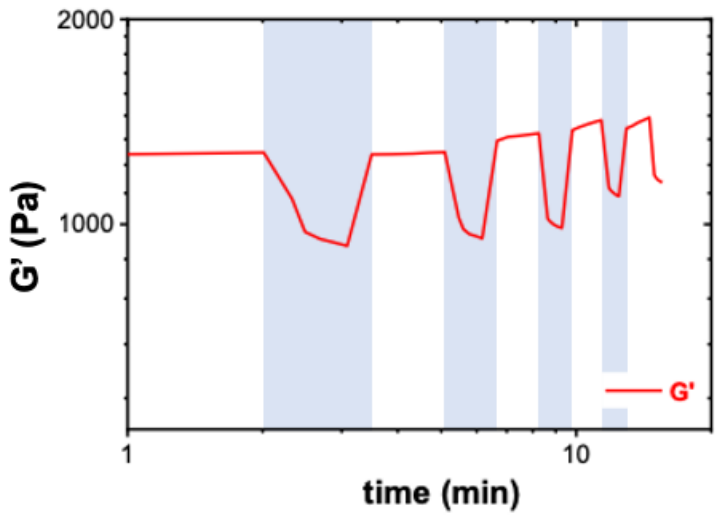

Figure 3.10. Cyclic strain time sweep data of the keratin hydrogel, shaded regions represent high strain (40%) and unshaded regions corresponds to low strain (0.2%) exposures.

The hydrogels showing shear-thinning behavior properties can be injected into the application area. In the shear-thinning behavior, viscosity decreased with increasing shear strain. Thus, shear-thinning hydrogels can be formed in the syringes, extruded from the syringe under increased shear strain thereby transforming from solid to liquid phase, and then rapidly re-form (or gel) in the injected area. The re-formation of hydrogel upon removing strain is known as self-healing. The self-healing behavior is mostly observed in the physically crosslinked hydrogels rather than in the chemically crosslinked hydrogels with some exceptions (H. D. Lu et al., 2013; Rodell et al., 2015). The self-healing nature of the keratin-based hydrogels was analyzed with the cyclic strain time sweep test.

According to the strain sweep experiment results, 40% strain (in the non-linear viscoelastic region) (1 min) and 0.2% strain value (in the for LVE region) (2 min) were selected for the liquefaction and restoration of the gel, respectively in this test. The cyclic strain time sweep test was repeated five times. The hydrogel structure was observed to restore itself up to four cycles. However, in the fifth cycle of the high strain exposure, no data was obtained due to the irreversible deformation in the hydrogel as shown in Figure 3.10. Thus, this test indicates that the 15 wt.% keratin-based hydrogel has limited self-healed nature and cannot withstand the repeated deformations in its non-linear viscoelastic region.

Due to the deformation of the hydrogel in the cyclic strain time sweep experiments, another hydrogel sample was used in the continuous flow tests. The resultant flow curve is shown in Figure 3.11. The data indicate that viscosity values increase to a certain point (shear thickening behavior) and then viscosity starts to decrease with increasing shear rate indicating a shear-thinning behavior. Thus, the 15 wt.% keratin-based hydrogel was shown to have a shear-thinning behavior if high shear rate is applied and exposure of the hydrogel to small shear rates is resulted in the stiffening of the gel.

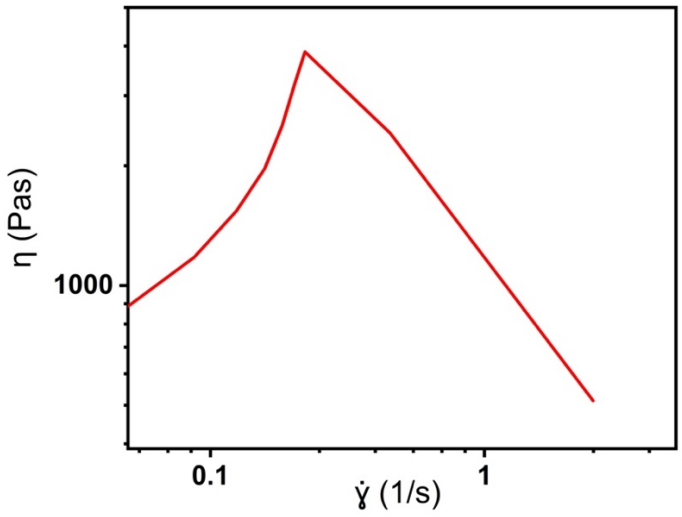

Figure 3.11. Continuous flow curve of the keratin hydrogel

For swelling test, the keratin-based hydrogels were prepared in deionized water at pH 7.4 and lyophilized. The dried hydrogel samples were immersed in excess filtered

PBS (10 mM NaH_2PO_4 and 150 mM NaCl) at pH 7.4 at room temperature and the samples swollen during specified time periods (15 min, 30 min, 45 min, 1h, 2h, 3h, 6h, 12 h, 24h, 48h, 72h, 99 h) were weighed after removing excess PBS solution. Using Equation 3.2, swelling ratios were calculated, and swelling ratio curve is shown in Figure 3.12. The keratin-based hydrogels had been maintained their integrity up to 4 days (99 h) with an average swelling ratio of 6.41 ± 0.36, which was lower than the THPC crosslinked hydrogels with lower storage moduli. Generally, swelling ratio decreases if a hydrogel has large number of crosslinking points or it is stiff corroborating with our observation (Muratoglu et al., 1999; Phillips & Lambert, 1990; Ryu et al., 2018; Yalçın & Top, 2022).

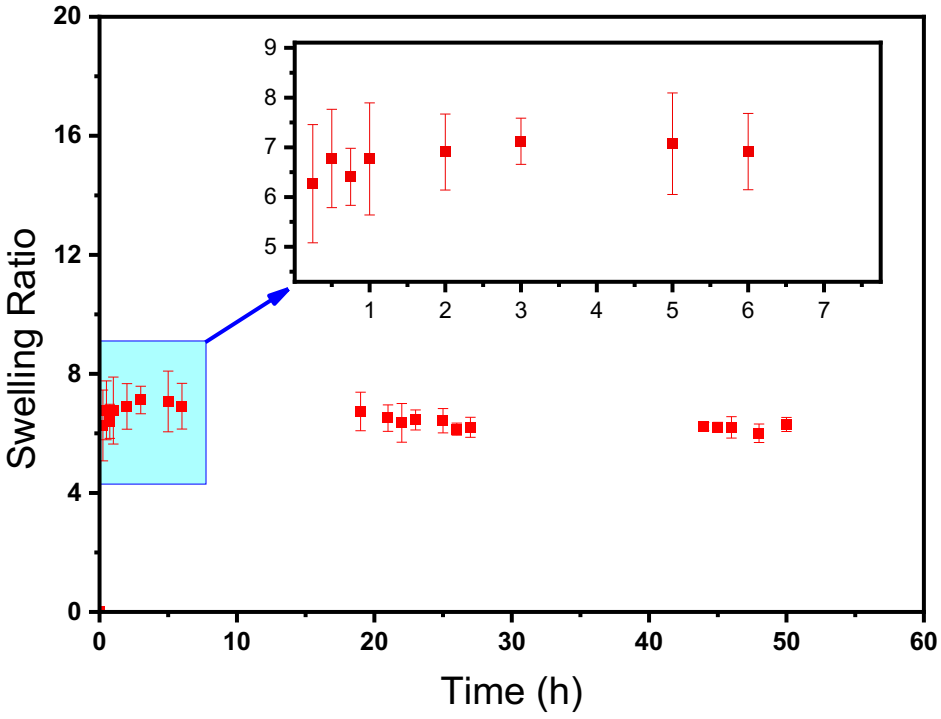

Figure 3.12. Swelling results of the freeze-dried keratin-based hydrogel.

Cytocompatibility of 15 wt.% keratin-based hydrogel cell was tested using CCK-8 assay. 2.5 x 10^3 L929 fibroblast cells were seeded onto the keratin-based hydrogels and empty tissue culture polystyrene (TCPS) was used as a control system. Cell proliferation results are given in Figure 3.13. Cell proliferation rates obtained at the end of Day 1, Day 4, and Day 7 indicate that the keratin-based hydrogel supports proliferation of the cells

but with a lower rate compared to the control system which provides more space for the cells to grow. After Day 4, cell proliferation in the hydrogel accelerated, which can be attributed to the dissolution of the hydrogel as observed in the swelling results.

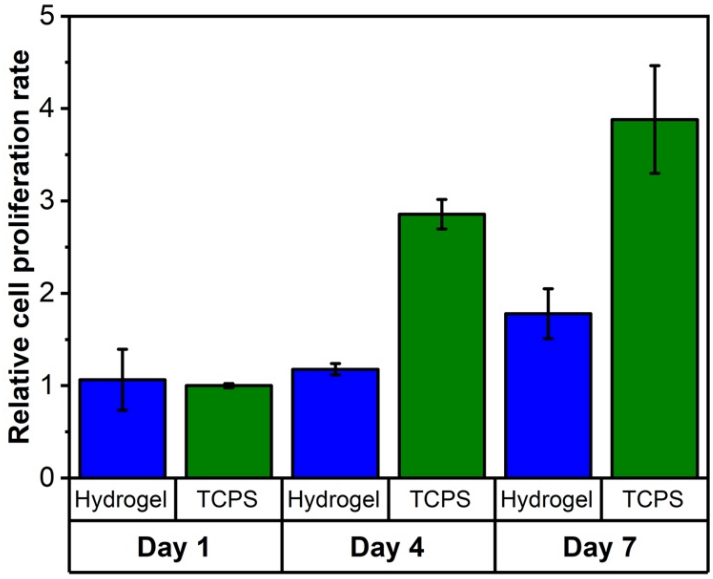

Figure 3. 13. Cell proliferation results of the keratin-based hydrogel.

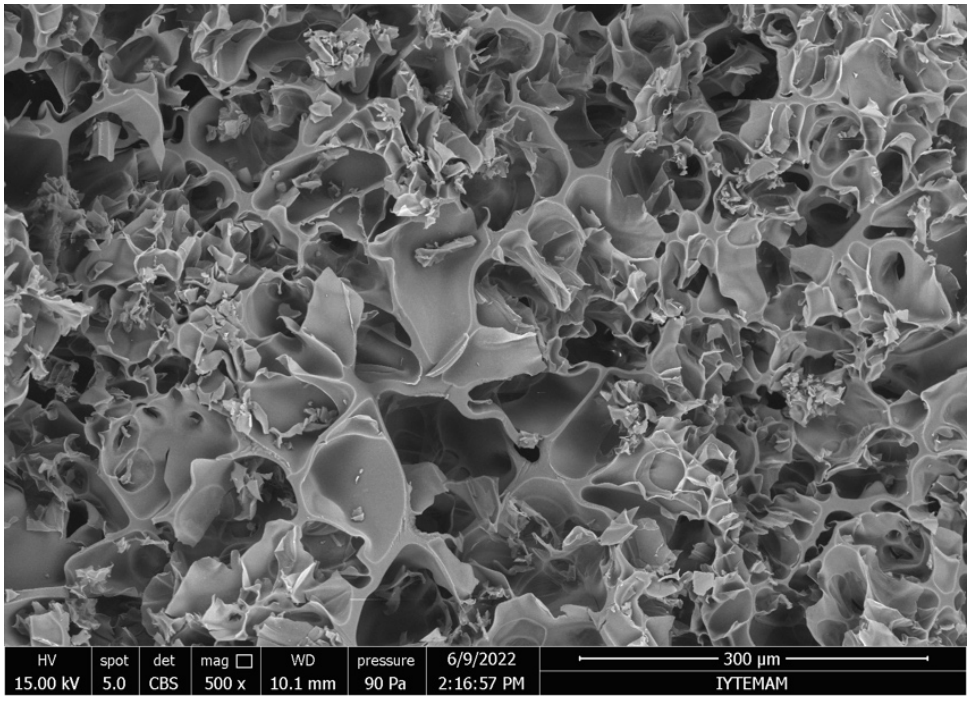

Figure 3.14. SEM picture of the freeze-dried keratin-based hydrogel.

Figure 3.14 indicates SEM images of freeze-dried keratin-based hydrogel. Highly irregular pore structure with an average pore size of 81.7 ± 19 μm was observed in the SEM picture of the hydrogel. Surprisingly, the pore size of keratin-based hydrogel is higher than those of the self-assembled keratose hydrogels and the chemically crosslinked keratose hydrogels prepared at lower protein concentrations (Pakkaner et al., 2019; Yalçın & Top, 2022). This can be attributed to highly heterogeneous pore structure of the keratin hydrogel.

3.4. Conclusions

The keratin proteins were obtained from Merino sheep wool with three different sulfitolysis extraction methods. Method NP with lower reaction time and high keratin protein yield was used to extract keratin to form hydrogels. Highly stiff and self-supported hydrogel was obtained by incubating 15 wt.% keratin at 37°C overnight. The hydrogel formation is triggered by self-assembly and reformation of disulfide bridges. The hydrogel was shown to have limited self-healing properties and exhibited shear thinning behavior at high shear strains. Swelling ratio of the hydrogel was obtained to be lower than those of the keratose hydrogels prepared at lower protein concentrations. Cell proliferation results confirm the cytocompatibility of the hydrogel. This low-cost and biocompatible hydrogel will be tested for wound healing applications.

CHAPTER 4

PEG-KERATIN HYDROGELS THROUGH THIOL MALEIMIDE REACTIONS

4.1. Introduction

Keratin hydrogels have been received increased attention due to their inherent biocompatibility, sustainability and low cost and ease of modification due to the reactive side chain functional groups. Additionally, the wool keratin also has bioactive sites such as LDV (Leu-Asp-Val), EDS (Glu-Asp-Ser), RGD (Arg-Gly-Asp), and glutamic acid-serine (EDS) cell attachment motifs, which trigger cell proliferation and migration (Hill et al., 2010; Su et al., 2020).

Chemical crosslinking offers strong mechanical properties but the toxicity of the crosslinking agent and the byproducts is a concern. For this reason, non-toxic crosslinking agents and addition reactions are preferred in the crosslinking reactions. The thiol-engaged crosslinking methods consist of two sub-groups that undergo addition reactions and substitution reactions. In the substitution reactions, low molecular weight by-products are generated. In the addition reactions, on the other hand, no by-product is formed.

Michael-type addition reaction and photoinitiated thiol-ene addition reaction are categorized as the addition reactions and frequently used as bioconjugation methods. The Michael-type addition reaction is involved in the reaction between free thiol groups and acrylates, maleimide and vinyl sulfones. The reaction between free thiol groups and maleimide has been widely used as it requires no catalyst, releases no by-product and provides rapid gelation with high crosslinking (Stenzel, 2013). In the study of Fu et al. (2011), PEG-dithiol reacted with 2000 Da PEG bismaleimide to form hydrogel network structure. This PEG based hydrogel was shown to be non-toxic and, therefore, it was proposed for drug delivery applications. In another study, 4 arm PEG maleimide was modified with thiol containing adhesive peptide GRGDSPC and crosslinked with dithiol protease-cleavable peptide crosslinker GCRDVPMSMRGGDRCG (Phelps et al., 2012).

PEG-4MAL hydrogels formed quite quickly and can be utilized in the applications where in situ gelation is required.

In this study, we aim to prepare chemically crosslinked hydrogels via thiol-maleimide reaction. Keratin proteins were obtained using a sulfitolysis method (Method NP) and the number of free thiol groups increased by applying DTT reduction method. Then, these thiol groups in the keratin structure reacted with 6000 Da or 2000 Da PEG-$(C_2H_4\text{-mal})_2$ to form crosslinked hydrogel network structures. Effect of molecular weight of PEG-MAL on the viscoelastic, swelling, morphological properties of the chemically crosslinked keratin hydrogels were be investigated. Cytocompatibility of these hydrogels was confirmed.

4.2. Experimental

4.2.1. Materials

Karacabey Merino sheep wool was kindly provided by the Sheep Breeding Research Institute (Balıkesir, Turkey). Chloroform (Sigma-Aldrich) and methanol (Sigma-Aldrich) were used for defatting of the Merinos wools. Sodium sulfite (Sigma-Aldrich), hydrochloric acid (HCl) (Sigma-Aldrich), urea (Sigma-Aldrich), ethylenediaminetetraacetic acid (EDTA) (Sigma-Aldrich) and cellulose membrane dialysis tubing (Sigma-Aldrich, MWCO ~14000) were employed in the extraction and isolation of the keratoses. DL-Dithiothreitol (DTT) (Sigma-Aldrich) was used for reducing keratin proteins. 6000 Da PEG-$(C_2H_4\text{-mal})_2$ and 2000 Da PEG-$(C_2H_4\text{-mal})_2$ (RAPP Polymere) was used as the chemically crosslinking agents to form chemically crosslinked keratin-based hydrogels. FT-IR grade potassium bromide was purchased from Sigma-Aldrich. Sodium hydroxide (NaOH) (Sigma-Aldrich) and hydrochloric acid (HCl) (Merck) were used for adjusting pH value of the solutions. 5,5'-dithio-bis-(2-nitrobenzoic acid) (DTNB = Ellman's reagent), was purchased from Sigma-Aldrich. $NaH_2PO_4.H_2O$ (Merck) was used in the preparation of phosphate buffer saline. Acrylamide (Sigma-Aldrich), bisacrylamide (Amresco), sodium dodecyl sulfate (Merck), ammonium persulfate (Merck), tetramethylethylenediamine (TEMED, Merck), bromophenol blue (Amresco), glycerol (Merck), 2-mercaptoethanol, PageRulerTM pre-

stained protein ladder (Thermo Fisher Scientific), glycine (Amresco), coomasie brilliant blue G-250 (Merck), acetic acid (Sigma-Aldrich), methanol (Sigma-Aldrich), Tris-HCl (Sigma-Aldrich), Tris-base (ChemCruz) were employed in sodium dodecyl sulfate polyacrylamide gel electrophoresis (SDS-PAGE) analysis. DMEM cell culture medium (high glucose), fetal bovine serum (FBS, European grade), gentamycin sulfate, 0.25% trypsin-EDTA solution and trypan blue solution (5 mg/ml) were obtained from Biological Industries. CCK-8 cell counting kit was purchased from Cayman Chemical Company.

4.2.2. Methods

4.2.2.1. Pre-extraction of the keratin proteins

In this study, the keratin proteins were extracted from Merino sheep wool. The wools were cleaned and defatted using previous methods (Pakkaner et al., 2019; Yalçın & Top, 2022).

4.2.2.2. Extraction of the keratin proteins with sodium sulfide

1 gram cleaned, and defatted wools were extracted with 125 mM sodium sulfide in 50 ml solution at 40ºC by shaking at 150 rpm for 4 h. The keratin extraction solution was filtered and dialyzed against deionized water using a pretreated dialysis membrane tubing. Dialysis medium was changed thrice a day, and the dialysis process was carried out for 3 days. Lastly, the dialyzed keratin proteins were lyophilized and stored at -20 ºC.

4.2.2.3. Reduction of the keratin proteins with DTT

500 mg lyophilized keratin was dissolved in 10 ml deionized water at pH 7.4, and at room temperature. Then, 200 mg 1.4-dithiothreitol (DTT) was added to the keratin solution to break the disulfide bonds and the solution is stirred at room temperature overnight. Then, the reduced keratins were purified using centrifugal filter units (Amicon Ultra-15 with Ultracel-3k membrane, MWCO 3000) by spinning 4500 rpm for 30 minutes. The concentrated protein solution in the filter was diluted to 15 ml with degassed deionized water, and then spined for another 30 minutes at 4500 rpm. The purification

steps were repeated for ten cycles to remove the excess DTT. Lastly, the purified keratin proteins were lyophilized and stored at -20 ºC.

4.2.2.4. Characterization of the keratin proteins

The yield of DTT reduction extraction method was calculated by using the following equation:

$$\text{Yield } \% = \left(\frac{\text{Amount of obtained keratin proteins}}{\text{Amount of initial Merino sheep wool}}\right) * 100\% \qquad (4.1)$$

DTNB (Ellman's Reagent) (5,5-dithio-bis-(2-nitrobenzoic acid)) assay was used to determine the free thiol groups of the keratin protein structures by applying the method proposed by Aitken and Learmonth (1996) as given in Chapter 3. Free thiol content concentration was determined using the extinction coefficient of 14150 $M^{-1}cm^{-1}$ at 412 nm (Riddles et al., 1983).

Thermogravimetric analyses (TGA) of the keratin reduced with DTT was carried out using a Shimadzu TGA-51 (Tokyo, Japan) model instrument. The sample was heated from room temperature to 600 ºC with a heating rate of 10 ºC/min under nitrogen flow.

X-ray diffraction (XRD) experiment was conducted using a Philips PANalytical X'Pert Pro (Almelo, Netherlands) model diffractometer with an incident CuKα radiation at 1.54 Å. XRD pattern of the sample was recorded between 2θ range of 5º and 80º with a scan rate of 0.08 degree/s.

Lastly, SDS-PAGE gel analysis of the extracted keratin proteins was performed using the method described in Chapter 3.

4.3.3.5. Preparation of the chemically crosslinked keratin hydrogels

After determined free thiol amount, 10 w/v % chemically crosslinked PEG-keratin hydrogels were prepared by reacting the reduced keratin with 6000 Da or 2000 Da PEG-$(C_2H_4$-mal$)_2$ in filtered PBS (10 mM NaH_2PO_4 and 150 mM NaCl) at pH 7.4 or in deionized water at pH 7.4 followed by incubating the immediately formed viscous solution at 37°C overnight. In the crosslinking reaction, thiol to maleimide molar ratio was set as 1:0.5.

4.2.2.6. Characterization of the keratin hydrogels

Oscillatory rheology tests were performed at 25°C, by using a Thermo Fisher Scientific HAAKE MARS (Waltham, MA, USA) model rheometer equipped with a 35 mm diameter of stainless-steel parallel plate. The tests were performed by following the protocol of Chen et al. (2017) as described in Chapter 3.

Cytocompatibility of the PEG-keratin hydrogels was investigated using CCK-8 assay by applying the procedure reported earlier (Pakkaner et al., 2019; Yalçın & Top, 2022). Absorbance values at 450 nm (A450) correlated to cell viability were measured using Thermo Fisher Varioskan Flash microplate reader (Waltham, MA, USA). Relative proliferation rate was determined using three replicates of keratin hydrogels 6000 Dalton PEG-$(C_2H_4\text{-mal})_2$ and 2000 Dalton PEG-$(C_2H_4\text{-mal})_2$ prepared in PBS. Empty tissue culture treated polystyrene (TCPS) wells were used as the control sample. Relative proliferation rate was calculated by the following equation:

$$\text{Relative cell proliferation rate} = \frac{A_{450} \text{ of the hydrogel}}{A_{450} \text{ of TCPS at the end of Day 1}} \tag{4.1}$$

For swelling test, the keratin hydrogels were prepared in the wells of a 24-well flat-bottom plate. Crosslinking reactions of the PEG-keratin hydrogels were performed in deionized water. Hydrogel samples were lyophilized, and the mass of each freeze-dried sample (number of replicates = 3) was determined. Then, dry samples were immersed in excess filtered PBS (10 mM NaH_2PO_4 and 150 mM NaCl) at pH 7.4 at room temperature and the samples swollen during specified time periods (15 min, 30 min, 45 min, 1h, 2h, 3h, 6h, 12 h, 24h, 48h, 72h, 148 h) were weighed after removing excess PBS solution. Swelling ratio values at time t were determined using the following equation (Y. Chen et al., 2020):

$$\text{Swelling ratio at time t} = \frac{W_t - W_d}{W_d} \tag{4.2}$$

where W_d is the initial weight of the freeze-dried sample, and W_t is the weight of the swollen hydrogel measured at time t.

Pore structure of the hydrogels were observed using scanning electron microscopy (SEM) FEI Quanta 250 FEG (Oregon, USA) model. PEG-keratin hydrogels were prepared in deionized water, freeze-dried at -80 ºC, and then frozen in liquid nitrogen prior to fracture. The samples were coated with gold and cross-sectionally fractured portion of the samples were investigated. Average pore size values of the freeze-dried hydrogels were measured using ImageJ software.

4.3. Results and Discussions

The keratin proteins were extracted from Merino sheep wool with Method NP that was mentioned in Section 3.2.2.2. After the sulfitolysis reaction, disulfide bonds are cleaved and free thiols form. Free thiol amount obtained in Method NP is quite low due to the reformation of disulfide bonds during dialysis (Table 3.1). For this reason, the keratin was reduced using dithiothreitol (DTT) and purified very quickly with a centrifugal filter. Dithiothreitol (DTT) is very strong reducing agent which breaks to form free thiols as given in Figure 4.1.

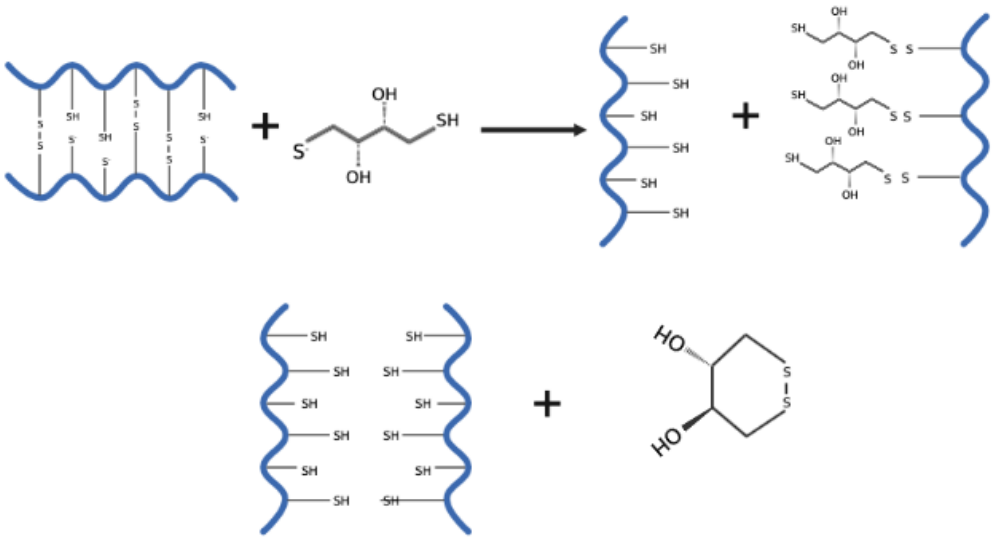

Figure 4.1. Reaction of DTT chemical with disulfide bonds.

The yield of DTT reduction was obtained as 88% and the overall yield of the combined sulfitolysis and DTT reduction was calculated as 39% as given in Table 4.1. Figure 4.2 shows the UV spectra of the keratins obtained from Method NP and Method

NP+DTT after reacting with Ellman's reagent. Maximum absorbance value of DTT reduced keratin was observed as ~1.75 at 412 nm. On the other hand, maximum absorbance of the keratin from Method NP is ~0.25 at 412 nm. These results indicate that upon DTT reduction, free thiol amount increased more than nine times (Table 4.1).

Similar to other study, keratin proteins were extracted from human hair using sodium sulfide, and the free thiol amount of the keratin proteins was calculated as less than 0.01 mmol/g keratin. However, after sodium sulfide extraction step, the human keratin proteins were treated with DTT reducing agent and purified with a centrifugal filter system. After the reduction process, amount of free thiols in the hair keratin increased to 0.55 mmol/g keratin (Yue et al., 2018).

Table 4.1. The yields and the free thiol amounts of the keratins obtained from the Method NP and the Method NP+DTT reduction methods.

Method	**Reduction Extraction Method**	**Yield (%)**	**Free Thiol Amounts [mmol/g keratin]**
NP	Sodium sulfide	44 ± 2	0.07 ± 0.02
NP+DTT	Sodium sulfide + DTT	88 ± 3	0.62 ± 0.07

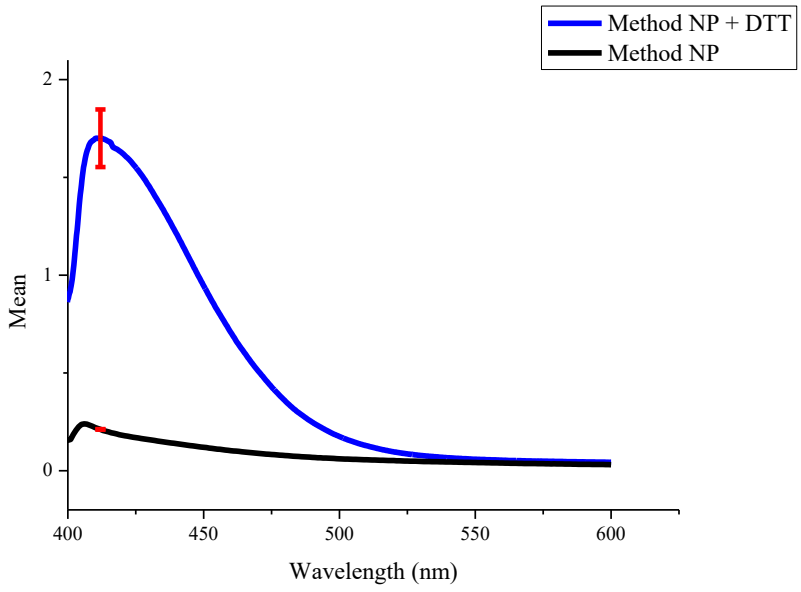

Figure 4.2. UV spectrum of keratins obtained from the Method NP and Method NP+DTT with Ellman's reagent.

The crystallinity structure of the keratin proteins from NP+DTT was analyzed using X-ray diffraction (XRD) spectroscopy. The diffraction pattern of the DTT reduced keratin exhibit two peaks at 2Θ = 9° and 2Θ = 20° similar to the parent keratin obtained by Method NP as shown in Figure 4.3. different extraction method. This result indicates that DTT reduction method did not disrupt the crystal structure of the keratin.

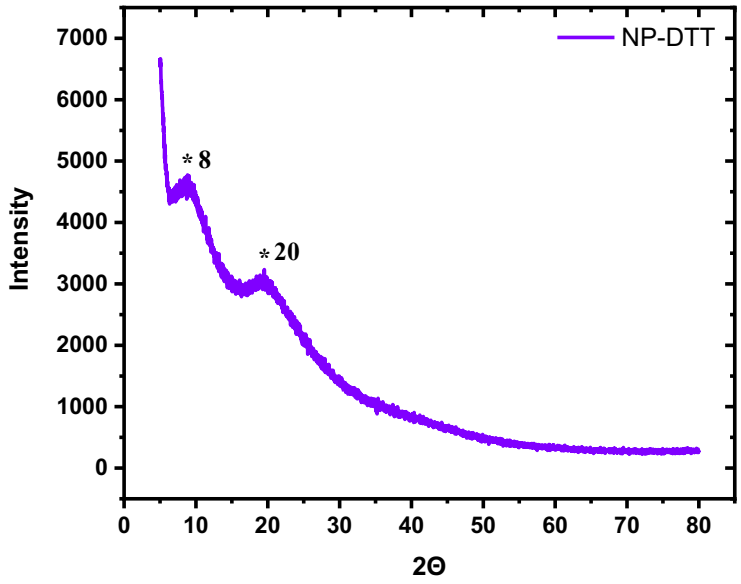

Figure 4.3. XRD pattern of the keratin proteins reduced by DTT.

Thermal behavior of DTT reduced keratin was investigated using thermogravimetric analysis (TGA) and derivative thermogravimetric analysis (DTGA) methods. The resultant curves are shown in Figure 4.4. Likewise, the other samples three endotherms were observed. The first endotherm is at ~89 °C and corresponds to the removal of volatiles and moisture with a ~4.38 % weight loss. The second endotherm was observed at ~337 °C mainly indicating the degradation of the side chains of the keratin proteins (Kakkar et al., 2014; Rama Rao & Gupta, 1992). Lastly, there is one more endotherm at ~523 °C, which can be attributed to pyrolytic decomposition reactions (Rama Rao & Gupta, 1992).

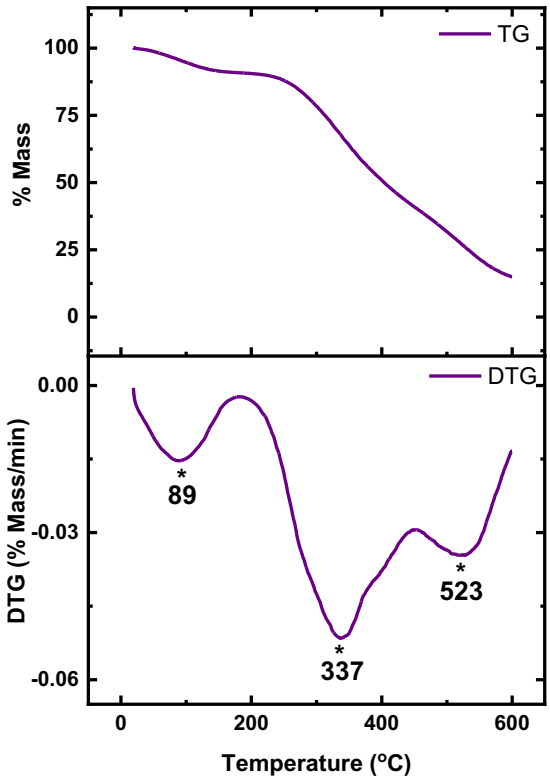

Figure 4.4. TGA and DTG of the keratins reduced by DTT.

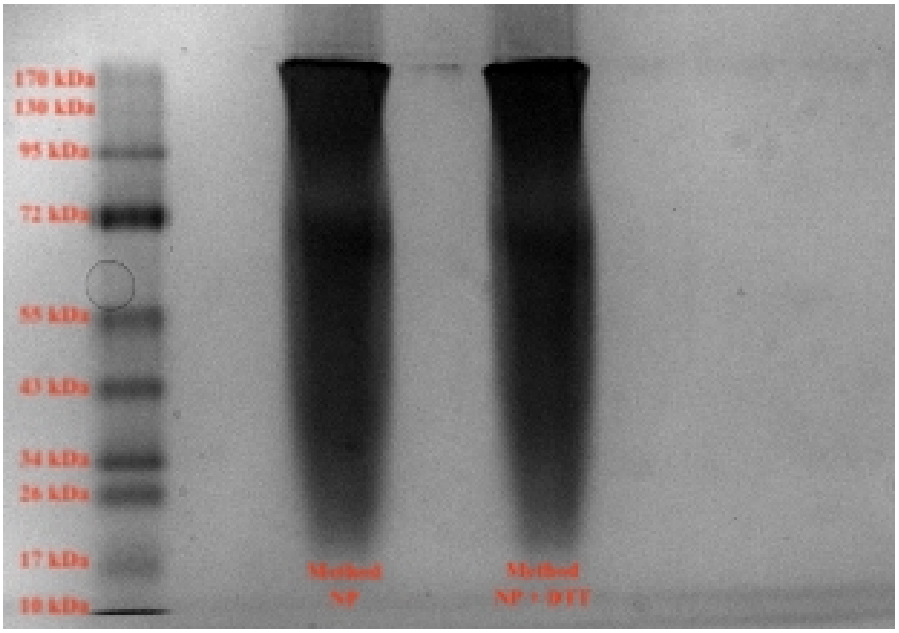

Figure 4.5. SDS-PAGE results of the extracted keratin proteins; from the left to right, lane 1 = protein molecular weight marker, lane 2 = Method NP, and lane 3 = Method NP+DTT.

Sodium dodecyl sulfate-polyacrylamide gel electrophoresis (SDS-PAGE) analysis results of the keratin extracted sulfitolysis and DTT reduced keratin with the molecular weight marker were given in Figure 4.5. According to SDS-PAGE results, diffusive bands were populated between >170 kDa and ~17 kDa indicating highly polydisperse nature of the keratins. The results obtained in lane 2 and lane 3 are quite similar confirming that DTT reduction did not change the composition and molecular weight distribution of the keratin.

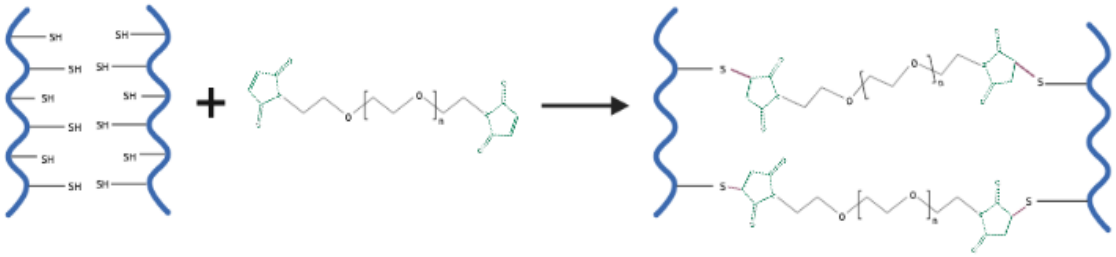

Figure 4. 6. Reaction scheme of the thiols of the reduced keratin and PEG-(C_2H_4-mal)$_2$.

PEG-keratin hydrogels were prepared using Michael addition reaction at 1:0.5 thiol to maleimide ratio. The reaction scheme is given in Figure 4.6. After mixing reduced keratin with 2000 Da or 6000 Da PEG-(C_2H_4-mal)$_2$ at pH 7.4 and incubating at 37 ^oC, self-standing hydrogels were obtained as given in Figure 4.7.

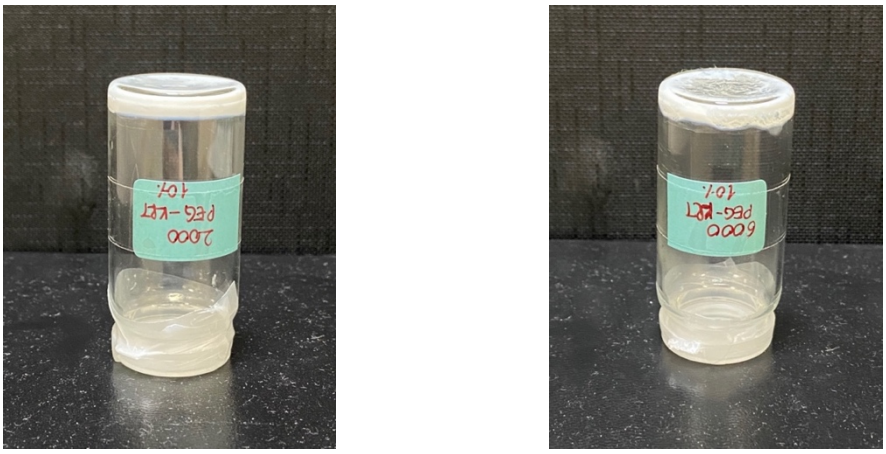

(a) **(b)**

Figure 4.7. Pictures of the 10 wt.% PEG-keratin hydrogels; (a) KRT-2000 PEG-(C_2H_4-mal)$_2$ and (b) KRT-6000 PEG-(C_2H_4-mal)$_2$ hydrogels.

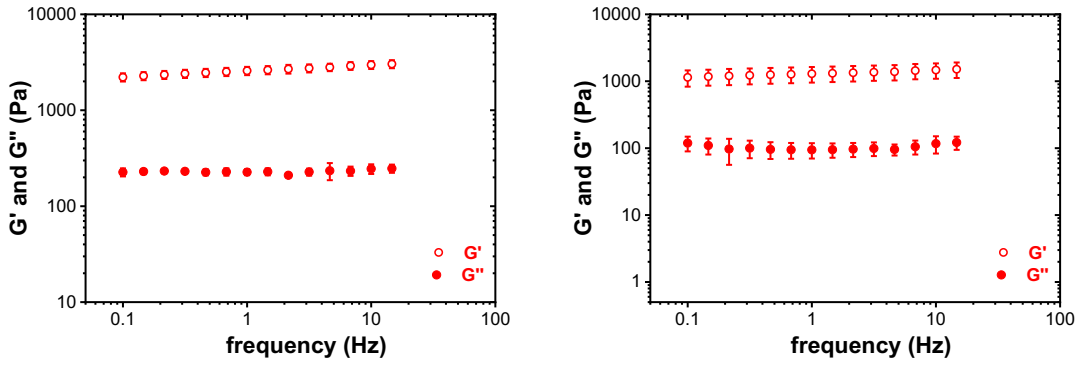

Figure 4.8. Frequency sweep data of the 10 wt.% keratin hydrogels; (a) KRT-2000 PEG-$(C_2H_4\text{-mal})_2$ and (b) KRT-6000 PEG-$(C_2H_4\text{-mal})_2$ hydrogels.

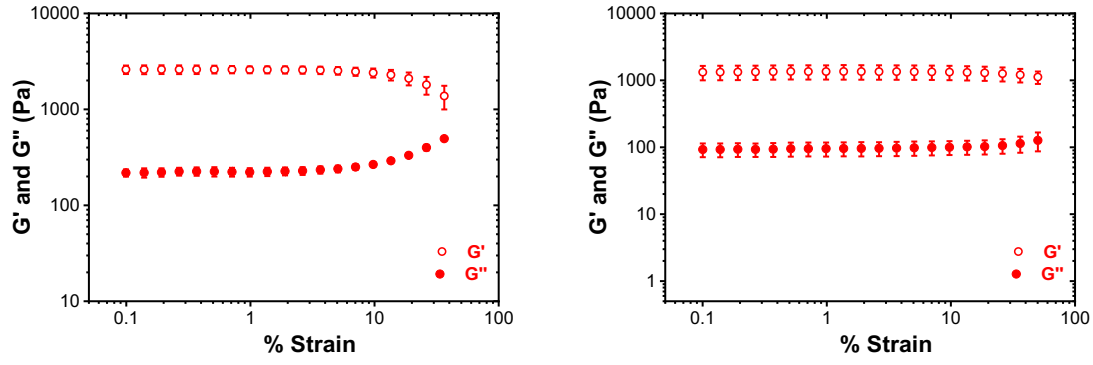

Figure 4.9. Strain sweep data of the 10 wt.% keratin hydrogels; (a) KRT-2000 PEG-$(C_2H_4\text{-mal})_2$ and (b) KRT-6000 PEG-$(C_2H_4\text{-mal})_2$ hydrogels.

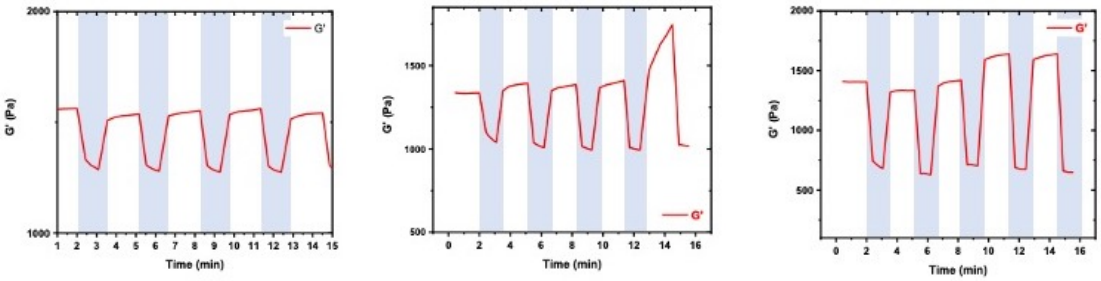

Figure 4.10. Cyclic strain time sweep data of the KRT-6000 PEG-$(C_2H_4\text{-mal})_2$ hydrogels, shaded regions were obtained at high strain values (a) 40%, (b) 60% and (c) 100%, and unshaded regions were obtained at low strain (0.2%).

Viscoelastic behavior of the PEG-keratin hydrogels was investigated using frequency sweep, strain sweep, cyclic strain time sweep experiments and flow curves. Firstly, the frequency sweep tests were done from 0.1 Hz to 15 Hz at constant 0.2% strain, and the results are shown in Figure 4.8. Likewise, the other hydrogels investigated, G' values of the PEG-keratin hydrogels were obtained to be higher than those of the G'' values confirming solid like structures. Plateau values of storage moduli were determined as 2613 ± 254 and 1313 ± 345 Pa for KRT-2000 PEG-$(C_2H_4\text{-mal})_2$ and KRT-6000 PEG-$(C_2H_4\text{-mal})_2$ hydrogels, respectively. Higher stiffness of the KRT-2000 PEG-$(C_2H_4\text{-mal})_2$ hydrogel can be attributed to its higher number of crosslinking points. G' values of the PEG-keratin hydrogels are much higher than those of the THPC crosslinked hydrogels but comparable to the keratin hydrogel at 15 w/v % concentration. On the other hand, KRT-6000 PEG-$(C_2H_4\text{-mal})_2$ hydrogel has a broader range of LVE up to 40% strain, whereas LVE range of KRT-2000 PEG-$(C_2H_4\text{-mal})_2$ was observed to ne less than 10% strain (Figure 4.9). These results indicate that KRT-6000 PEG-$(C_2H_4\text{-mal})_2$ hydrogel is more elastic compared to KRT-2000 PEG-$(C_2H_4\text{-mal})_2$ hydrogel. Self-healing behavior of the PEG-hydrogels were determined using cyclic strain time sweep experiments. For KRT-2000 PEG-$(C_2H_4\text{-mal})_2$ hydrogel self-healing behavior could not be observed due to much higher number of crosslinking points and stiffness of the hydrogel. However, more elastic KRT-6000 PEG-$(C_2H_4\text{-mal})_2$ hydrogel exhibited self-healing behavior at 40%, 60% and 100% strains which are outside of its LVE region of the hydrogel as given in Figure 4.10.

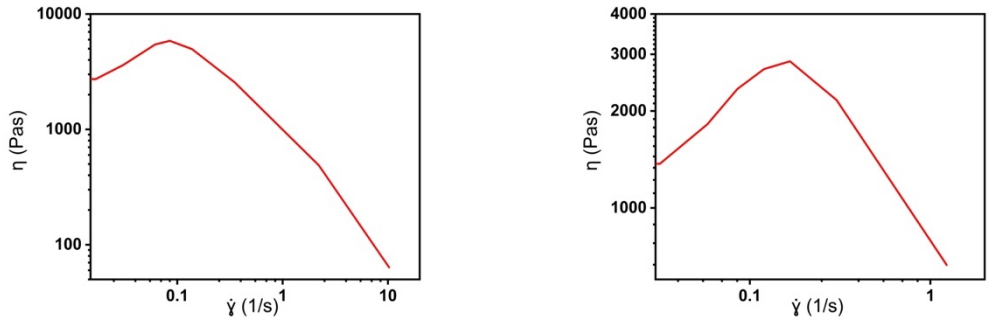

(a) **(b)**

Figure 4.11. Continuous flow curve of the 10 wt.% keratin hydrogels; (a) KRT-2000 PEG-$(C_2H_4\text{-mal})_2$ and (b) KRT-6000 PEG-$(C_2H_4\text{-mal})_2$ hydrogels.

Flow curves of KRT-2000 PEG-(C_2H_4-mal)$_2$ and KRT-6000 PEG-(C_2H_4-mal)$_2$ hydrogels are shown in Figure 4.11. Likewise, the keratin hydrogel prepared in Chapter 3, up to a certain shear rate viscosity of the hydrogels increased. Above shear rate of 0.1-0.15 s^{-1}, shear-thinning behavior was observed.

Swelling kinetic curves of the PEG-hydrogels are shown in Figure 4.12. KRT-2000 PEG-(C_2H_4-mal)$_2$ and KRT-6000 PEG-(C_2H_4-mal)$_2$ hydrogels maintained their structures up to 6 days (148 h). After 148 h, the samples started to dissolve in the PBS. Average swelling ratios of the KRT-2000 PEG-(C_2H_4-mal) and KRT-6000 PEG-(C_2H_4-mal)$_2$ hydrogels were determined as 13.7 ± 1.0 % and 17.6 ± 0.5 %, respectively. The higher swelling ratio of KRT-2000 PEG-(C_2H_4-mal)$_2$ hydrogel can be explained by its stiffness which restrict water penetration into the structure (Muratoglu et al., 1999; Phillips & Lambert, 1990; Ryu et al., 2018; Yalçın & Top, 2022).

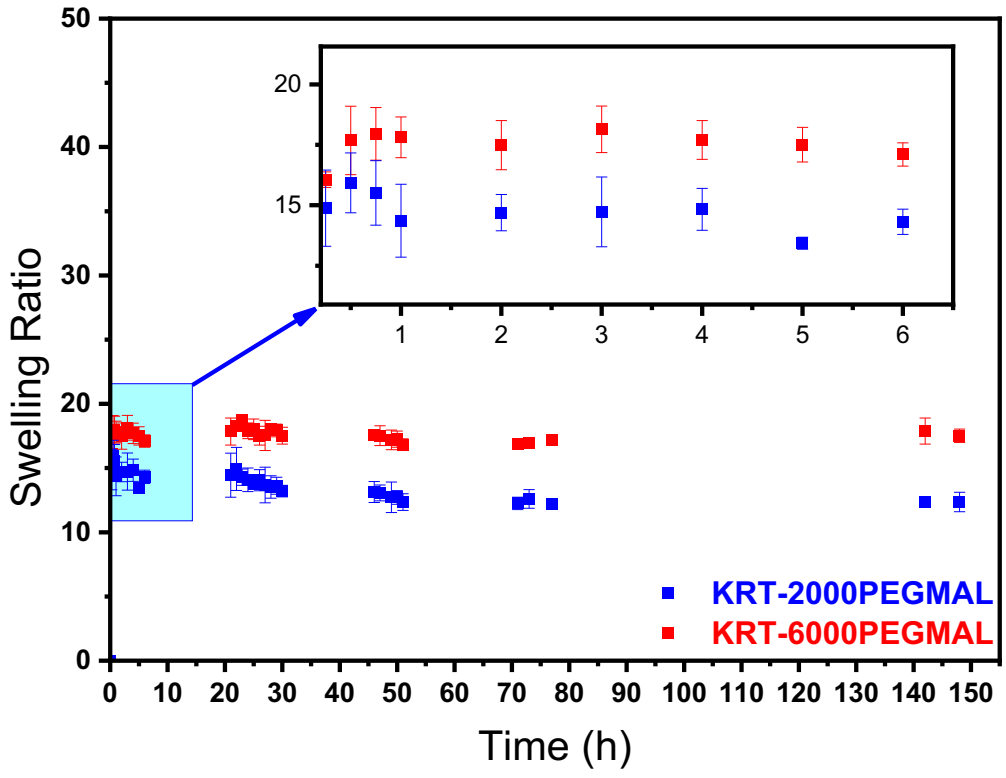

Figure 4.12. Swelling results of the freeze-dried KRT-2000 PEG-(C_2H_4-mal)$_2$ and KRT-6000 PEG-(C_2H_4-mal)$_2$ hydrogels.

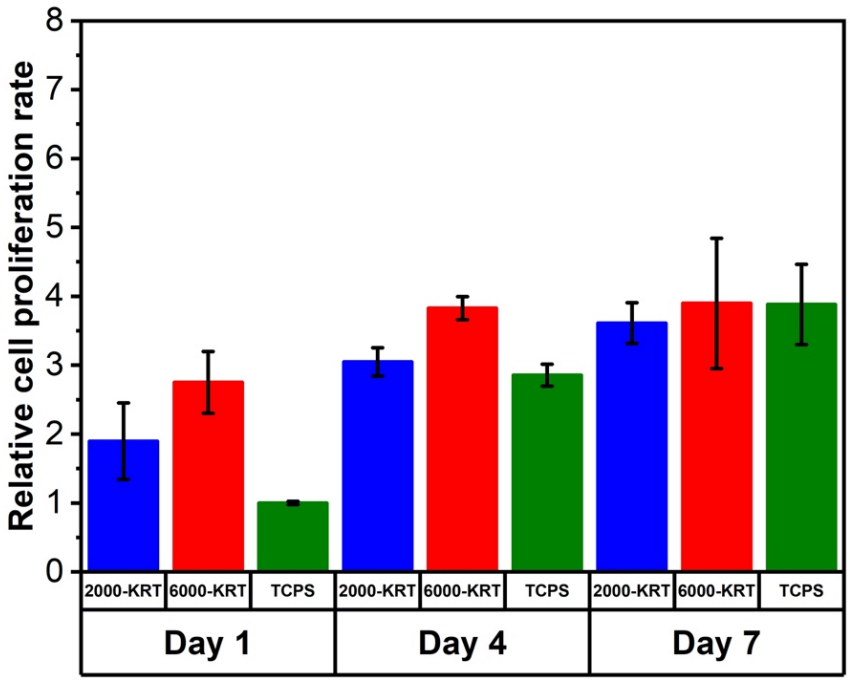

Figure 4.13. Cell proliferation results of KRT-2000 PEG-(C_2H_4-mal)$_2$ and KRT-6000 PEG-(C_2H_4-mal)$_2$ hydrogels.

Cell proliferation tests were performed to examine the interactions between KRT-2000 PEG-(C_2H_4-mal)$_2$ and KRT-6000 PEG-(C_2H_4-mal)$_2$ hydrogels with L929 fibroblast cell line using CCK-8 assay. Relative cell proliferation rate results are presented on Figure 4.13. For Day 1 and Day 4, both hydrogels promoted cell proliferation with a rate higher than TCPS. However, at the end of the seventh day, similar proliferation rates were obtained. These results indicate that PEG-keratin hydrogels are not toxic and can find biomedical applications such as soft tissue engineering and drug delivery. Especially, KRT-6000 PEG-(C_2H_4-mal)$_2$ hydrogel can be evaluated as an injectable biomaterial.

Figure 4.14 shows SEM images of freeze-dried KRT-2000 PEG-(C_2H_4-mal)$_2$ and KRT-6000 PEG-(C_2H_4-mal)$_2$ hydrogels. Highly irregular pore structure with open and closed pores was obtained for both hydrogels. Average pore sizes of KRT-2000 PEG-(C_2H_4-mal)$_2$ and KRT-6000 PEG-(C_2H_4-mal)$_2$ hydrogels were measured as 113 ± 26 μm and 154 ± 38 μm, respectively. The higher pore size of KRT-6000 PEG-(C_2H_4-mal)$_2$ hydrogel can be attributed to higher molar mass of PEG and lower number of crosslinking points of this hydrogel compared to that of KRT-2000 PEG-(C_2H_4-mal)$_2$ hydrogel.

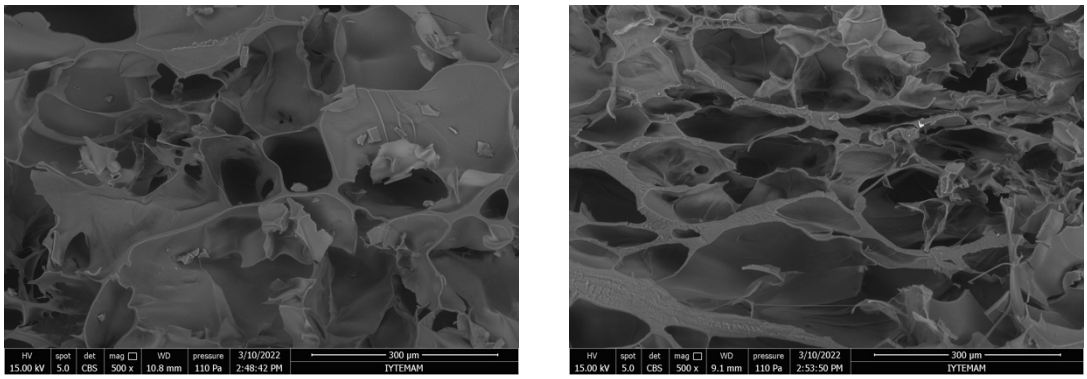

(a) **(b)**

Figure 4.14. SEM pictures of the freeze-dried of the 10 wt.% keratin hydrogels; (a) KRT-2000 PEG-$(C_2H_4\text{-mal})_2$ and (b) KRT-6000 PEG-$(C_2H_4\text{-mal})_2$ hydrogels.

4.4. Conclusions

The keratin proteins obtained via sulfitolysis extraction method was reduced using DTT to increase the number of free thiols. Reduced keratin proteins reacted with 2000 Da PEG-$(C_2H_4\text{-mal})_2$ or 6000 Da PEG-$(C_2H_4\text{-mal})_2$ to form 10 wt.% chemically crosslinked PEG-keratin based hydrogels. Frequency sweep experiments indicate KRT-2000 PEG-$(C_2H_4\text{-mal})_2$ hydrogel is stiffer than KRT-6000 PEG-$(C_2H_4\text{-mal})_2$ hydrogel due to the higher number of crosslinking points of KRT-2000 PEG-$(C_2H_4\text{-mal})_2$ hydrogel. However, KRT-6000 PEG-$(C_2H_4\text{-mal})_2$ hydrogel exhibited self-healing behavior as indicated by cyclic strain time sweep experiment. Swelling ratio of KRT-6000 PEG-$(C_2H_4\text{-mal})_2$ hydrogel was found to be higher than that of KRT-2000 PEG-$(C_2H_4\text{-mal})_2$ hydrogel which can be attributed to higher flexibility of KRT-6000 PEG-$(C_2H_4\text{-mal})_2$ hydrogel. Average pore size of KRT-6000 PEG-$(C_2H_4\text{-mal})_2$ hydrogel was also higher compared to the hydrogel crosslinked with shorter PEG chain. Thus, molecular weight of the PEG macro-crosslinker affected viscoelastic, swelling, and morphological properties of the hydrogels. Up to 4 days, both hydrogels were shown to promote cell proliferation with a higher rate than empty TCPS wells indicating cytocompatibility of these hydrogels.

CHAPTER 5

CONCLUSIONS & FUTURE STUDIES

Wool keratins were extracted by oxidation, sulfitolysis, and reduction methods. Keratins were characterized using XRD and FTIR spectroscopy and thermal analysis methods. Molar mass distributions of the keratins were determined by SDS-PAGE gel analysis. Keratin based hydrogel systems were prepared via different strategies. In Chapter 2, oxidized keratins (keratoses) reacted with a small molecular weight crosslinker THPC to form chemically crosslinked keratose hydrogels. In Chapter 3, keratins obtained from sulfitolysis reaction formed hydrogels at physiological temperature upon oxidation of the free thiols and self-assembly of the keratin chains. In Chapter 4, the keratin proteins obtained by sulfitolysis and DTT reduction were reacted with macromolecular crosslinkers, 2000 Da PEG-$(C_2H_4$-mal$)_2$ and 6000 Da PEG-$(C_2H_4$-mal$)_2$ to prepare PEG-keratin hydrogels. Viscoelastic, swelling, and morphological properties of the hydrogels were investigated and were shown to be tuned by the amount and molar mass of the crosslinkers and dictated by the hydrogel preparation methods. Finally, cytocompatibility of the hydrogels was confirmed by CCK-8 assay. Thus, these hydrogels can serve as low cost and efficient scaffolds in the biomedical applications as an alternative to other polymer/biopolymer-based materials.

As a future work, we will investigate wound healing properties of curcumin loaded keratin hydrogels. Additionally, doxorubicin loaded KRT - 6000 Da PEG-$(C_2H_4$-mal$)_2$ will be tested as an injectable hydrogel in cancer therapy.

REFERENCES

Agarwal, V., Panicker, A. G., Indrakumar, S., & Chatterjee, K. (2019). Comparative study of keratin extraction from human hair. *International Journal of Biological Macromolecules*, *133*, 382–390. https://doi.org/10.1016/j.ijbiomac.2019.04.098

Aitken, A., & Learmonth, M. (1996). *Estimation of Disulfide Bonds Using Ellman's Reagent* (pp. 487–488). https://doi.org/10.1007/978-1-60327-259-9_82

Allpress, J. D., Mountain, G., & Gowland, P. C. (2002). Production, purification and characterization of an extracellular keratinase from Lysobacter NCIMB 9497. *Letters in Applied Microbiology*, *34*(5), 337–342. https://doi.org/10.1046/j.1472-765X.2002.01093.x

Aluigi, A., Tonetti, C., Rombaldoni, F., Puglia, D., Fortunati, E., Armentano, I., Santulli, C., Torre, L., & Kenny, J. M. (2014). Keratins extracted from Merino wool and Brown Alpaca fibres as potential fillers for PLLA-based biocomposites. *Journal of Materials Science*, *49*(18), 6257–6269. https://doi.org/10.1007/s10853-014-8350-9

Aluigi, A., Vineis, C., Varesano, A., Mazzuchetti, G., Ferrero, F., & Tonin, C. (2008). Structure and properties of keratin/PEO blend nanofibres. *European Polymer Journal*, *44*(8), 2465–2475. https://doi.org/10.1016/j.eurpolymj.2008.06.004

Anbu, P., Hilda, A., Sur, H.-W., Hur, B.-K., & Jayanthi, S. (2008). Extracellular keratinase from Trichophyton sp. HA-2 isolated from feather dumping soil. *International Biodeterioration & Biodegradation*, *62*(3), 287–292. https://doi.org/10.1016/j.ibiod.2007.07.017

Ayatullah Hosne Asif, A. K. M., Rahman, M., Sarker, P., Hasan, Md. Z., & Paul, D. (2019). Hydrogel Fibre: Future Material of Interest for Biomedical Applications. *Journal of Textile Science and Technology*, *05*(04), 92–107. https://doi.org/10.4236/jtst.2019.54009

Azmi, N. A., Idris, A., & Yusof, N. S. M. (2018). Ultrasonic technology for value added products from feather keratin. *Ultrasonics Sonochemistry*, *47*, 99–107. https://doi.org/10.1016/j.ultsonch.2018.04.016

Bertini, F., Canetti, M., Patrucco, A., & Zoccola, M. (2013). Wool keratin-polypropylene composites: Properties and thermal degradation. In *Polymer degradation and stability: Vol. v. 98*. Elsevier Ltd.

Bhavsar, P., Zoccola, M., Patrucco, A., Montarsolo, A., Rovero, G., & Tonin, C. (2017). Comparative study on the effects of superheated water and high temperature alkaline hydrolysis on wool keratin. *Textile Research Journal*, *87*(14), 1696–1705.

Blackburn, S., & Lee, G. R. (1956). The reaction of wool keratin with alkali. *Biochimica et Biophysica Acta*, *19*, 505–512.

Bohacz, J. (2017). Biodegradation of feather waste keratin by a keratinolytic soil fungus of the genus Chrysosporium and statistical optimization of feather mass loss. *World Journal of Microbiology and Biotechnology*, *33*(1), 13. https://doi.org/10.1007/s11274-016-2177-2

Bose, A., Pathan, S., Pathak, K., & Keharia, H. (2014). Keratinolytic Protease Production by Bacillus amyloliquefaciens 6B Using Feather Meal as Substrate and Application of Feather Hydrolysate as Organic Nitrogen Input for Agricultural Soil. *Waste and Biomass Valorization*, *5*(4), 595–605. https://doi.org/10.1007/s12649-013-9272-5

Brandelli, A. (2008). *Bacterial keratinases: useful enzymes for bioprocessing agroindustrial wastes and beyond. Food Bioprocess Technol 1: 105–116*.

Brandelli, A., Sala, L., & Kalil, S. J. (2015). Microbial enzymes for bioconversion of poultry waste into added-value products. *Food Research International*, *73*, 3–12. https://doi.org/10.1016/j.foodres.2015.01.015

Brown, E. M., Pandya, K., Taylor, M. M., & Liu, C.-K. (2016). Comparison of Methods for Extraction of Keratin from Waste Wool. *Agricultural Sciences*, *07*(10), 670–679. https://doi.org/10.4236/as.2016.710063

Buchanan, J. H. (1977). A cystine-rich protein fraction from oxidized α-keratin. *Biochemical Journal*, *167*(2), 489–491. https://doi.org/10.1042/bj1670489

C Marshall, R., & Gillespie, J. (1977). The Keratin Proteins of Wool, Horn and Hoof from Sheep. *Australian Journal of Biological Sciences*, *30*(5), 389. https://doi.org/10.1071/BI9770389

Călin, M., Constantinescu-Aruxandei, D., Alexandrescu, E., Răut, I., Doni, M. B., Arsene, M.-L., Oancea, F., Jecu, L., & Lazăr, V. (2017). Degradation of keratin substrates by keratinolytic fungi. *Electronic Journal of Biotechnology*, *28*, 101–112. https://doi.org/10.1016/j.ejbt.2017.05.007

Calin, Raut, Liliana, Capra, Gurban, Doni, & Jecu. (2019). Applications of Fungal Strains with Keratin-Degrading and Plant Growth Promoting Characteristics. *Agronomy*, *9*(9), 543. https://doi.org/10.3390/agronomy9090543

Canetti, M., Cacciamani, A., & Bertini, F. (2013). Structural characterization and thermal behaviour of wool keratin hydrolizates-polypropylene composites. *Journal of Polymer Research*, *20*(7), 181. https://doi.org/10.1007/s10965-013-0181-x

Cao, Y., Yao, Y., Li, Y., Yang, X., Cao, Z., & Yang, G. (2019). Tunable keratin hydrogel based on disulfide shuffling strategy for drug delivery and tissue engineering. *Journal of Colloid and Interface Science*, *544*, 121–129. https://doi.org/10.1016/j.jcis.2019.02.049

Cao, Z.-J., Zhang, Q., Wei, D.-K., Chen, L., Wang, J., Zhang, X.-Q., & Zhou, M.-H. (2009). Characterization of a novel Stenotrophomonas isolate with high keratinase activity and purification of the enzyme. *Journal of Industrial*

Microbiology & Biotechnology, *36*(2), 181–188. https://doi.org/10.1007/s10295-008-0469-8

Cardamone, J. M. (2010). Investigating the microstructure of keratin extracted from wool: Peptide sequence (MALDI-TOF/TOF) and protein conformation (FTIR). *Journal of Molecular Structure*, *969*(1–3), 97–105. https://doi.org/10.1016/j.molstruc.2010.01.048

Cardamone, J. M., Nuñez, A., Garcia, R. A., & Aldema-Ramos, M. (2009). Characterizing Wool Keratin. *Research Letters in Materials Science*, *2009*, 1–5. https://doi.org/10.1155/2009/147175

Cavello, I. A., Hours, R. A., Rojas, N. L., & Cavalitto, S. F. (2013). Purification and characterization of a keratinolytic serine protease from Purpureocillium lilacinum LPS # 876. *Process Biochemistry*, *48*(5–6), 972–978. https://doi.org/10.1016/j.procbio.2013.03.012

Caven, B., Redl, B., & Bechtold, T. (2019). An investigation into the possible antibacterial properties of wool fibers. *Textile Research Journal*, *89*(4), 510–516. https://doi.org/10.1177/0040517517750645

Chaitanya Reddy, C., Khilji, I. A., Gupta, A., Bhuyar, P., Mahmood, S., Saeed AL-Japairai, K. A., & Chua, G. K. (2021). Valorization of keratin waste biomass and its potential applications. *Journal of Water Process Engineering*, *40*, 101707. https://doi.org/10.1016/j.jwpe.2020.101707

Chatterjee, K., Lin-Gibson, S., Wallace, W. E., Parekh, S. H., Lee, Y. J., Cicerone, M. T., Young, M. F., & Simon, C. G. (2010). The effect of 3D hydrogel scaffold modulus on osteoblast differentiation and mineralization revealed by combinatorial screening. *Biomaterials*, *31*(19), 5051–5062. https://doi.org/10.1016/j.biomaterials.2010.03.024

Chaturvedi, V., Bhange, K., Bhatt, R., & Verma, P. (2014). Production of kertinases using chicken feathers as substrate by a novel multifunctional strain of Pseudomonas stutzeri and its dehairing application. *Biocatalysis and Agricultural Biotechnology*, *3*(2), 167–174. https://doi.org/10.1016/j.bcab.2013.08.005

Chen, J., Ding, S., Ji, Y., Ding, J., Yang, X., Zou, M., & Li, Z. (2015). Microwave-enhanced hydrolysis of poultry feather to produce amino acid. *Chemical Engineering and Processing: Process Intensification*, *87*, 104–109. https://doi.org/10.1016/j.cep.2014.11.017

Chen, M. H., Wang, L. L., Chung, J. J., Kim, Y.-H., Atluri, P., & Burdick, J. A. (2017). Methods To Assess Shear-Thinning Hydrogels for Application As Injectable Biomaterials. *ACS Biomaterials Science & Engineering*, *3*(12), 3146–3160. https://doi.org/10.1021/acsbiomaterials.7b00734

Chen, M., Ren, X., Dong, L., Li, X., & Cheng, H. (2021). Preparation of dynamic covalently crosslinking keratin hydrogels based on thiol/disulfide bonds exchange strategy. *International Journal of Biological Macromolecules*, *182*, 1259–1267. https://doi.org/10.1016/j.ijbiomac.2021.05.057

Chen, Y. (2020). Chapter 1 - Properties and development of hydrogels. In Y. Chen (Ed.), *Hydrogels Based on Natural Polymers* (pp. 3–16). Elsevier. https://doi.org/https://doi.org/10.1016/B978-0-12-816421-1.00001-X

Chen, Y., Liu, T., Wang, G., Liu, J., Zhao, L., & Yu, Y. (2020). Highly swelling, tough intelligent self-healing hydrogel with body temperature-response. *European Polymer Journal*, *140*, 110047. https://doi.org/10.1016/j.eurpolymj.2020.110047

Chung, C., Lampe, K. J., & Heilshorn, S. C. (2012). Tetrakis(hydroxymethyl) Phosphonium Chloride as a Covalent Cross-Linking Agent for Cell Encapsulation within Protein-Based Hydrogels. *Biomacromolecules*, *13*(12), 3912–3916. https://doi.org/10.1021/bm3015279

Cohen, D. J., Hyzy, S. L., Haque, S., Olson, L. C., Boyan, B. D., Saul, J. M., & Schwartz, Z. (2018). Effects of Tunable Keratin Hydrogel Erosion on Recombinant Human Bone Morphogenetic Protein 2 Release, Bioactivity, and Bone Induction. *Tissue Engineering Part A*, *24*(21–22), 1616–1630. https://doi.org/10.1089/ten.tea.2017.0471

Costa, F., Silva, R., & Boccaccini, A. R. (2018). Fibrous protein-based biomaterials (silk, keratin, elastin, and resilin proteins) for tissue regeneration and repair. In *Peptides and Proteins as Biomaterials for Tissue Regeneration and Repair* (pp. 175–204). Elsevier. https://doi.org/10.1016/B978-0-08-100803-4.00007-3

DANG, J., & LEONG, K. (2006). Natural polymers for gene delivery and tissue engineering☆. *Advanced Drug Delivery Reviews*, *58*(4), 487–499. https://doi.org/10.1016/j.addr.2006.03.001

Darling, N. J., Hung, Y.-S., Sharma, S., & Segura, T. (2016). Controlling the kinetics of thiol-maleimide Michael-type addition gelation kinetics for the generation of homogenous poly(ethylene glycol) hydrogels. *Biomaterials*, *101*, 199–206. https://doi.org/10.1016/j.biomaterials.2016.05.053

de Guzman, R. C., Merrill, M. R., Richter, J. R., Hamzi, R. I., Greengauz-Roberts, O. K., & van Dyke, M. E. (2011). Mechanical and biological properties of keratose biomaterials. *Biomaterials*, *32*(32), 8205–8217. https://doi.org/10.1016/j.biomaterials.2011.07.054

de Oliveira Martinez, J., Cai, G., Nachtschatt, M., Navone, L., Zhang, Z., Robins, K., & Speight, R. (2020). Challenges and Opportunities in Identifying and Characterising Keratinases for Value-Added Peptide Production. *Catalysts*, *10*(2), 184. https://doi.org/10.3390/catal10020184

Deb-Choudhury, S., Plowman, J. E., & Harland, D. P. (2016). *Isolation and Analysis of Keratins and Keratin-Associated Proteins from Hair and Wool* (pp. 279–301). https://doi.org/10.1016/bs.mie.2015.07.018

Duer, M. J., McDougal, N., & Murray, R. C. (2003). A solid-state NMR study of the structure and molecular mobility of α-keratin. *Phys. Chem. Chem. Phys.*, *5*(13), 2894–2899. https://doi.org/10.1039/B302506C

Duncan, W. J., Greer, P. F. C., Lee, M.-H., Loch, C., & Gay, J. H. A. (2018). Wool-derived keratin hydrogel enhances implant osseointegration in cancellous bone. *Journal of Biomedical Materials Research Part B: Applied Biomaterials*, *106*(6), 2447–2454. https://doi.org/10.1002/jbm.b.34047

Earland, C., & Knight, C. S. (1955). Studies on the structure of keratin. *Biochimica et Biophysica Acta*, *17*, 457–461. https://doi.org/10.1016/0006-3002(55)90406-6

Edwards, A., Jarvis, D., Hopkins, T., Pixley, S., & Bhattarai, N. (2015). Poly(ε-caprolactone)/keratin-based composite nanofibers for biomedical applications. *Journal of Biomedical Materials Research Part B: Applied Biomaterials*, *103*(1), 21–30. https://doi.org/10.1002/jbm.b.33172

Engler, A. J., Richert, L., Wong, J. Y., Picart, C., & Discher, D. E. (2004). Surface probe measurements of the elasticity of sectioned tissue, thin gels and polyelectrolyte multilayer films: Correlations between substrate stiffness and cell adhesion. *Surface Science*, *570*(1–2), 142–154. https://doi.org/10.1016/j.susc.2004.06.179

Engler, A. J., Sen, S., Sweeney, H. L., & Discher, D. E. (2006). Matrix Elasticity Directs Stem Cell Lineage Specification. *Cell*, *126*(4), 677–689. https://doi.org/10.1016/j.cell.2006.06.044

Esparza, Y., Ullah, A., & Wu, J. (2018). Molecular mechanism and characterization of self-assembly of feather keratin gelation. *International Journal of Biological Macromolecules*, *107*, 290–296. https://doi.org/10.1016/j.ijbiomac.2017.08.168

Fagbemi, O. D., Sithole, B., & Tesfaye, T. (2020). Optimization of keratin protein extraction from waste chicken feathers using hybrid pre-treatment techniques. *Sustainable Chemistry and Pharmacy*, *17*, 100267. https://doi.org/10.1016/j.scp.2020.100267

Fang, Z., Zhang, J., Liu, B., Du, G., & Chen, J. (2013). Biochemical characterization of three keratinolytic enzymes from Stenotrophomonas maltophilia BBE11-1 for biodegrading keratin wastes. *International Biodeterioration & Biodegradation*, *82*, 166–172. https://doi.org/10.1016/j.ibiod.2013.03.008

Farmer, R. S., Argust, L. M., Sharp, J. D., & Kiick, K. L. (2006). Conformational Properties of Helical Protein Polymers with Varying Densities of Chemically Reactive Groups. *Macromolecules*, *39*(1), 162–170. https://doi.org/10.1021/ma051534t

Farmer, R. S., & Kiick, K. L. (n.d.). Conformational behavior of chemically reactive alanine-rich repetitive protein polymers. *Biomacromolecules*, *6*(3), 1531–1539. https://doi.org/10.1021/bm049216+

Fernández, J. F., Waterkamp, D., & Thöming, J. (2008). Recovery of ionic liquids from wastewater: Aggregation control for intensified membrane filtration. *Desalination*, *224*(1–3), 52–56. https://doi.org/10.1016/j.desal.2007.04.079

Fernández-d'Arlas, B. (2018). Improved aqueous solubility and stability of wool and feather proteins by reactive-extraction with H2O2 as bisulfide (S S) splitting

agent. *European Polymer Journal*, *103*, 187–197. https://doi.org/10.1016/j.eurpolymj.2018.04.010

Feroz, S., Muhammad, N., Ratnayake, J., & Dias, G. (2020). Keratin - Based materials for biomedical applications. *Bioactive Materials*, *5*(3), 496–509. https://doi.org/10.1016/j.bioactmat.2020.04.007

Fu, Y., & Kao, W. J. (2011). In situ forming poly(ethylene glycol)-based hydrogels via thiol-maleimide Michael-type addition. *Journal of Biomedical Materials Research Part A*, *98A*(2), 201–211. https://doi.org/10.1002/jbm.a.33106

Gaidau, C., Stanca, M., Niculescu, M.-D., Alexe, C.-A., Becheritu, M., Horoias, R., Cioineag, C., Râpă, M., & Stanculescu, I. R. (2021). Wool Keratin Hydrolysates for Bioactive Additives Preparation. *Materials*, *14*(16), 4696. https://doi.org/10.3390/ma14164696

George, A., Shah, P. A., & Shrivastav, P. S. (2019). Natural biodegradable polymers based nano-formulations for drug delivery: A review. *International Journal of Pharmaceutics*, *561*, 244–264. https://doi.org/10.1016/j.ijpharm.2019.03.011

Ghosh, A., Clerens, S., Deb-Choudhury, S., & Dyer, J. M. (2014). Thermal effects of ionic liquid dissolution on the structures and properties of regenerated wool keratin. *Polymer Degradation and Stability*, *108*, 108–115. https://doi.org/10.1016/j.polymdegradstab.2014.06.007

Gillespie, J. M. (1972). Proteins rich in glycine and tyrosine from keratins. *Comparative Biochemistry and Physiology Part B: Comparative Biochemistry*, *41*(4), 723–734. https://doi.org/10.1016/0305-0491(72)90085-5

Gough, C. R., Rivera-Galletti, A., Cowan, D. A., Salas-de la Cruz, D., & Hu, X. (2020). Protein and Polysaccharide-Based Fiber Materials Generated from Ionic Liquids: A Review. *Molecules*, *25*(15), 3362. https://doi.org/10.3390/molecules25153362

Gradišar, H., Kern, S., & Friedrich, J. (2000). Keratinase of Doratomyces microsporus. *Applied Microbiology and Biotechnology*, *53*(2), 196–200. https://doi.org/10.1007/s002530050008

Grazziotin, A., Pimentel, F. A., Sangali, S., de Jong, E. v., & Brandelli, A. (2007). Production of feather protein hydrolysate by keratinolytic bacterium Vibrio sp. kr2. *Bioresource Technology*, *98*(16), 3172–3175. https://doi.org/10.1016/j.biortech.2006.10.034

Guo, L., Lu, L., Yin, M., Yang, R., Zhang, Z., & Zhao, W. (2020). Valorization of refractory keratinous waste using a new and sustainable bio-catalysis. *Chemical Engineering Journal*, *397*, 125420. https://doi.org/10.1016/j.cej.2020.125420

Gupta, R., & Ramnani, P. (2006). Microbial keratinases and their prospective applications: an overview. *Applied Microbiology and Biotechnology*, *70*(1), 21–33. https://doi.org/10.1007/s00253-005-0239-8

Ham, T. R., Lee, R. T., Han, S., Haque, S., Vodovotz, Y., Gu, J., Burnett, L. R., Tomblyn, S., & Saul, J. M. (2016). Tunable Keratin Hydrogels for Controlled Erosion and Growth Factor Delivery. *Biomacromolecules*, *17*(1), 225–236. https://doi.org/10.1021/acs.biomac.5b01328

Han, D., & Row, K. H. (2010). Recent Applications of Ionic Liquids in Separation Technology. *Molecules*, *15*(4), 2405–2426. https://doi.org/10.3390/molecules15042405

Han, S., Ham, T. R., Haque, S., Sparks, J. L., & Saul, J. M. (2015). Alkylation of human hair keratin for tunable hydrogel erosion and drug delivery in tissue engineering applications. *Acta Biomaterialia*, *23*, 201–213. https://doi.org/10.1016/j.actbio.2015.05.013

Hill, P., Brantley, H., & van Dyke, M. (2010). Some properties of keratin biomaterials: Kerateines. *Biomaterials*, *31*(4), 585–593. https://doi.org/10.1016/j.biomaterials.2009.09.076

HILTERHAUS-BONG, S., & ZAHN, H. (1987). Contributions to the chemistry of human hair. 1. Analyses of cystine, cysteine and cystine oxides in untreated human hair. *International Journal of Cosmetic Science*, *9*(3), 101–110. https://doi.org/10.1111/j.1467-2494.1987.tb00467.x

Holkar, C. R., Jain, S. S., Jadhav, A. J., & Pinjari, D. v. (2018). Valorization of keratin based waste. *Process Safety and Environmental Protection*, *115*, 85–98. https://doi.org/10.1016/j.psep.2017.08.045

Hong, S.-J., Park, G.-S., Jung, B. K., Khan, A. R., Park, Y.-J., Lee, C.-H., & Shin, J.-H. (2015). Isolation, Identification, and Characterization of a Keratin-degrading Bacterium Chryseobacterium sp. P1-3. *Journal of Applied Biological Chemistry*, *58*(3), 247–251. https://doi.org/10.3839/jabc.2015.039

Idris, A., Vijayaraghavan, R., Rana, U. A., Patti, A. F., & MacFarlane, D. R. (2014). Dissolution and regeneration of wool keratin in ionic liquids. *Green Chem.*, *16*(5), 2857–2864. https://doi.org/10.1039/C4GC00213J

Ishihara, M., Kishimoto, S., Nakamura, S., Sato, Y., & Hattori, H. (2019). Polyelectrolyte Complexes of Natural Polymers and Their Biomedical Applications. *Polymers*, *11*(4), 672. https://doi.org/10.3390/polym11040672

Isik, M., Sardon, H., & Mecerreyes, D. (2014). Ionic Liquids and Cellulose: Dissolution, Chemical Modification and Preparation of New Cellulosic Materials. *International Journal of Molecular Sciences*, *15*(7), 11922–11940. https://doi.org/10.3390/ijms150711922

Jackson, M., & Mantsch, H. H. (1995). The Use and Misuse of FTIR Spectroscopy in the Determination of Protein Structure. *Critical Reviews in Biochemistry and Molecular Biology*, *30*(2), 95–120. https://doi.org/10.3109/10409239509085140

Jaouadi, N. Z., Rekik, H., Badis, A., Trabelsi, S., Belhoul, M., Yahiaoui, A. B., Aicha, H. ben, Toumi, A., Bejar, S., & Jaouadi, B. (2013). Biochemical and Molecular Characterization of a Serine Keratinase from Brevibacillus brevis US575 with

Promising Keratin-Biodegradation and Hide-Dehairing Activities. *PLoS ONE*, *8*(10), e76722. https://doi.org/10.1371/journal.pone.0076722

Jeong, J.-H., Lee, O.-M., Jeon, Y.-D., Kim, J.-D., Lee, N.-R., Lee, C.-Y., & Son, H.-J. (2010). Production of keratinolytic enzyme by a newly isolated feather-degrading Stenotrophomonas maltophilia that produces plant growth-promoting activity. *Process Biochemistry*, *45*(10), 1738–1745. https://doi.org/10.1016/j.procbio.2010.07.020

Ji, Y., Chen, J., Lv, J., Li, Z., Xing, L., & Ding, S. (2014). Extraction of keratin with ionic liquids from poultry feather. *Separation and Purification Technology*, *132*, 577–583. https://doi.org/10.1016/j.seppur.2014.05.049

Kadirvelu, K., & Fathima, N. N. (2016). Self-assembly of keratin peptides: Its implication on the performance of electrospun PVA nanofibers. *Scientific Reports*, *6*(1), 36558. https://doi.org/10.1038/srep36558

Kakkar, P., Madhan, B., & Shanmugam, G. (2014). Extraction and characterization of keratin from bovine hoof: A potential material for biomedical applications. *SpringerPlus*, *3*(1), 596. https://doi.org/10.1186/2193-1801-3-596

Kim, J. W., Kim, M. J., Ki, C. S., Kim, H. J., & Park, Y. H. (2017). Fabrication of bi-layer scaffold of keratin nanofiber and gelatin-methacrylate hydrogel: Implications for skin graft. *International Journal of Biological Macromolecules*, *105*, 541–548. https://doi.org/10.1016/j.ijbiomac.2017.07.067

KONG, J., & YU, S. (2007). Fourier Transform Infrared Spectroscopic Analysis of Protein Secondary Structures. *Acta Biochimica et Biophysica Sinica*, *39*(8), 549–559. https://doi.org/10.1111/j.1745-7270.2007.00320.x

Korniłłowicz-Kowalska, T., & Bohacz, J. (2011). Biodegradation of keratin waste: Theory and practical aspects. *Waste Management*, *31*(8), 1689–1701. https://doi.org/10.1016/j.wasman.2011.03.024

Kumar, A. G., Swarnalatha, S., Gayathri, S., Nagesh, N., & Sekaran, G. (2007). Characterization of an alkaline active – thiol forming extracellular serine keratinase by the newly isolated Bacillus pumilus. *Journal of Applied Microbiology*, *0*(0), 071008041820010-??? https://doi.org/10.1111/j.1365-2672.2007.03564.x

Kuo, J.-M., Yang, J.-I., Chen, W.-M., Pan, M.-H., Tsai, M.-L., Lai, Y.-J., Hwang, A., Pan, B. S., & Lin, C.-Y. (2012). Purification and characterization of a thermostable keratinase from Meiothermus sp. I40. *International Biodeterioration & Biodegradation*, *70*, 111–116. https://doi.org/10.1016/j.ibiod.2012.02.006

Lateef, A., Adelere, I. A., & Gueguim-Kana, E. B. (2015). *Bacillus safensis* LAU 13: a new source of keratinase and its multi-functional biocatalytic applications. *Biotechnology & Biotechnological Equipment*, *29*(1), 54–63. https://doi.org/10.1080/13102818.2014.986360

Ledford, B. T., Simmons, J., Chen, M., Fan, H., Barron, C., Liu, Z., van Dyke, M., & He, J.-Q. (2017). Keratose Hydrogels Promote Vascular Smooth Muscle Differentiation from C-kit-Positive Human Cardiac Stem Cells. *Stem Cells and Development*, *26*(12), 888–900. https://doi.org/10.1089/scd.2016.0351

Leitner, W. (2004). Recent advances in catalyst immobilization using supercritical carbon dioxide. *Pure and Applied Chemistry*, *76*(3), 635–644.

Li, R., & Wang, D. (2013). Preparation of regenerated wool keratin films from wool keratin-ionic liquid solutions. *Journal of Applied Polymer Science*, *127*(4), 2648–2653. https://doi.org/10.1002/app.37527

Lin, C., Chen, Y., Tang, K., Yang, K., Cheng, N., & Yu, J. (2019). Keratin scaffolds with human adipose stem cells: Physical and biological effects toward wound healing. *Journal of Tissue Engineering and Regenerative Medicine*, term.2855. https://doi.org/10.1002/term.2855

Liu, D. K., & Chang, S. G. (1987). Kinetic study of the reaction between cystine and sulfide in alkaline solutions. *Canadian Journal of Chemistry*, *65*(4), 770–774. https://doi.org/10.1139/v87-131

Liu, X., Nie, Y., Meng, X., Zhang, Z., Zhang, X., & Zhang, S. (2017). DBN-based ionic liquids with high capability for the dissolution of wool keratin. *RSC Advances*, *7*(4), 1981–1988. https://doi.org/10.1039/C6RA26057H

Lloyd, A. W., Faragher, R. G. A., & Denyer, S. P. (2001). Ocular biomaterials and implants. *Biomaterials*, *22*(8), 769–785. https://doi.org/10.1016/S0142-9612(00)00237-4

Lo, W.-H., Too, J.-R., & Wu, J.-Y. (2012). Production of keratinolytic enzyme by an indigenous feather–degrading strain Bacillus cereus Wu2. *Journal of Bioscience and Bioengineering*, *114*(6), 640–647. https://doi.org/10.1016/j.jbiosc.2012.07.014

Lu, H. D., Soranno, D. E., Rodell, C. B., Kim, I. L., & Burdick, J. A. (2013). Secondary Photocrosslinking of Injectable Shear-Thinning Dock-and-Lock Hydrogels. *Advanced Healthcare Materials*, *2*(7), 1028–1036. https://doi.org/10.1002/adhm.201200343

Lu, T.-Y., Huang, W.-C., Chen, Y., Baskaran, N., Yu, J., & Wei, Y. (2020). Effect of varied hair protein fractions on the gel properties of keratin/chitosan hydrogels for the use in tissue engineering. *Colloids and Surfaces B: Biointerfaces*, *195*, 111258. https://doi.org/10.1016/j.colsurfb.2020.111258

Mazotto, A. M., Couri, S., Damaso, M. C. T., & Vermelho, A. B. (2013). Degradation of feather waste by Aspergillus niger keratinases: Comparison of submerged and solid-state fermentation. *International Biodeterioration & Biodegradation*, *85*, 189–195. https://doi.org/10.1016/j.ibiod.2013.07.003

McBath, R. A., & Shipp, D. A. (2010). Swelling and degradation of hydrogels synthesized with degradable poly(β-amino ester) crosslinkers. *Polymer Chemistry*, *1*(6), 860. https://doi.org/10.1039/c0py00074d

McKittrick, J., Chen, P.-Y., Bodde, S. G., Yang, W., Novitskaya, E. E., & Meyers, M. A. (2012). The Structure, Functions, and Mechanical Properties of Keratin. *JOM*, *64*(4), 449–468. https://doi.org/10.1007/s11837-012-0302-8

Miyamoto, T., Amiya, T., & Inagaki, H. (1982). Preparation of wool powder by explosive-puffing treatment. *Kobunshi Ronbunshu*, *39*(11), 679–685.

Muratoglu, O. K., Bragdon, C. R., O'Connor, D. O., Jasty, M., Harris, W. H., Gul, R., & McGarry, F. (1999). Unified wear model for highly crosslinked ultra-high molecular weight polyethylenes (UHMWPE). *Biomaterials*, *20*(16), 1463–1470. https://doi.org/10.1016/S0142-9612(99)00039-3

Nakamura, A., Arimoto, M., Takeuchi, K., & Fujii, T. (2002). A Rapid Extraction Procedure of Human Hair Proteins and Identification of Phosphorylated Species. *Biological and Pharmaceutical Bulletin*, *25*(5), 569–572. https://doi.org/10.1248/bpb.25.569

Nakata, R., Osumi, Y., Miyagawa, S., Tachibana, A., & Tanabe, T. (2015). Preparation of keratin and chemically modified keratin hydrogels and their evaluation as cell substrate with drug releasing ability. *Journal of Bioscience and Bioengineering*, *120*(1), 111–116. https://doi.org/10.1016/j.jbiosc.2014.12.005

Nnolim, N. E., Okoh, A. I., & Nwodo, U. U. (2020). Bacillus sp. FPF-1 Produced Keratinase with High Potential for Chicken Feather Degradation. *Molecules*, *25*(7), 1505. https://doi.org/10.3390/molecules25071505

Nuutinen, E.-M., Willberg-Keyriläinen, P., Virtanen, T., Mija, A., Kuutti, L., Lantto, R., & Jääskeläinen, A.-S. (2019). Green process to regenerate keratin from feathers with an aqueous deep eutectic solvent. *RSC Advances*, *9*(34), 19720–19728. https://doi.org/10.1039/C9RA03305J

Onifade, A. A., Al-Sane, N. A., Al-Musallam, A. A., & Al-Zarban, S. (1998). A review: Potentials for biotechnological applications of keratin-degrading microorganisms and their enzymes for nutritional improvement of feathers and other keratins as livestock feed resources. *Bioresource Technology*, *66*(1), 1–11. https://doi.org/10.1016/S0960-8524(98)00033-9

Ozbas, B., Kretsinger, J., Rajagopal, K., Schneider, J. P., & Pochan, D. J. (2004). Salt-Triggered Peptide Folding and Consequent Self-Assembly into Hydrogels with Tunable Modulus. *Macromolecules*, *37*(19), 7331–7337. https://doi.org/10.1021/ma0491762

Pace, L. A., Plate, J. F., Smith, T. L., & van Dyke, M. E. (2013). The effect of human hair keratin hydrogel on early cellular response to sciatic nerve injury in a rat model. *Biomaterials*, *34*(24), 5907–5914. https://doi.org/10.1016/j.biomaterials.2013.04.024

Pakkaner, E., Yalçın, D., Uysal, B., & Top, A. (2019). Self-assembly behavior of the keratose proteins extracted from oxidized Ovis aries wool fibers. *International Journal of Biological Macromolecules*, *125*, 1008–1015. https://doi.org/https://doi.org/10.1016/j.ijbiomac.2018.12.129

Park, M., Shin, H. K., Kim, B.-S., Kim, M. J., Kim, I.-S., Park, B.-Y., & Kim, H.-Y. (2015). Effect of discarded keratin-based biocomposite hydrogels on the wound healing process in vivo. *Materials Science and Engineering: C*, *55*, 88–94. https://doi.org/10.1016/j.msec.2015.03.033

Parry, D. A. D., & Creamer, L. K. (1979). *Fibrous proteins, scientific, industrial, and medical aspects*. Academic Presss.

Peppas, N. A., Bures, P., Leobandung, W., & Ichikawa, H. (2000). Hydrogels in pharmaceutical formulations. *European Journal of Pharmaceutics and Biopharmaceutics*, *50*(1), 27–46. https://doi.org/https://doi.org/10.1016/S0939-6411(00)00090-4

Perța-Crișan, S., Ursachi, C. Ștefan, Gavrilaș, S., Oancea, F., & Munteanu, F.-D. (2021). Closing the Loop with Keratin-Rich Fibrous Materials. *Polymers*, *13*(11), 1896. https://doi.org/10.3390/polym13111896

Petek, B., & Marinšek Logar, R. (2021). Management of waste sheep wool as valuable organic substrate in European Union countries. *Journal of Material Cycles and Waste Management*, *23*(1), 44–54. https://doi.org/10.1007/s10163-020-01121-3

Phelps, E. A., Enemchukwu, N. O., Fiore, V. F., Sy, J. C., Murthy, N., Sulchek, T. A., Barker, T. H., & García, A. J. (2012). Maleimide Cross-Linked Bioactive PEG Hydrogel Exhibits Improved Reaction Kinetics and Cross-Linking for Cell Encapsulation and In Situ Delivery. *Advanced Materials*, *24*(1), 64–70. https://doi.org/10.1002/adma.201103574

Phillips, P. J., & Lambert, W. S. (1990). Regime transitions in a non-reptating polymer: crosslinked linear polyethylene. *Macromolecules*, *23*(7), 2075–2081. https://doi.org/10.1021/ma00209a033

Poole, A. J., Lyons, R. E., & Church, J. S. (2011). Dissolving Feather Keratin Using Sodium Sulfide for Bio-Polymer Applications. *Journal of Polymers and the Environment*, *19*(4), 995–1004. https://doi.org/10.1007/s10924-011-0365-6

Potter, N. A., & van Dyke, M. (2018). Effects of Differing Purification Methods on Properties of Keratose Biomaterials. *ACS Biomaterials Science & Engineering*, *4*(4), 1316–1323. https://doi.org/10.1021/acsbiomaterials.7b00964

Pourjavaheri, F., Ostovar Pour, S., Jones, O. A. H., Smooker, P. M., Brkljača, R., Sherkat, F., Blanch, E. W., Gupta, A., & Shanks, R. A. (2019). Extraction of keratin from waste chicken feathers using sodium sulfide and l-cysteine. *Process Biochemistry*, *82*, 205–214. https://doi.org/10.1016/j.procbio.2019.04.010

Purchase, D. (2016). Microbial keratinases: characteristics, biotechnological applications and potential. In *The handbook of microbial bioresources* (pp. 634–674). CABI. https://doi.org/10.1079/9781780645216.0634

Rahayu, S., Syah, D., & Thenawidjaja Suhartono, M. (2012). Degradation of keratin by keratinase and disulfide reductase from Bacillus sp. MTS of Indonesian origin. *Biocatalysis and Agricultural Biotechnology*, *1*(2), 152–158. https://doi.org/10.1016/j.bcab.2012.02.001

Rajabi, M., Ali, A., McConnell, M., & Cabral, J. (2020). Keratinous materials: Structures and functions in biomedical applications. *Materials Science and Engineering: C*, *110*, 110612. https://doi.org/10.1016/j.msec.2019.110612

Rajabinejad, H., Zoccola, M., Patrucco, A., Montarsolo, A., Chen, Y., Ferri, A., Muresan, A., & Tonin, C. (2020). Fabrication and properties of keratoses/polyvinyl alcohol blend films. *Polymer Bulletin*, *77*(6), 3033–3046. https://doi.org/10.1007/s00289-019-02889-7

Rajabinejad, H., Zoccola, M., Patrucco, A., Montarsolo, A., Rovero, G., & Tonin, C. (2018). Physicochemical properties of keratin extracted from wool by various methods. *Textile Research Journal*, *88*(21), 2415–2424. https://doi.org/10.1177/0040517517723028

Rama Rao, D., & Gupta, V. B. (1992). Thermal characteristics of wool fibers. *Journal of Macromolecular Science, Part B*, *31*(2), 149–162. https://doi.org/10.1080/00222349208215509

Ramya, K. R., Thangam, R., & Madhan, B. (2020). Comparative analysis of the chemical treatments used in keratin extraction from red sheep's hair and the cell viability evaluations of this keratin for tissue engineering applications. *Process Biochemistry*, *90*, 223–232. https://doi.org/10.1016/j.procbio.2019.11.015

Reddy, N. (2017). *Keratin-based biomaterials and bioproducts*.

Riddles, P. W., Blakeley, R. L., & Zerner, B. (1983). *[8] Reassessment of Ellman's reagent* (pp. 49–60). https://doi.org/10.1016/S0076-6879(83)91010-8

Riffel, A., Lucas, F., Heeb, P., & Brandelli, A. (2003). Characterization of a new keratinolytic bacterium that completely degrades native feather keratin. *Archives of Microbiology*, *179*(4), 258–265. https://doi.org/10.1007/s00203-003-0525-8

Rippon, J. A. (2013). The Structure of Wool. In *The Coloration of Wool and other Keratin Fibres* (pp. 1–42). John Wiley & Sons, Ltd. https://doi.org/10.1002/9781118625118.ch1

Robbins, C. R. (2012). *Chemical and Physical Behavior of Human Hair*. Springer Berlin Heidelberg. https://doi.org/10.1007/978-3-642-25611-0

Rodell, C. B., MacArthur, J. W., Dorsey, S. M., Wade, R. J., Wang, L. L., Woo, Y. J., & Burdick, J. A. (2015). Shear-Thinning Supramolecular Hydrogels with Secondary Autonomous Covalent Crosslinking to Modulate Viscoelastic Properties In Vivo. *Advanced Functional Materials*, *25*(4), 636–644. https://doi.org/10.1002/adfm.201403550

Rodríguez-Clavel, I. S., Paredes-Carrera, S. P., Flores-Valle, S. O., Paz-García, E. J., Sánchez-Ochoa, J. C., & Pérez-Gutiérrez, R. M. (2019). Effect of Microwave or Ultrasound Irradiation in the Extraction from Feather Keratin. *Journal of Chemistry*, *2019*, 1–9. https://doi.org/10.1155/2019/1326063

Rouse, J. G., & van Dyke, M. E. (2010). A Review of Keratin-Based Biomaterials for Biomedical Applications. *Materials*, *3*(2), 999–1014. https://doi.org/10.3390/ma3020999

Ryu, J., Lee, H., Kim, H., & Sohn, D. (2018). Lamellar Thickness of Poly(ethylene oxide) Film Crystallized from the Gel State. *Macromolecules*, *51*(19), 7745–7755. https://doi.org/10.1021/acs.macromol.8b01232

Saleem, M., Rehman, A., Yasmin, R., & Munir, B. (2012). Biochemical analysis and investigation on the prospective applications of alkaline protease from a Bacillus cereus strain. *Molecular Biology Reports*, *39*(6), 6399–6408. https://doi.org/10.1007/s11033-011-1033-6

Sánchez, Ó. J., & Cardona, C. A. (2008). Trends in biotechnological production of fuel ethanol from different feedstocks. *Bioresource Technology*, *99*(13), 5270–5295. https://doi.org/10.1016/j.biortech.2007.11.013

Sando, L., Kim, M., Colgrave, M. L., Ramshaw, J. A. M., Werkmeister, J. A., & Elvin, C. M. (2010). Photochemical crosslinking of soluble wool keratins produces a mechanically stable biomaterial that supports cell adhesion and proliferation. *Journal of Biomedical Materials Research Part A*, *95A*(3), 901–911. https://doi.org/10.1002/jbm.a.32913

Sangali, S., & Brandelli, A. (2000). Feather keratin hydrolysis by a Vibrio sp. strain kr2. *Journal of Applied Microbiology*, *89*(5), 735–743. https://doi.org/10.1046/j.1365-2672.2000.01173.x

Santos, R. M. D. B., Firmino, A. A. P., de Sá, C. M., & Felix, C. R. (1996). Keratinolytic Activity of Aspergillus fumigatus Fresenius. *Current Microbiology*, *33*(6), 364–370. https://doi.org/10.1007/s002849900129

Saul, J. M., Ellenburg, M. D., de Guzman, R. C., & Dyke, M. van. (2011). Keratin hydrogels support the sustained release of bioactive ciprofloxacin. *Journal of Biomedical Materials Research Part A*, *98A*(4), 544–553. https://doi.org/10.1002/jbm.a.33147

Sharma, S., Gupta, A., & Kumar, A. (2019). *Keratin: An Introduction* (pp. 1–18). https://doi.org/10.1007/978-3-030-02901-2_1

Shavandi, A., Carne, A., Bekhit, A. A., & Bekhit, A. E.-D. A. (2017). An improved method for solubilisation of wool keratin using peracetic acid. *Journal of Environmental Chemical Engineering*, *5*(2), 1977–1984. https://doi.org/10.1016/j.jece.2017.03.043

Shavandi, A., Silva, T. H., Bekhit, A. A., & Bekhit, A. E.-D. A. (2017). Keratin: dissolution, extraction and biomedical application. *Biomaterials Science*, *5*(9), 1699–1735. https://doi.org/10.1039/C7BM00411G

Sierpinski, P., Garrett, J., Ma, J., Apel, P., Klorig, D., Smith, T., Koman, L. A., Atala, A., & van Dyke, M. (2008). The use of keratin biomaterials derived from human hair for the promotion of rapid regeneration of peripheral nerves. *Biomaterials*, *29*(1), 118–128. https://doi.org/10.1016/j.biomaterials.2007.08.023

Sinkiewicz, I., Staroszczyk, H., & Śliwińska, A. (2018). Solubilization of keratins and functional properties of their isolates and hydrolysates. *Journal of Food Biochemistry*, *42*(2), e12494. https://doi.org/10.1111/jfbc.12494

Sionkowska, A. (2011). Current research on the blends of natural and synthetic polymers as new biomaterials: Review. *Progress in Polymer Science*, *36*(9), 1254–1276. https://doi.org/10.1016/j.progpolymsci.2011.05.003

Snyder, S. L., & Sobocinski, P. Z. (1975). An improved 2,4,6-trinitrobenzenesulfonic acid method for the determination of amines. *Analytical Biochemistry*, *64*(1), 284–288. https://doi.org/10.1016/0003-2697(75)90431-5

Sowmiah, S., Srinivasadesikan, V., Tseng, M.-C., & Chu, Y.-H. (2009). On the Chemical Stabilities of Ionic Liquids. *Molecules*, *14*(9), 3780–3813. https://doi.org/10.3390/molecules14093780

Stenzel, M. H. (2013). Bioconjugation Using Thiols: Old Chemistry Rediscovered to Connect Polymers with Nature's Building Blocks. *ACS Macro Letters*, *2*(1), 14–18. https://doi.org/10.1021/mz3005814

Su, C., Gong, J., Ye, J., He, J., Li, R., Jiang, M., Geng, Y., Zhang, Y., Chen, J., Xu, Z., & Shi, J. (2020). Enzymatic Extraction of Bioactive and Self-Assembling Wool Keratin for Biomedical Applications. *Macromolecular Bioscience*, *20*(9), 2000073. https://doi.org/10.1002/mabi.202000073

Sun, P., Liu, Z.-T., & Liu, Z.-W. (2009). Particles from bird feather: A novel application of an ionic liquid and waste resource. *Journal of Hazardous Materials*, *170*(2–3), 786–790. https://doi.org/10.1016/j.jhazmat.2009.05.034

Sun, X. F., Xu, F., Sun, R. C., Geng, Z. C., Fowler, P., & Baird, M. S. (2005). Characteristics of degraded hemicellulosic polymers obtained from steam exploded wheat straw. *Carbohydrate Polymers*, *60*(1), 15–26. https://doi.org/10.1016/j.carbpol.2004.11.012

Suvarnapathaki, S., Nguyen, M. A., Wu, X., Nukavarapu, S. P., & Camci-Unal, G. (2019). Synthesis and characterization of photocrosslinkable hydrogels from bovine skin gelatin. *RSC Advances*, *9*(23), 13016–13025. https://doi.org/10.1039/C9RA00655A

Swetha, M., Sahithi, K., Moorthi, A., Srinivasan, N., Ramasamy, K., & Selvamurugan, N. (2010). Biocomposites containing natural polymers and hydroxyapatite for bone tissue engineering. *International Journal of Biological Macromolecules*, *47*(1), 1–4. https://doi.org/10.1016/j.ijbiomac.2010.03.015

Syed, D. G., Lee, J. C., Li, W.-J., Kim, C.-J., & Agasar, D. (2009). Production, characterization and application of keratinase from Streptomyces gulbargensis. *Bioresource Technology*, *100*(5), 1868–1871. https://doi.org/10.1016/j.biortech.2008.09.047

Tachibana, A., Nishikawa, Y., Nishino, M., Kaneko, S., Tanabe, T., & Yamauchi, K. (2006). Modified keratin sponge: Binding of bone morphogenetic protein-2 and

osteoblast differentiation. *Journal of Bioscience and Bioengineering*, *102*(5), 425–429. https://doi.org/10.1263/jbb.102.425

Teasdale, D. C. (1988). *Wool testing and marketing handbook / D.C. Teasdale: Vol. viii*.

Tomblyn, S., Pettit Kneller, E. L., Walker, S. J., Ellenburg, M. D., Kowalczewski, C. J., van Dyke, M., Burnett, L., & Saul, J. M. (2016a). Keratin hydrogel carrier system for simultaneous delivery of exogenous growth factors and muscle progenitor cells. *Journal of Biomedical Materials Research Part B: Applied Biomaterials*, *104*(5), 864–879. https://doi.org/10.1002/jbm.b.33438

Tomblyn, S., Pettit Kneller, E. L., Walker, S. J., Ellenburg, M. D., Kowalczewski, C. J., van Dyke, M., Burnett, L., & Saul, J. M. (2016b). Keratin hydrogel carrier system for simultaneous delivery of exogenous growth factors and muscle progenitor cells. *Journal of Biomedical Materials Research Part B: Applied Biomaterials*, *104*(5), 864–879. https://doi.org/10.1002/jbm.b.33438

Tonin, C., Zoccola, M., Aluigi, A., Varesano, A., Montarsolo, A., Vineis, C., & Zimbardi, F. (2006). Study on the Conversion of Wool Keratin by Steam Explosion. *Biomacromolecules*, *7*(12), 3499–3504. https://doi.org/10.1021/bm060597w

Tran, C. D., & Mututuvari, T. M. (2015). Cellulose, Chitosan, and Keratin Composite Materials. Controlled Drug Release. *Langmuir*, *31*(4), 1516–1526. https://doi.org/10.1021/la5034367

Turkish Statistical Institute. (n.d.).

Varaprasad, K., Vimala, K., Raghavendra, G. M., Jayaramudu, T., Sadiku, E. R., & Ramam, K. (2015). Cell Encapsulation in Polymeric Self-Assembled Hydrogels. In *Nanotechnology Applications for Tissue Engineering* (pp. 149–171). Elsevier. https://doi.org/10.1016/B978-0-323-32889-0.00010-8

Veerasubramanian, P. K., Thangavel, P., Kannan, R., Chakraborty, S., Ramachandran, B., Suguna, L., & Muthuvijayan, V. (2018). An investigation of konjac glucomannan-keratin hydrogel scaffold loaded with Avena sativa extracts for diabetic wound healing. *Colloids and Surfaces B: Biointerfaces*, *165*, 92–102. https://doi.org/10.1016/j.colsurfb.2018.02.022

Ventura, S. P. M., e Silva, F. A., Quental, M. v., Mondal, D., Freire, M. G., & Coutinho, J. A. P. (2017). Ionic-Liquid-Mediated Extraction and Separation Processes for Bioactive Compounds: Past, Present, and Future Trends. *Chemical Reviews*, *117*(10), 6984–7052. https://doi.org/10.1021/acs.chemrev.6b00550

Vidal, L., Christen, P., & Coello, M. N. (2000). Feather degradation by Kocuria rosea in submerged culture. *World Journal of Microbiology and Biotechnology*, *16*(6), 551–554. https://doi.org/10.1023/A:1008976802181

Villa, A. L. V., Aragão, M. R. S., dos Santos, E. P., Mazotto, A. M., Zingali, R. B., de Souza, E. P., & Vermelho, A. B. (2013). Feather keratin hydrolysates obtained

from microbial keratinases: effect on hair fiber. *BMC Biotechnology*, *13*(1), 15. https://doi.org/10.1186/1472-6750-13-15

Wang, J., Hao, S., Luo, T., Cheng, Z., Li, W., Gao, F., Guo, T., Gong, Y., & Wang, B. (2017). Feather keratin hydrogel for wound repair: Preparation, healing effect and biocompatibility evaluation. *Colloids and Surfaces B: Biointerfaces*, *149*, 341–350. https://doi.org/10.1016/j.colsurfb.2016.10.038

Wang, K., Li, R., Ma, J. H., Jian, Y. K., & Che, J. N. (2016). Extracting keratin from wool by using <scp>l</scp> -cysteine. *Green Chemistry*, *18*(2), 476–481. https://doi.org/10.1039/C5GC01254F

Wang, S., Wang, Z., Foo, S. E. M., Tan, N. S., Yuan, Y., Lin, W., Zhang, Z., & Ng, K. W. (2015). Culturing Fibroblasts in 3D Human Hair Keratin Hydrogels. *ACS Applied Materials & Interfaces*, *7*(9), 5187–5198. https://doi.org/10.1021/acsami.5b00854

Wang, X., Shi, Z., Zhao, Q., & Yun, Y. (2021). Study on the structure and properties of biofunctional keratin from rabbit hair. *Materials*, *14*(2), 379.

Wang, Y.-X., & Cao, X.-J. (2012). Extracting keratin from chicken feathers by using a hydrophobic ionic liquid. *Process Biochemistry*, *47*(5), 896–899. https://doi.org/10.1016/j.procbio.2012.02.013

Xie, H., Li, S., & Zhang, S. (2005). Ionic liquids as novel solvents for the dissolution and blending of wool keratin fibers. *Green Chemistry*, *7*(8), 606. https://doi.org/10.1039/b502547h

Xie, Y., Hill, C. A. S., Xiao, Z., Militz, H., & Mai, C. (2010). Silane coupling agents used for natural fiber/polymer composites: A review. *Composites Part A: Applied Science and Manufacturing*, *41*(7), 806–819. https://doi.org/https://doi.org/10.1016/j.compositesa.2010.03.005

Xu, W., Ke, G., Wu, J., & Wang, X. (2006). Modification of wool fiber using steam explosion. *European Polymer Journal*, *42*(9), 2168–2173. https://doi.org/10.1016/j.eurpolymj.2006.03.026

Yalçın, D., & Top, A. (2022). Novel biopolymer-based hydrogels obtained through crosslinking of keratose proteins using tetrakis(hydroxymethyl) phosphonium chloride. *Iranian Polymer Journal*. https://doi.org/10.1007/s13726-022-01058-4

Yang, G., Yao, Y., & Wang, X. (2018). Comparative study of kerateine and keratose based composite nanofibers for biomedical applications. *Materials Science and Engineering: C*, *83*, 1–8. https://doi.org/10.1016/j.msec.2017.07.057

Yang, J., Shen, M., Luo, Y., Wu, T., Chen, X., Wang, Y., & Xie, J. (2021). Advanced applications of chitosan-based hydrogels: From biosensors to intelligent food packaging system. *Trends in Food Science & Technology*, *110*, 822–832. https://doi.org/10.1016/j.tifs.2021.02.032

Yin, J., Rastogi, S., Terry, A. E., & Popescu, C. (2007). Self-organization of Oligopeptides Obtained on Dissolution of Feather Keratins in Superheated Water. *Biomacromolecules*, *8*(3), 800–806. https://doi.org/10.1021/bm060811g

Yue, K., Liu, Y., Byambaa, B., Singh, V., Liu, W., Li, X., Sun, Y., Zhang, Y. S., Tamayol, A., Zhang, P., Ng, K. W., Annabi, N., & Khademhosseini, A. (2018). Visible light crosslinkable human hair keratin hydrogels. *Bioengineering & Translational Medicine*, *3*(1), 37–48. https://doi.org/10.1002/btm2.10077

Zahn, H., & Kusch, P. (1981). Melliand Textilber. *English Edn*, *10*, 75.

Zhang, Y., Yang, R., & Zhao, W. (2014). Improving Digestibility of Feather Meal by Steam Flash Explosion. *Journal of Agricultural and Food Chemistry*, *62*(13), 2745–2751. https://doi.org/10.1021/jf405498k

Zhang, Y., Zhao, W., & Yang, R. (2015). Steam Flash Explosion Assisted Dissolution of Keratin from Feathers. *ACS Sustainable Chemistry & Engineering*, *3*(9), 2036–2042. https://doi.org/10.1021/acssuschemeng.5b00310

Zhao, J., Yan, Y., Shang, Y., Du, Y., Long, L., Yuan, X., & Hou, X. (2017). Thermosensitive elastin-derived polypeptide hydrogels crosslinked by genipin. *International Journal of Polymeric Materials and Polymeric Biomaterials*, *66*(8), 369–377. https://doi.org/10.1080/00914037.2016.1217534

Zhao, W., Yang, R., Zhang, Y., & Wu, L. (2012). Sustainable and practical utilization of feather keratin by an innovative physicochemical pretreatment: high density steam flash-explosion. *Green Chemistry*, *14*(12), 3352. https://doi.org/10.1039/c2gc36243k

Zoccola, M., Aluigi, A., Patrucco, A., Vineis, C., Forlini, F., Locatelli, P., Sacchi, M. C., & Tonin, C. (2012). Microwave-assisted chemical-free hydrolysis of wool keratin. *Textile Research Journal*, *82*(19), 2006–2018. https://doi.org/10.1177/0040517512452948

Zuidema, J. M., Rivet, C. J., Gilbert, R. J., & Morrison, F. A. (2014). A protocol for rheological characterization of hydrogels for tissue engineering strategies. *Journal of Biomedical Materials Research Part B: Applied Biomaterials*, *102*(5), 1063–1073. https://doi.org/10.1002/jbm.b.33088

APPENDIX A

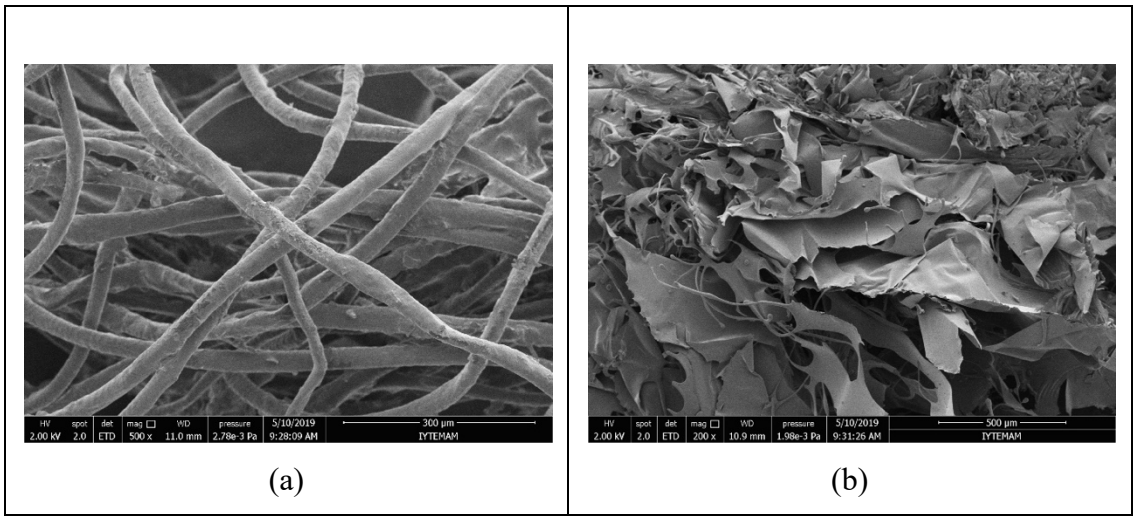

Figure A.1. SEM of the washed wool and the extracted keratose.

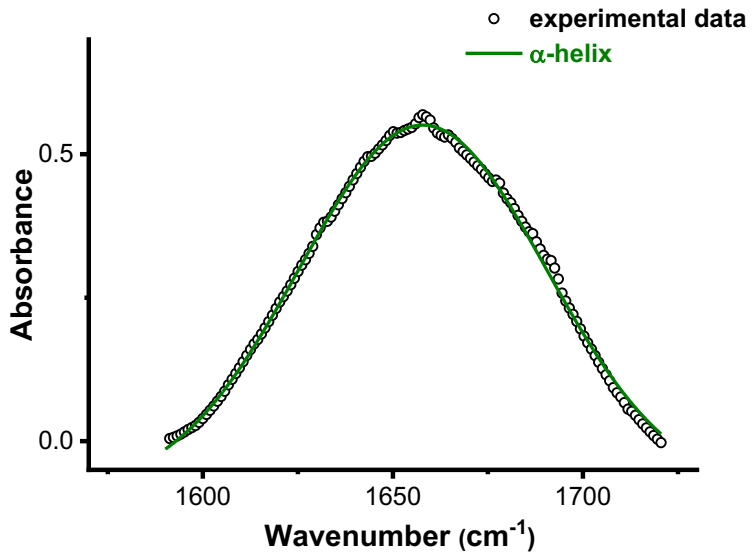

Figure A.2. Deconvolution of the Amide I region of the FTIR spectrum of the keratose.

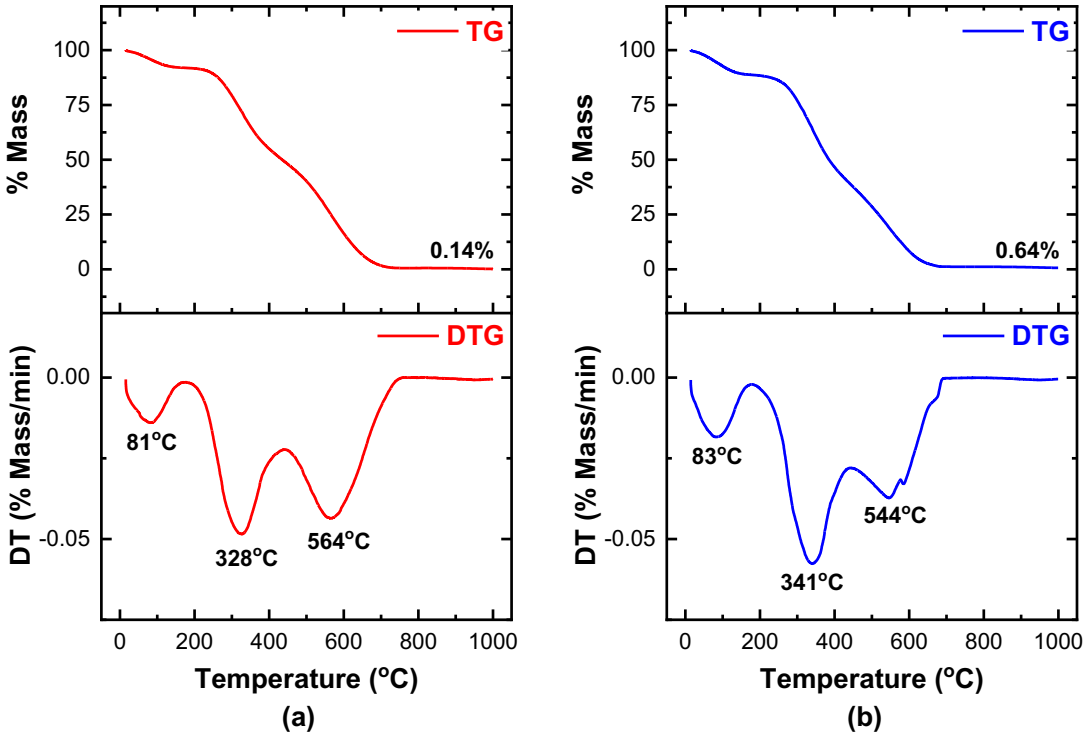

Figure A.3. TGA and DTG of the (a) defatted wool and (b) extracted keratose.

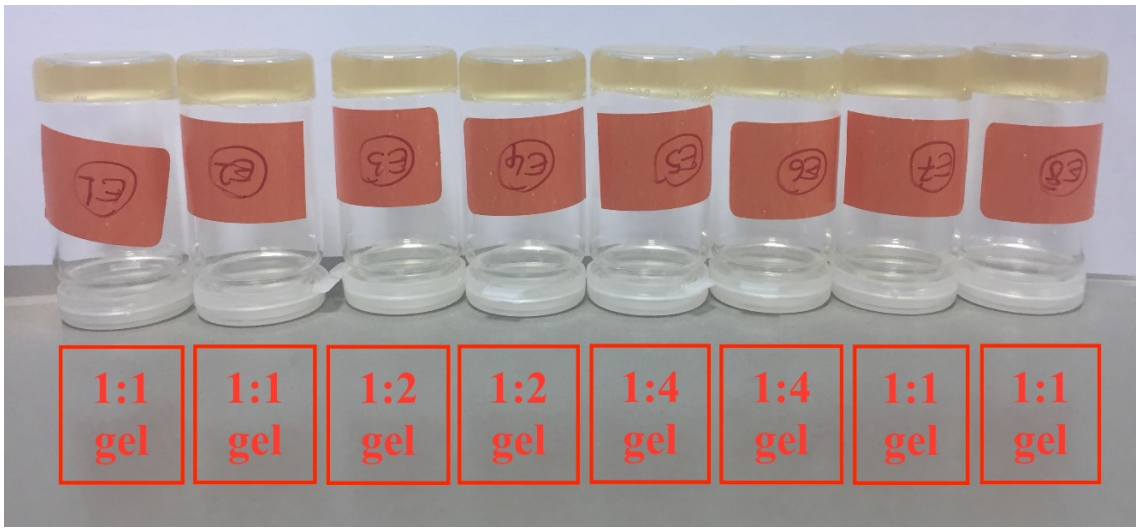

Figure A.4. Pictures of the hydrogels prepared at different keratose:THPC reactive groups ratio

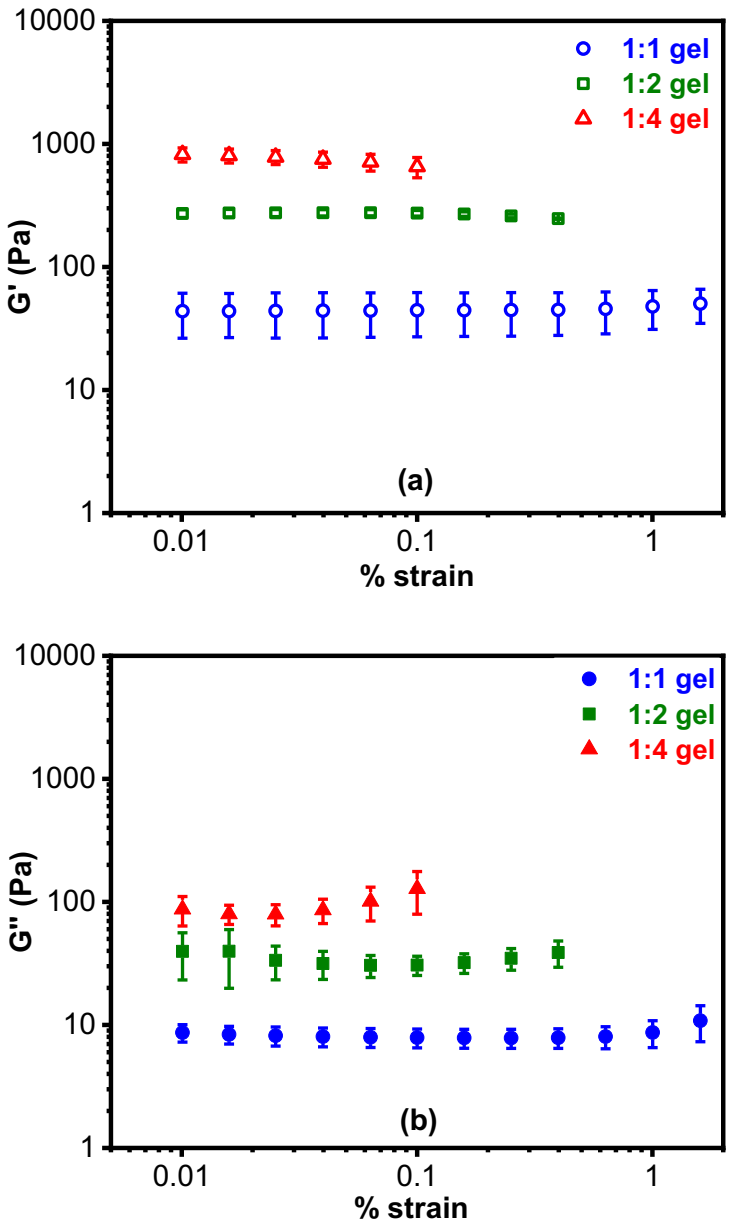

Figure A.5. Strain sweep data of the crosslinked hydrogels.

APPENDIX B

PERMISSIONS TO REPRODUCE FIGURES AND TEXTS

The permission has been taken to reproduce the full text presented in Chapter 2 through Copyright Clearance Center. The documentation of the approval is shown below.

SPRINGER NATURE LICENSE
TERMS AND CONDITIONS

Aug 04, 2022

This Agreement between İzmir Institute of Technology -- Damla Yalçın ("You") and Springer Nature ("Springer Nature") consists of your license details and the terms and conditions provided by Springer Nature and Copyright Clearance Center.

License Number	5362010613222
License date	Aug 04, 2022
Licensed Content Publisher	Springer Nature
Licensed Content Publication	Iranian Polymer Journal
Licensed Content Title	Novel biopolymer-based hydrogels obtained through crosslinking of keratose proteins using tetrakis(hydroxymethyl) phosphonium chloride
Licensed Content Author	Damla Yalçın et al
Licensed Content Date	May 18, 2022
Type of Use	Thesis/Dissertation
Requestor type	academic/university or research institute
Format	print and electronic